# University of Alberta

Reconsidering the pre-industrial mercury cycle using lake sediment archives

by

Colin Alexander Cooke

A thesis submitted to the Faculty of Graduate Studies and Research
in partial fulfillment of the requirements for the degree of

Doctor of Philosophy

Earth and Atmospheric Sciences



Spring, 2010
Edmonton, Alberta

## Examining Committee

Alexander Wolfe, Earth and Atmospheric Sciences

Marianne Douglas, Earth and Atmospheric Sciences

Michael Wayman, Chemical and Materials Engineering

Vincent St.Louis, Biological Sciences

Marc Lucotte, Centre GEOTOP, Université du Québec à Montréal

**ABSTRACT**

Human activities have profoundly altered the biogeochemical cycle of many elements including mercury (Hg). Since ~1850 AD, industrial processes are suggested to have led to a 3-fold increase in Hg deposition above natural, pre-industrial levels. Despite extensive historical evidence for pre-industrial Hg extraction, there has been little evidence for any pre-industrial Hg pollution. This dissertation contains five research papers which critically investigate our understanding of pre-industrial Hg cycling using the geochemical record preserved in lake sediments.

Pre-industrial Hg pollution has long been hypothesized on the basis of historical records but has never been proven. Using lake sediment cores from three regions in the Peruvian and Bolivian Andes, I show that pre-industrial Hg pollution resulted from a multitude of mineral-extractive activities including: (i) Colonial (1532-1900 AD) and pre-Colonial (pre-1532 AD) cinnabar (HgS) extraction (Chapter 2); (ii) Colonial Hg amalgamation (Chapter 3), and; (iii) pre-Colonial smelting of argentiferous ores (Chapter 4). All three of these activities resulted in atmospheric Hg emissions, and Hg speciation analyses demonstrate that at least some of these emissions were transported long distances.

Chapter 5 explores how sediment core chronologies influence the calculation of pre-industrial Hg accumulation rates (fluxes), and suggests $^{14}C$ dates are necessary if accurate Hg flux histories are sought. Relying on $^{210}Pb$ chronologies alone overestimates pre-industrial Hg fluxes, resulting in an

underestimation in the degree to which human activities have altered the natural biogeochemical cycle of Hg.

The final paper presented here (Chapter 6) places 20$^{th}$-century Arctic Hg enrichment in an unparalleled long-term, multi-proxy perspective using two unique paleolimnological records, both of which are from Baffin Island, Canada. These records span the Holocene at high resolution but also include sediment from the last and penultimate interglacials. 20$^{th}$-century Hg fluxes at both lakes are shown to be >10 times higher than pre-industrial fluxes, and 20$^{th}$-century Hg concentrations are exceeded during both the early Holocene and the early last-interglacial. These results suggest natural processes are capable of generating Hg burdens in lakes which exceed those associated with anthropogenic pollution.

**ACKNOWLEDGEMENTS**

Numerous people contributed to my experience in producing this thesis and I owe them all a debt of gratitude for their assistance.

First and foremost, I need to thank my supervisor Dr. Alexander Wolfe. Alex encouraged me to ignore traditional disciplinary boundaries, gave me the freedom to develop my ideas, and inspired me with his passion for science everyday. Every student would lucky to work under the mentorship of a great advisor, scientist and friend like Alex.

Many colleagues and friends generously provided me with help, support and encouragement during my studies. Dr. Duane Froese always listened to my ideas, dilemmas and problems, and provided me with advice and assistance. My committee members, Drs. Vincent St. Louis and Marianne Douglas provided excellent guidance and feedback, and were always available. To Dr. Mike Wayman, thank you for your genuine interest and excitement for my research. My project would not have been the same without the involvement of Prentiss Balcom, who welcomed me into his lab, and was always quick with helpful revisions. My collaborators Drs. Harald Biester, Mark Abbott, Jason Briner, Charles Kerfoot, Neal Micheluti, and William Hobbs generously contributed their cores, data and expertise. I am also grateful to Dr. Marc Lucotte for his time and efforts as external examiner.

My time in the Andes was spent with my good friends William Hobbs and Alberto Reyes. For their help, their efforts, and their friendship, I am truly grateful; I very much look forward to our future adventures together. I would also like to thank Drs. Pedro Tapia, Alejandro Chu, and Broxton Bird for their invaluable help in Peru over the years.

My greatest thanks is to my wife, Tara Bond. Tara's adventurist spirit is only exceeded by her excitement the night before our next journey. Tara remains my most important collaborator of all, in all things. Any successes I've enjoyed are due in no small part to her love and support.

# TABLE OF CONTENTS

**LIST OF TABLES**

## LIST OF FIGURES

# CHAPTER 1: INTRODUCTION

## Metals and the environment

Human activities have profoundly altered the biogeochemical cycle of many metals, and metal pollution is an important environmental issue in many parts of the world (Kessler, 1994). A common assumption is that large-scale metal pollution began with the industrial era (~1850 AD). Indeed, between 1930 and 1985, production of chromium (Cr), copper (Cu), nickel (Ni), and zinc (Zn) increased by 18-, 5-, 35-, and 4-fold, respectively (Nriagu, 1988), and anthropogenic activities are the most important mobilizing mechanism in the global biogeochemical cycling of many trace metals (Pacyna and Pacyna, 2001). Thus, there is considerable interest in tracking the trajectory of these biogeochemical changes, and knowledge about metal pollution histories is relevant for understanding present-day metal burdens in the environment (Renberg et al., 2009; Smol, 2010).

The longest observational dataset of atmospheric metal concentrations typically only span a few decades (e.g., Slemr et al., 2003) making it difficult to quantify the degree to which human activities have altered key biogeochemical cycles. Fortunately, natural archives, including lake sediments, can be exploited to provide data on past environmental conditions including the past biogeochemical cycling of many elements (Smol, 2008, 2010) (Fig. 1.1). For example, paleolimnological records can be used to determine pre-disturbance metal burdens, constrain the range of natural variability in biogeochemical cycling, and asses the rate, magnitude, and drivers of recent biogeochemical change (Renberg et al., 2009).

This thesis focuses on improving our understanding of the pre-industrial

global biogeochemical cycle of mercury (Hg) using paleolimnological archives. This introductory chapter is not intended to serve as an exhaustive literature review, but rather aims to provide the necessary foundation for a careful assessment of the papers presented as part of this dissertation.

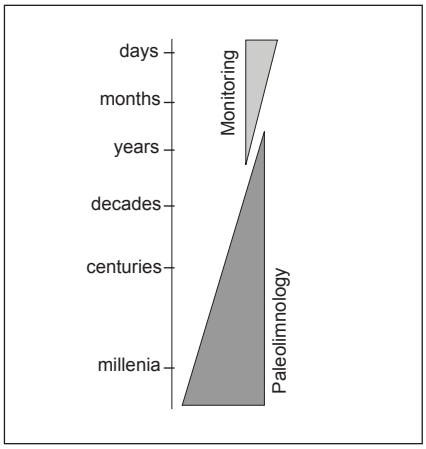


**Fig. 1.1.** Conceptual timescale model of the overlap between environmental monitoring and paleolimnology. Adapted from Smol (2008).

**Metal pollution and natural archives**

Clair Patterson was among the first to recognize and intensively study widespread metal pollution within the environment (Patterson, 1965). Patterson's geochemical research was initially focused on examining the evolution of the earth. It was during these efforts, which provided the first accurate estimates of the absolute age of the earth, that Patterson first recognized that the environment was severely contaminated with lead (Pb) pollution. The recognition that human activities had demonstrably altered the global biogeochemical cycle of Pb prompted Patterson to shift his focus towards quantifying the magnitude and rate of 20$^{th}$-century Pb pollution, and documenting its impact on human health and society. Patterson and his collaborators accomplished this by making, for example, the first reliable measurements of Pb in aerosols (Patterson, 1965) and in ice cores (Murozumi et al., 1969), and by contrasting Pb burdens within ancient and modern human skeletons (Ericson et al., 1979).

As the evidence for industrial-era Pb pollution became indubitable, Hong et al. (1994) and Renberg et al. (1994) used the Pb geochemical records preserved in an ice core from Greenland and lake sediment cores from Sweden, respectively, to convincingly demonstrate the existence of widespread pre-

industrial Pb pollution associated with Greek and Roman mining and metallurgy (Fig. 1.2). These results were later confirmed by measurements of stable Pb isotopes (Renberg et al., 2002; Rosman et al., 1997) and concentrations of Cu, Zn, and Cd pollution (Hong et al., 1998) within ice cores from Greenland. Since this pioneering work, Bindler et al. (2008), have demonstrated that in Europe about half of the cumulative burden of atmospherically deposited Pb dates to the pre-industrial era. Collectively, these results have firmly established the existence, hemispheric nature, and contemporary biogeochemical importance of atmospheric metal pollution from industrial and pre-industrial metal extraction.

Just as metal mining and pollution have a long history in the Old World, environmental scientists have recently revealed a long history of metal pollution associated with New World mining and metallurgy. The Peruvian and Bolivian Andes represent the cradle of New World metallurgy, and Abbott and Wolfe (2003) were the first to document atmospheric metal pollution resulting from pre-industrial New World metallurgy. At Cerro Rico de Potosí, Bolivia, which was historically the world's largest silver deposit, the authors used the geochemical record preserved in nearby lake sediments to reconstruct a ~1000-year history of silver extraction associated with Colonial, Incan, and pre-Incan mining practices. Subsequent efforts by Cooke et al. (2007, 2008) utilized lake sediment records to identify patterns in the expansion and evolution of New World

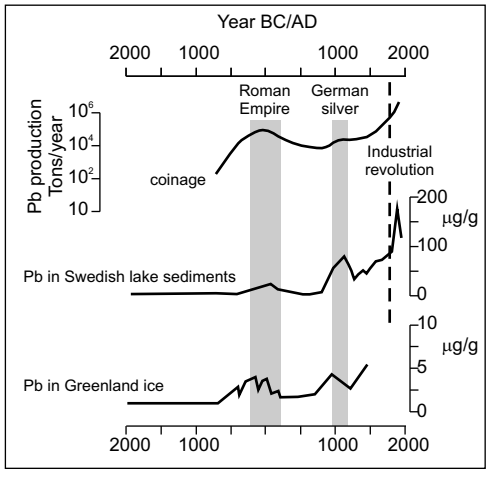


**Fig. 1.2.** Stratigraphic profiles of European Pb production, and associated Pb pollution preserved in both Swedish lake sediments and Greenland ice cores. Modified from Hong et al. (1994) and Renberg et al. (1994).

metallurgy, highlighting the contribution paleolimnological methods can make towards understanding technological and cultural evolution. Collectively, these studies in both the Old and New Worlds have firmly established the usefulness of natural archives in documenting the impact of pre-industrial mining activities on global biogeochemical cycles.

**The global cycle of mercury**

Mercury exists in the environment in several chemical species. Gaseous elemental Hg ($Hg^0$) comprises >95% of atmospheric Hg, and has an atmospheric residence time of about one year (Fitzgerald and Lamborg, 2005; Mason and Sheu, 2002). This long residence time results in the hemispheric homogenization of atmospheric Hg (Lindberg et al., 2007). Wet deposition of Hg occurs following oxidation to divalent Hg ($Hg^{2+}$), though dry deposition (of both $Hg^{2+}$ and $Hg^0$) can also be important (Schroeder and Munthe, 1998). Methylmercury ($CH_3Hg^+$) is of the most concern to living organisms because of its high toxicity, and its propensity to bioaccumulate through food chains.

Mercury exhibits a scientifically challenging biogeochemical cycle which has been profoundly altered by anthropogenic activities. Natural sources are currently thought to emit between 21 and 26 Mmol of Hg annually to the atmosphere, part of which is composed of previously deposited Hg, from both natural and anthropogenic sources, that has been reemitted and recycled (Lindberg et al., 2007; Pirrone et al., 2009). Anthropogenic sources of Hg are thought to emit 12-15 Mmol of Hg annually, with the major contributions being from fossil fuel combustion (~7 Mmol $yr^{-1}$), small-scale gold mining (~2 Mmol $yr^{-1}$), non-ferrous metals manufacturing (~2 Mmol $yr^{-1}$), and waste disposal (~1 Mmol $yr^{-1}$) (Pirrone et al., 2009). Each of these categories and their respective flux estimates carry a

minimum uncertainty of ±30%.

Attempts to model the current global Hg cycle are often juxtaposed with models of the pre-industrial (i.e. natural) Hg cycle. These pre-industrial Hg models assume no anthropogenic emissions of Hg to the atmosphere prior to the industrial era (~1850 AD) (Mason and Sheu, 2002). While there is a great deal of historical evidence for pre-industrial Hg exploitation (see summary below), there has been considerable debate about the importance of pre-industrial Hg emissions for the pre-industrial global Hg cycle (c.f., Camargo, 1993, 2002; Lamborg et al., 2002; Nriagu, 1993, 1994; Strode et al., 2009). Resolving this debate will afford us a better understanding of how and to what degree human activities have altered the global Hg cycle.

**Pre-industrial mercury exploitation**

Natural deposits of Hg (Fig. 1.3) have been known about and exploited for at least the last 3500 years, and by the 1st century BC the mercuric ore cinnabar (HgS) was widely used by the Romans as a pigment (Nriagu, 1979). The development of Hg amalgamation in New Spain (Mexico) in 1554 AD by Bartonome de Medina marks the onset of industrial-scale Hg production and the widespread use of Hg amalgamation to extract silver (Nriagu, 1994). Globally, approximately one million tons of Hg has been mined since ~1500 AD (Hylander and Meili, 2003), and virtually all of the Hg mined before 1900 AD was exported to the silver mines of Mexico, Peru, and Bolivia. The location and approximate start-date of Colonial silver mining for each mine is

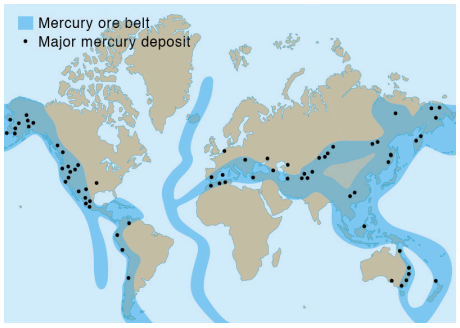


**Fig. 1.3.** Map of the mercury ore belt and major mercury deposits globally. Adapted from Kessler 1994.

indicated in Fig. 1.4. New World Hg amalgamation was carried out in large open-air courts or patios, and thus became known as the "patio process". The process itself consisted of five separate operations, which were conducted over a few weeks to months. (1) The ore was crushed using a stamp, crusher, or Chilean mill. (2) The crushed ore was then mixed with liquid Hg in a lined pit or *arrastra*. (3) Once combined, the material from the *arrastra* was spread out on the patio in the shape of a large flat cake (called a *torta*) to which both *magistral* (roasted copper or iron sulfate) and more Hg were added. The ratio of Hg added to silver in the ore was ~6-8, and the *torta* was treaded by men, horses, or mules for anywhere

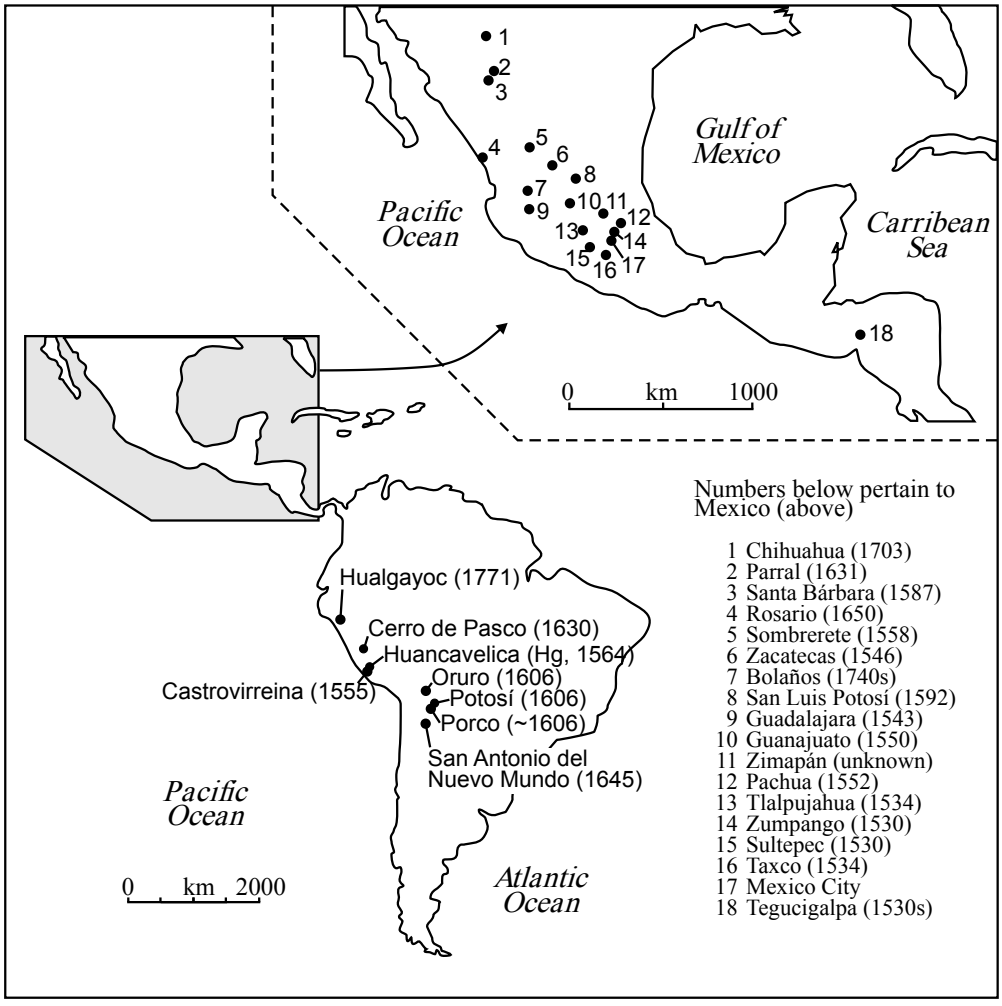


**Fig. 1.4.** Major silver mining centers in Colonial Latin America. Dates indiate the onset of significant Colonial silver mining activites. Study sites investigated as part of this dissertation are shown in red. The map is adapted from Nriagu, 1994.

from 3 weeks to 5 months. In the high-altitude silver mines of the Andes, the mixture was often heated in large stone tanks called *cajones*. (4) Once the reaction was deemed to be complete, the silver amalgam (the *pella*) was mechanically separated using large beaters. (5) Finally, more Hg was added to coagulate any extra Hg and to make the mixture more fluid. Excess Hg was then expelled from the *pella* by first squeezing it through canvas bags and then heating it in a retort to drive off the last remaining Hg.

This patio process of silver extraction remained unchallenged as the predominant method for silver and gold extraction for over 300 years, and is still used today in small-scale mining operations (Telmer and Veiga, 2009). The process was cheap, required only the simplest of tools, could be set up anywhere, and most importantly required little water and no firewood (Nriagu, 1994).

Losses of Hg occurred at many stages both prior to and during the amalgamation process. Significant points of Hg loss include: (1) during mining and retorting of cinnabar (HgS) which supplied the Hg to the silver mines; (2) during the transport of the Hg to the silver mines (the Hg was carried in leather bags which often broke), and; (3) at multiple stages during the amalgamation process itself. Due to its expense and important commercial role, losses of Hg were closely monitored. Using historical records of Hg production (from the cinnabar mines) and Hg consumption (from the silver mines), Nriagu (1994) estimated that between 1580 and 1900 AD Hg amalgamation resulted in the emission of 257,400 Mg (1283 Mmol) of Hg to the atmosphere. This amount is nearly identical to the approximately 260,100 Mg (1300 Mmol) of Hg emitted since 1900 AD by industrial anthropogenic activities. These estimates of Colonial and modern Hg emissions represent minimum and maximum values, respectively, because (1) the former assumes that all Hg mined was accounted for and that losses during amalgamation occurred at a rate comparable to modern Hg

amalgamation operations when in realty, losses were probably much greater over the Colonial era; and (2) the latter assumes that anthropogenic activities have been emitting ~13 Mmol per year to the atmosphere for the entire 20th century, when in fact, emissions during the first half of the 20th century were probably much lower than today. Thus, it seems clear that pre-industrial Hg emissions contained as much potential, if not more, to influence the global biogeochemical cycle of Hg. The difference between the Colonial and industrial era Hg emissions is that the former was spread out over a ~400 year period, while the latter has occurred in only the past ~100 years. Because of the high volatility of Hg, any deposited Hg can readily be re-emitted to the atmosphere. Thus, the continued recycling of this large mass of Colonial Hg emissions may have elevated background levels of mercury in the global environment.

**Pre-industrial Hg emissions and their legacy in natural archives**

Following the publication of Nriagu's (1993, 1994) hypothesis that ancient mining practices generated substantial Hg emissions, many studies attempted to exploit the geochemical record preserved in natural archives to ascertain if, and to what degree, pre-industrial Hg emissions impacted the pre-industrial Hg cycle. Indeed, a few peat bog cores (Givelet et al., 2003; Martínez-Cortizas et al., 1999; Roos-Barraclough et al., 2002, 2006; Roos-Barraclough and Shotyk, 2003) and a single ice core (Schuster et al., 2002) do suggest the presence of pre-industrial Hg pollution. In the peat cores, pre-industrial increases in Hg content have been attributed not only to ancient mining and metallurgy, but also to volcanism, and even biomass burning by Native Americans. However, there are no lake-sediment records of pre-industrial Hg pollution (Biester et al., 2007). This is despite the fact that many of the lake core sites are located very near to the peat core and ice core

collection sites.

The evidence for pre-industrial Hg enrichment in peat cores, and the lack of any evidence in lake sediment cores, has engendered considerable debate (e.g., Biester et al., 2007; Lamborg et al., 2002; Lindberg et al., 2007). Unlike Pb, for which clear increases in [Pb] are confirmed by changes in Pb stable isotopic ratios, recognizing pre-industrial Hg pollution in peat cores has not been straightforward, and has relied upon distinguishing between natural and anthropogenic Hg contributions from the peat geochemical record. Various methods have been suggested, including normalization to bromine (Br) and selenium (Se) (Givelet et al., 2003; Roos-Barraclough et al., 2002, 2006; Roos-Barraclough and Shotyk, 2003; Shotyk et al., 2005), and simple averaging and subtraction of background (natural) Hg concentrations (Martínez-Cortizas et al., 1999). However, Biester and colleagues (Biester et al., 2002, 2003, 2006, 2007; Martínez-Cortizas et al., 2007) have demonstrated that Hg retention in peat is strongly dependent on the degree of peat humification, which in turn depends on climate and the depth of the local water table (Ise et al., 2008; Martínez-Cortizas et al., 2007). Furthermore, many elements (including Br) display a linear or near-linear correlation with the degree of peat humification (Y. Hermanns and H. Biester, unpublished data). Thus, the reliability of peat as a faithful archive of pre-industrial Hg pollution seems questionable.

Ice cores may prove to be more reliable archives of pre-industrial Hg pollution than peat cores, but published ice core Hg profiles are limited to the Upper Fremont Glacier in Wyoming (Schuster et al., 2002) and a short firn core from Greenland spanning <70 years (Faïn et al., 2009). The Upper Fremont Glacier record does preserve a significant increase in Hg deposition during the 19$^{th}$ century, which the authors attributed to Hg use in gold and silver processing in the United States. However, we know little about the processes which govern

Hg retention in ice, especially over centennial (or longer) time scales, making firm conclusions from a single ice core difficult.

Despite the above-mentioned peat and ice core evidence for pre-industrial Hg emissions, previous investigations using lake sediment cores have revealed no evidence for any preindustrial Hg pollution (Heyvaert et al., 2000; Lamborg et al., 2002; Pirrone et al., 1998). The South American Andes had not been investigated systematically previously, despite the fact that they were the center of pre-industrial Hg use. My dissertation utilizes lake sediment records from the Peruvian and Bolivian Andes to test the hypothesis that intensive pre-industrial Hg use generated local- to regional-scale Hg pollution in the Andes. By establishing the existence or lack of pre-industrial Hg pollution in the Andes, we can then expand out to other regions to track the impact of these emissions at the extra-regional, hemispheric, and global scale.

**Lake sediment reconstructions of Hg deposition**

Unlike peat deposits, lake sediments are faithful recorders of past Hg accumulation. For example, using a unique collection of varved sediment cores collected annually since 1971, Rydberg et al. (2008) were able to track the burial and possible diagenetic alteration of Hg (as well as a wide range of other proxies including: %C, %N, and %S, and C and N isotopes). The authors demonstrated that even after 40 years of burial within the sediment there was negligible diagenetic alteration of the Hg geochemical record. Moreover, sediment Hg remained stable despite significant loss of both C (~30%) and N (~40%) over the same period (Gälman et al., 2008). A similar conclusion was reached by Lockhart et al. (2000) using well-dated sediment cores recovered from lakes in British Columbia with known histories of industrial mercury input. Collectively, these

studies have demonstrated that lake sediments reliably archive Hg with little diagenetic alteration.

There have been many lake-sediment studies aimed at quantifying the degree of industrial-era anthropogenic impact on the biogeochemical cycle of Hg. Swain et al. (1992) were among the first when they used sediment cores from seven lakes located in Minnesota and Wisconsin to show that Hg deposition to terrestrial environments had increased by a factor of ~four over the past ~100 years. Since then, many lake sediment cores have been collected and analyzed from across North America. Collectively, these cores suggest an approximately three-fold increase in the rate of Hg deposition since the industrial revolution (see Biester et al., 2007; Lucotte et al., 1995; Muir et al., 2009 and references therein).

Despite this relatively large body of research, most studies completed to date have focused on reconstructing the rate and magnitude of change in Hg deposition during the industrial era. These studies have relied upon short $^{210}$Pb-dated lake cores from the Northern Hemisphere. There is a paucity of multi-proxy studies aimed at investigating natural variability in the biogeochemical cycle of Hg, and only a handful of sites from the Southern Hemisphere. Moreover, there have been few rigorous attempts to investigate pre-industrial Hg pollution using well-dated lake cores. The research presented in this thesis has focused on addressing these key knowledge gaps, with the larger goal of improving our understanding of the pre-industrial Hg cycle.

**Progression of papers**

This dissertation represents an investigation into the biogeochemical cycle of Hg across disparate geographical regions (Fig. 1.4). The evolution of both natural and anthropogenic drivers of Hg cycling is explored at decadal to millennial

time-scales. Ultimately, the paleolimnological records presented here represent a concerted effort to identify and address key knowledge gaps in our understanding of the pre-industrial biogeochemical cycle of Hg.


**Fig. 1.4.** Location of the study lakes considered in this dissertation.

Chapters 2, 3, and 4 collectively make the case that pre-industrial anthropogenic activity released large quantities of Hg to the atmosphere. The paleolimnological study presented in Chapter 2, which is co-authored by Prentiss H. Balcom (University of Connecticut), Harald Biester (Technical University of Braunschweig), and Alexander P. Wolfe (University of Alberta), utilizes the geochemical stratigraphies from three lakes located near the world's second largest deposit of cinnabar: Huancavelica, Peru. The lake records demonstrate over three millennia of regional and extra-regional Hg pollution associated with the mining and processing of cinnabar at Huancavelica. Chapter 3, which is co-authored by William O. Hobbs (St. Croix Watershed Research Station, Science Museum of Minnesota) and Alexander P. Wolfe (University of Alberta), builds on these results by confirming the existence of Hg emissions directly resulting from Colonial Hg amalgamation. These results are the first to confirm the hypothesis,

first suggested by Nriagu in *Nature* over a decade ago (Nriagu, 1993), that Colonial amalgamation resulted in widespread Hg pollution. Chapter 4, which is co-authored by Prentiss H. Balcom (University of Connecticut), Charles Kerfoot (Michigan Technological University), Mark B. Abbott (University of Pittsburgh), and Alexander P. Wolfe (University of Alberta), makes the case that early smelting of non-ferrous ores constitute a hitherto now unrecognized but significant source of pre-industrial Hg emissions. Both Chapters 2 and 3 are previously published and are reprinted here with permission (Cooke et al., 2009a, 2009b). Chapter 4 has been submitted for publication to the scientific journal *Ambio: A journal of the human environment*.

Chapter 5 is a methodological study that uses four lake sediment cores (two from the Peruvian Andes and two from the east coast of Baffin Island, Canada) to show that the common practice of relying on $^{210}$Pb dating to construct geochronological models of lake sedimentation results in a systematic overestimation of pre-industrial Hg accumulation rates and an underestimation of the degree to which humans have impacted the global cycle of Hg. This Chapter is published in the journal *Environmental Science & Technology* and is co-authored by William O. Hobbs (St. Croix Watershed Research Station, Science Museum of Minnesota), Neal Michelutti (Queen's University), and Alexander P. Wolfe (University of Alberta).

Chapter 6 places 20$^{th}$ century Hg enrichment in a long-term perspective by utilizing two cores collected from the east coast of Baffin Island, Canada. These two records include the longest Hg record generated to date from the Northern Hemisphere, spanning three interglacials and one interstadial. Chapter 6 remains unpublished and is co-authored by Prentiss H. Balcom (University of Connecticut), Alexander P. Wolfe (University of Alberta), and Jason P. Briner (State University of New York at Buffalo). My role in each of these chapters

included designing and performing the research, analyzing and interpreting the data, and writing the papers.

**References**


Abbott, M. B. & Wolfe, A. P. (2003) Intensive pre-Incan metallurgy recorded by lake sediments from the Bolivian Andes. *Science,* 301, 1893-1895.

Biester, H., Bindler, R. & Martínez-Cortizas, A. (2006) Mercury in mires. IN Martini, I. P., Martinez-Cortizas, A. & Chesworth, W. (Eds.) *Peatlands: Evolution and Records of Environmental and Climate Changes.* Elsevier.

Biester, H., Bindler, R., Martínez-Cortizas, A. & Engstrom, D. R. (2007) Modeling the past atmospheric deposition of mercury using natural archives. *Environmental Science & Technology,* 41, 4851-4860.

Biester, H., Kilian, R., Franzen, C., Woda, C., Mangini, A., et al. (2002) Elevated mercury accumulation in a peat bog of the Magellanic Moorlands, Chile (53°S) - an anthropogenic signal from the Southern Hemisphere. *Earth and Planetary Science Letters,* 201, 609-620.

Biester, H., Martínez-Cortizas, A., Birkenstock, S. & Kilian, R. (2003) Effect of peat decomposition and mass loss on historic mercury records in peat bogs from Patagonia. *Environmental Science & Technology,* 37, 32-39.

Bindler, R., Renberg, I. & Klaminder, J. (2008) Bridging the gap between ancient metal pollution and contemporary biogeochemistry. *Journal of Paleolimnology,* 40, 755-770.

Camargo, J. A. (1993) Which source of mercury pollution? *Nature,* 365, 302-302.

Camargo, J. A. (2002) Contribution of Spanish-American silver mines (1570-1820) to the present high mercury concentrations in the global environment: a review. *Chemosphere,* 48, 51-57.

Cooke, C. A., Abbott, M. B. & Wolfe, A. P. (2008) Late-Holocene atmospheric lead deposition in the Peruvian and Bolivian Andes. *The Holocene,* 18, 353-359.

Cooke, C. A., Abbott, M. B., Wolfe, A. P. & Kittleson, J. L. (2007) A millennium of metallurgy recorded by lake sediments from Morococha, Peruvian Andes. *Environmental Science & Technology,* 41, 3469-3474.

Cooke, C. A., Balcom, P. H., Biester, H. & Wolfe, A. P. (2009a) Over three millennia of mercury pollution in the Peruvian Andes. *Proceedings of the National Academy of Sciences,* 106, 8830-8834.

Cooke, C. A., Wolfe, A. P. & Hobbs, W. O. (2009b) Lake-sediment geochemistry reveals 1400 years of evolving extractive metallurgy at Cerro de Pasco, Peruvian Andes. *Geology,* 37, 1019-1022.

Ericson, J. E., Shirahata, H. & Patterson, C. C. (1979) Skeletal concentrations of lead in ancient Peruvians. *New England Journal of Medicine,* 300, 946-951.

Faïn, X., Ferrari, C. P., Dommergue, A., Albert, M. R., Battle, M., et al. (2009) Polar firn air reveals large-scale impact of anthropogenic mercury emissions during the 1970s. *Proceedings of the National Academy of Sciences,* 106, 16114-16119.

Fitzgerald, W. F. & Lamborg, C. H. (2005) Geochemistry of mercury in the environment. IN Sherwood Lollar, B. (Ed.) *Treatise on Geochemistry*. New York, Springer.

Gälman, V., Rydberg, J., de-Luna, S. S., Bindler, R. & Renberg, I. (2008) Carbon and nitrogen loss rates during aging of lake sediment: Changes over 27 years studied in varved lake sediment. *Limnology & Oceanography,* 53, 1076-1082.

Givelet, N., Roos-Barraclough, F. & Shotyk, W. (2003) Predominant anthropogenic sources and rates of atmospheric mercury accumulation in southern Ontario recorded by peat cores from three bogs: comparison with natural background values (past 8000 years). *Journal of Environmental*

*Monitoring,* 5, 935-949.

Heyvaert, A. C., Reuter, J. E., Slotton, D. G. & Goldman, C. R. (2000) Paleolimnological reconstruction of historical atmospheric lead and mercury deposition at Lake Tahoe, California-Nevada. *Environmental Science & Technology,* 34, 3588-3597.

Hong, S., Boutron, C. F., Edwards, R. & Morgan, V. I. (1998) Heavy metals in antarctic ice from Law Dome: initial results. *Environmental Research,* 78, 94-103.

Hong, S., Candelone, J.-P., Patterson, C. C. & Boutron, C. F. (1994) Greenland ice evidence of hemispheric lead pollution two millennia ago by Greek and Roman Civilizations. *Science,* 265, 1841-1843.

Hylander, L. D. & Meili, M. (2003) 500 years of mercury production: global annual inventory by region until 2000 and associated emissions. *The Science of the Total Environment,* 304, 13-27.

Ise, T., Dunn, A. L., Wofsy, S. C. & Moorcroft, P. R. (2008) High sensitivity of peat decomposition to climate change through water-table feedback. *Nature Geoscience,* 1, 763-766.

Kessler, S. E. (1994) *Mineral Resources, Economics and the Environment,* New York, Maxwell Macmillan International.

Lamborg, C. H., Fitzgerald, W. F., Damman, A. W. H., Benoit, J. M., Balcom, P. H., et al. (2002) Modern and historic atmospheric mercury fluxes in both hemispheres: global and regional mercury cycling implications. *Global Biogeochemical Cycles,* 16, 1104.

Lindberg, S., Bullock, R., Ebinghaus, R., Engstrom, D., Feng, X., et al. (2007) A synthesis of progress and uncertainties in attributing the sources of mercury in deposition. *Ambio: A Journal of the Human Environment,* 36, 19-33.

Lockhart, W. L., Macdonald, R. W., Outridge, P. M., Wilkinson, P., DeLaronde, J. B., et al. (2000) Tests of the fidelity of lake sediment core records of mercury deposition to known histories of mercury contamination. *The Science of the Total Environment,* 260, 171-180.

Lucotte, M., Mucci, A., Hillaire-Marcel, C., Pichet, P. & Grondin, A. (1995) Anthropogenic mercury enirichment in remote lakes of northern Québec (Canada). *Water, Air and Soil Pollution,* 80, 467-476.

Martínez-Cortizas, A., Biester, H., Mighall, T. & Bindler, R. (2007) Climate-driven enrichment of pollutants in peatlands. *Biogeosciences,* 4, 905-911.

Martínez-Cortizas, A., Pontevedra-Pombal, X., García-Rodeja, E., Nóvoa-Muñoz, J. C. & Shotyk, W. (1999) Mercury in a Spanish peat bog: Archive of climate change and atmospheric metal deposition. *Science,* 284, 939-942.

Mason, R. P. & Sheu, G. R. (2002) Role of the ocean in the global mercury cycle. *Global Biogeochemical Cycles,* 16, 1093.

Muir, D. C. G., Wang, X., Yang, F., Nguyen, N., Jackson, T. A., et al. (2009) Spatial trends and historical deposition of mercury in eastern and northern Canada inferred from lake sediment cores. *Environmental Science & Technology,* 43, 4802-4809.

Murozumi, M., Chow, T. J. & Patterson, C. (1969) Chemical concentrations of pollutant lead aerosols, terrestrial dusts and sea salts in Greenland and Antarctic snow strata. *Geochimica et Cosmochimica Acta,* 33, 1247-1294.

Nriagu, J. O. (1979) *Biogeochemistry of Mercury in the Environment,* New York, Elsevier/North-Holland Biomedical Press.

Nriagu, J. O. (1988) A silent epidemic of environmental metal poisoning? *Environmental Pollution,* 50, 139-161.

Nriagu, J. O. (1993) Legacy of mercury pollution. *Nature,* 363, 589.

Nriagu, J. O. (1994) Mercury pollution from the past mining of gold and silver in

the Americas. *The Science of the Total Environment,* 149, 167-181.

Pacyna, J. M. & Pacyna, E. G. (2001) An assessment of global and regional emissions of trace metals to the atmosphere from anthropogenic sources worldwide. *Environmental Reviews,* 9, 269-298.

Patterson, C. C. (1965) Contaminated and natural lead environments of man. *Archives of environmental health,* 11, 344-360.

Pirrone, N., Allegrini, I., Keeler, G. J., Nriagu, J. O., Rossmann, R., et al. (1998) Historical atmospheric mercury emissions and depositions in North America compared to mercury accumulations in sedimentary records. *Atmospheric Environment,* 32, 929-940.

Pirrone, N., Cinnirella, S., Feng, X., Finkelman, R. B., Friedli, H. R., et al. (2009) Global mercury emissions to the atmosphere from natural and anthropogenic sources IN Pirrone, N. & Mason, R. (Eds.) *Mercury Fate and Transport in the Global Atmosphere.* Springer.

Renberg, I., Bigler, C., Bindler, R., Norberg, M., Rydberg, J., et al. (2009) Environmental history: A piece in the puzzle for establishing plans for environmental management. *Journal of Environmental Management,* 90, 2794-2800.

Renberg, I., Brännvall, M. L., Bindler, R. & Emteryd, O. (2002) Stable lead isotopes and lake sediments—a useful combination for the study of atmospheric lead pollution history. *The Science of the Total Environment,* 292, 45-54.

Renberg, I., Persson, M. W. & Emteryd, O. (1994) Pre-industrial atmospheric lead contamination detected in Swedish lake sediments. *Nature,* 368, 323-326.

Roos-Barraclough, F., Givelet, N., Cheburkin, A. K., Shotyk, W. & Norton, S. A. (2006) Use of Br and Se in peat to reconstruct the natural and anthropogenic fluxes of atmospheric Hg: a 10000-year record from

Caribou Bog, Maine. *Environmental Science & Technology,* 40, 3188-3194.

Roos-Barraclough, F., Martínez-Cortizas, A., Garcia-Rodeja, E. & Shotyk, W. (2002) A 14500 year record of the accumulation of atmospheric mercury in peat: volcanic signals, anthropogenic influences and a correlation to bromine accumulation. *Earth and Planetary Science Letters,* 202, 435-451.

Roos-Barraclough, F. & Shotyk, W. (2003) Millennial-scale records of atmospheric mercury deposition obtained from ombrotrophic and minerotrophic peatlands in the Swiss Jura Mountains. *Environmental Science & Technology,* 37, 235-244.

Rosman, K. J. R., Chisholm, W., Hong, S., Candelone, J.-P. & Boutron, C. F. (1997) Lead from Carthaginian and Roman Spanish mines isotopically identified in Greenland ice dated from 600 B.C. to 300 A.D. *Environmental Science & Technology,* 31, 3413-3416.

Rydberg, J., Gälman, V., Renberg, I., Bindler, R., Lambertsson, L., et al. (2008) Assessing the stability of mercury and methylmercury in a varved lake sediment deposit. *Environmental Science & Technology,* 42, 4391-4396.

Schroeder, W. H. & Munthe, J. (1998) Atmospheric mercury-an overview. *Atmospheric Environment,* 32, 809-822.

Schuster, P. F., Krabbenhoft, D. P., Naftz, D. L., Cecil, L. D., Olson, M. L., et al. (2002) Atmospheric mercury deposition during the last 270 years: a glacial ice core record of natural and anthropogenic sources. *Environmental Science & Technology,* 36, 2303-2310.

Shotyk, W., Goodsite, M. E., Roos-Barraclough, F., Givelet, N., Le Roux, G., et al. (2005) Accumulation rates and predominant atmospheric sources of natural and anthropogenic Hg and Pb on the Faroe Islands. *Geochimica et*

*Cosmochimica Acta,* 69, 1-17.

Slemr, F., Brunke, E.-G., Ebinghaus, R., Temme, C., Munthe, J., et al. (2003) Worldwide trend of atmospheric mercury since 1977. *Geophysical Research Letters,* 30, 1516.

Smol, J. P. (2008) *Pollution of Lakes and Rivers: A Paleoenvironmental Perspective,* Oxford, Blackwell Publishing.

Smol, J. P. (2010) The power of the past: using sediments to track the effects of multiple stressors on lake ecosystems. *Freshwater Biology,* 55, 43-59.

Strode, S., Jaeglé, L. & Selin, N. E. (2009) Impact of mercury emissions from historic gold and silver mining: global modeli ng. *Atmospheric Environment,* 43, 2012-2017.

Swain, E. B., Engstrom, D. R., Brigham, M. E., Henning, T. A. & Brezonik, P. L. (1992) Increasing rates of atmospheric mercury deposition in midcontinental North America. *Science,* 257, 784-787.

Telmer, K. & Veiga, M. M. (2009) World emissions of mercury from artisanal and small scale gold mining. IN Pirrone, N. & Mason, R. (Eds.) *Mercury Fate and Transport in the Global Atmosphere.* New York, Springer.

# CHAPTER 2: OVER THREE MILLENNIA OF MERCURY POLLUTION IN THE PERUVIAN ANDES

## Introduction

Cinnabar (HgS) is the primary mineralogical source of mercury (Hg), and forms a bright red pigment (vermillion) when powdered. In the Andes, the use of vermillion is closely tied to that of precious metals, and vermillion has been recovered in burials of the elite from the first (Chavín) to the last (Inca) Andean empires, where it was used as either a body paint or a covering on ceremonial gold objects (Burger, 1992). During the Colonial era (1532-1900 AD), large-scale Hg mining began in earnest with the invention of Hg amalgamation in 1554 AD (Nriagu, 1994). For the next 350 years, Hg amalgamation became the dominant silver processing technique because it allowed for the extraction of silver from low-grade ores. Nriagu (1993, 1994) estimated Colonial Hg emissions totalled 196,000 tons, averaging ~600 tons $yr^{-1}$; roughly equivalent to current emissions from China (Wu et al., 2006). Estimates of Colonial Hg emissions represent minimum values for the region because they only incorporate state-registered Hg used during amalgamation. Hg emissions associated with early Hg mining therefore remain entirely unknown. Huancavelica, in the central Peruvian Andes, served as the single largest supplier of Hg to New World Colonial silver mines, and thus represents a potentially major source of pre-industrial Hg pollution.

---

* Previously published material: Cooke C. A., Balcom, P. H., Biester, H., & Wolfe, A. P. (2009) Over three millennia of mercury pollution in the Peruvian Andes. *Proceedings of the National Academy of Sciences*, **106**, 8830-8834.

## Materials and Methods

*Study region*

Huancavelica is on the eastern slope of the Cordillera Occidental in central Peru (Fig. 2.1). Hg deposits are related to high-grade Cenozoic magmatism intruding Mesozoic and Cenozoic sedimentary rocks. Cinnabar is the dominant mercuric ore, and over 90% of historically documented cinnabar production has been from the Santa Bárbara mine, immediately south of Huancavelica (Wise and Féraud, 2005). Frequent cave-ins and extensive Hg poisoning throughout Huancavelica's 450-year Colonial history have made it one of the most sinister examples of human exploitation and disastrous mining environments ever documented, earning it the nickname *mina de la muerte* (mine of death) (Brown, 2001; Wise and Féraud, 2005).

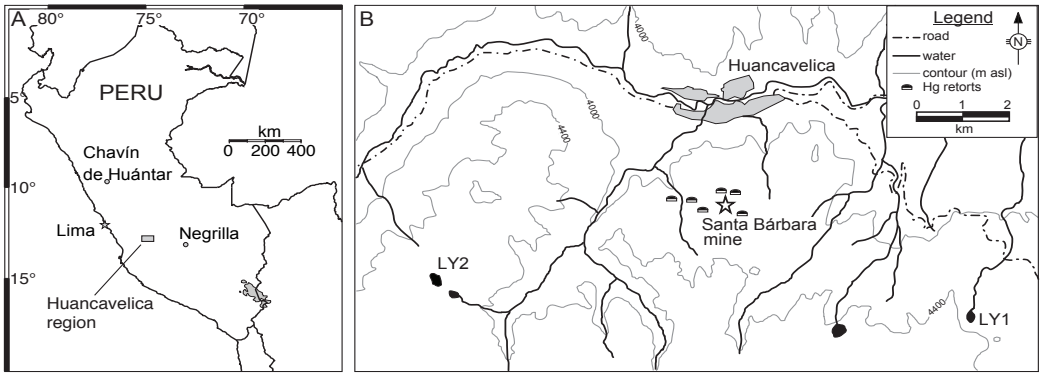


**Fig. 2.1.** Map of the study region. (A) Map of Peru with study region and location of Negrilla. (B) detailed map of Huancavelica region with locations of Santa Bárbara mine, the two study lakes (LY1 and LY2), and remains of Colonial Hg retorts.

We recovered lake-sediment cores from three lakes to reconstruct the history of mining at Huancavelica. Two of the study lakes presented here are named Laguna Yanacocha (hereafter LY1 and LY2; Fig. 2.1). LY1 is 10 km southeast of Huancavelica, while LY2 is approximately 6 km southwest and is

directly up-valley from Huancavelica and the Santa Bárbara mine. Both lakes are small (LY1: 0.03 $km^2$; LY2: 0.05 $km^2$) and relatively deep (maximum depths for LY1: 14 m; LY2: 11 m) headwater tarns that occupy undisturbed catchments of 0.71 $km^2$ and 0.31 $km^2$, respectively. Laguna Negrilla (hereafter Negrilla) is ~225 km east of Huancavelica in the Cordillera Vilcabamba (Fig. 2.1a). There are no major Hg deposits or mining centres in this latter region. Negrilla is a small (0.06 $km^2$), deep (33 m) headwater lake that occupies an undisturbed catchment of 0.32 $km^2$. Lakes with undisturbed catchments were deliberately targeted to minimize confounding impacts associated with catchment disturbance, and to maximize sensitivity to atmospheric deposition of Hg.

Sediment cores were recovered from the deepest part of each lake using a percussion corer fitted with a 7-cm-diameter polycarbonate tube. Cores were extruded into continuous 0.5-cm intervals in the field. At all three lakes, sediment excess $^{210}Pb$ activities decline in near-monotonic fashion (Table A.1). To constrain ages beyond the limit of $^{210}Pb$, Accelerator Mass Spectrometry (AMS) $^{14}C$ measurements of discrete carbonized grass macrofossils were obtained on five samples from LY1, three samples from LY2, and three samples from Negrilla (Fig. 2.2 and Table A.2). AMS $^{14}C$ ages were calibrated using SHCal04 (McCormac et al., 2004) within Calib 5.0 (Stuiver and Reimer, 1993). Concentrations of total Hg were determined on a DMA80 direct mercury analyzer. Measurements of sediment-Hg speciation were done by solid-phase Hg thermo-desorption (Biester and Scholz, 1997), which produces temperature-dependent Hg release curves enabling identification of species such as $Hg^0$, matrix-bound Hg, and inorganic HgS by comparison to reference materials (Fig. A.1).

## Results and Discussion

*Sediment Geochemistry*

Blank values, average relative standard deviations, and recoveries of standard reference materials [NRCC PACS-2 (marine sediment, certified value 3040±200 ng $g^{-1}$) and MESS-3 (marine sediment, certified value 91±9 ng $g^{-1}$)] associated with DMA80 measurements of Hg are presented in Table A.3. Solid-phase Hg thermo-desorption (SPTD) is an indirect method in which Hg species are determined by thermal desorption or decomposition temperatures (Biester and Scholz, 1997). The method has a detection limit of 0.4 μg $g^{-1}$ Hg, and a maximum sample size of ~ 200 mg. In SPTD analysis, the sample is placed in a quartz furnace and heated at a rate of 0.5 °C $s^{-1}$. Volatilized Hg compounds are carried from the furnace with $N_2$ 200 ml $min^{-1}$, and reduced to $Hg^0$ by thermal reduction in a quartz tube heated to 800 °C before being analyzed by flameless AAS. This method produces temperature-dependent Hg release curves that are species- and matrix-specific. These release curves enable identification of species such as $Hg^0$, matrix-bound Hg, and inorganic cinnabar (HgS) by comparison to pure Hg phases and reference materials (Fig. A.1). Quantification of Hg species was made by peak integration (Biester et al., 2000). Samples volumes used were between 20 and 200 mg dry sediment depending on sediment-Hg concentrations. Relative standard deviation on replicate measurements of Hg binding forms in sediments (matrix-bound non-cinnabar Hg compounds and cinnabar) of each sample ($n$=3-4) ranged 2.8% to 15.4% (mean 8.0%). Total organic matter was determined by loss-on-ignition (Heiri et al., 2001). Sediment chlorophyll *a* was inferred using visible-near infrared reflectance (VNIR) spectroscopy (Wolfe et al., 2006).

Despite different sedimentation rates (Fig. 2.2), the LY1 and LY2 geochemical profiles are highly concordant (Fig. 2.3) when plotted on their

respective age-depth models. For about one millennium prior to ~1600 BC, Hg accumulation within LY2 sediment is stable and low, averaging 6±1 μg $m^{-2}$ $yr^{-1}$. This represents the natural, background accumulation of non-pollution Hg within LY2 sediment. The Hg profile of the Negrilla core is somewhat different; however, background Hg accumulation rates are of similar magnitude (7±2 μg $m^{-2}$ $yr^{-1}$) for much of this lake's early record. Background Hg levels do not appear to have been reached at LY1, though Hg accumulation rates of 6 μg $m^{-2}$ $yr^{-1}$ are noted in the lowest-most intervals (Fig. 2.3). Thus, we conclude that the accumulation of natural, non-pollution Hg in these lakes is 6-7 μg $m^{-2}$ $yr^{-1}$. While this range is consistent with nearly all other lake-sediment reconstructions of pre-anthropogenic Hg deposition from around the globe (Biester et al., 2007), mechanisms such as catchment export and sediment focusing ultimately serve to confound reconstructions of Hg deposition to varying degrees (Engstrom et al., 2007). Therefore, to enhance comparability between these, and other lake-core records, sample to

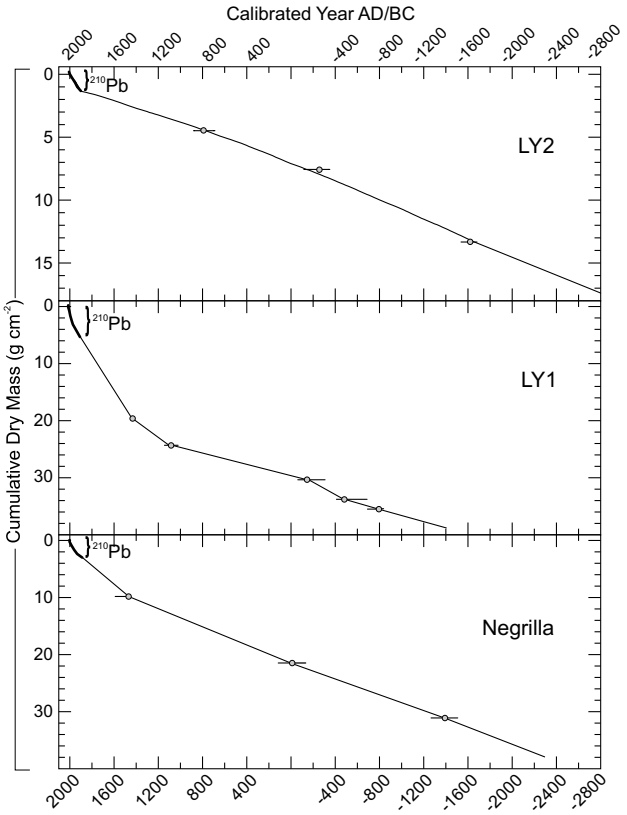


**Fig. 2.2.** Age models for the three lake-sediment cores. Age models for LY1 and Negrilla are based on linear interpolation between $^{210}$Pb dates and median ages of calibrated $^{14}$C dates, while a best-fit line was used between dates at LY2. AMS $^{14}$C ages were measured on terrestrial charcoal and calibrated age ranges are 2 σ.

background flux ratios were calculated for each lake (Fig. 2.3).

At both LY1 and LY2, dramatic increases in Hg accumulation rates are initiated ~1400 BC, and by 600 BC both lakes exceed background by ~10-fold (Fig. 2.3). The accumulation of Hg subsequently decreases in both lakes until

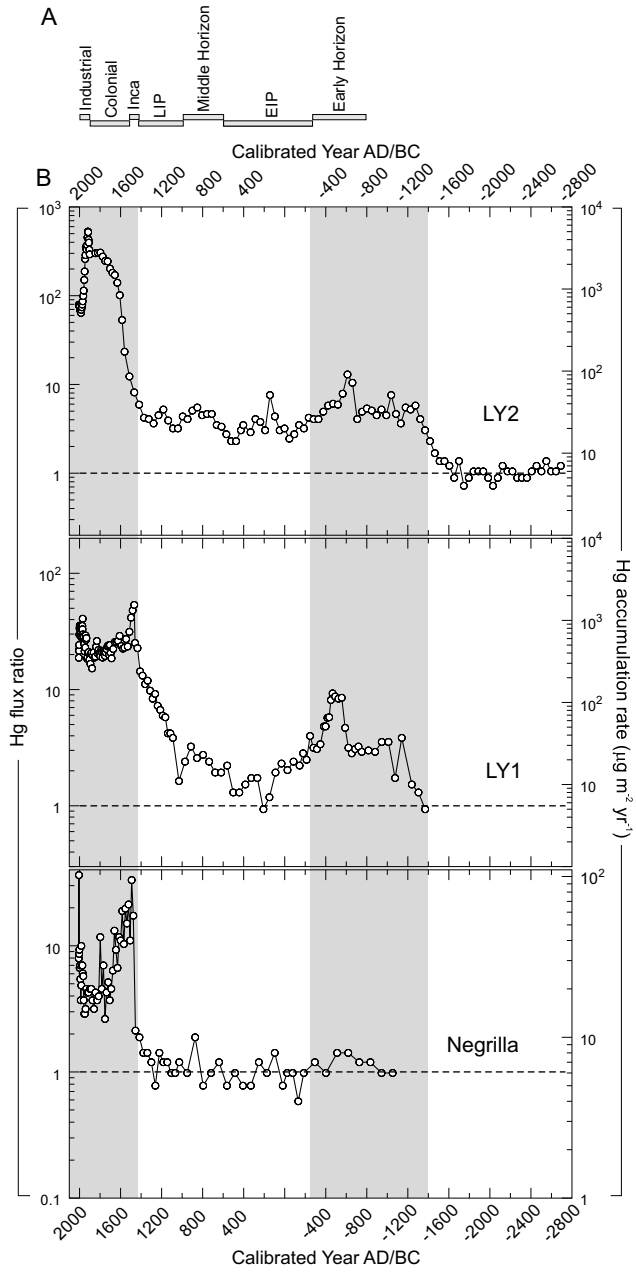


**Fig. 2.3.** Lake-sediment profiles of Hg deposition and Andean archaeology. (A) Compilation of central Andean archaeology (EIP: Early Intermediate Period and LIP: Late Intermediate Period), and (B) profiles of Hg accumulation rates and flux ratios for lakes LY2, LY1, and Negrilla. Two intervals of marked Hg enrichment are shaded. Pre-Colonial Hg deposition peaks during the height of the Chavín culture, while the later rise occurs under Inca and subsequent Colonial control. This second period of extensive mining activity witnessed the long-range transport of Hg emissions, as shown by the onset of Hg deposition to Negrilla, ~250 km east of Huancavelica.

~1200 AD at LY1 and ~1450 AD at LY2, before increasing once again. By the mid-16$^{th}$ century, sediment Hg accumulation rates at LY1 and LY2 are enriched by factors of ~55 and ~70 relative to background, respectively (Fig. 2.3). Only the latter increase in Hg deposition is preserved at Negrilla, where Hg accumulation rates rise dramatically ~1400 AD to over ~30 times background. After 1600 AD, the Hg records for all three lakes are all characterized by Hg accumulation rates and flux ratios well above background (Fig. 2.3).

The earliest (~1400 BC) rise in Hg at LY1 and LY2 is characterized by a 3- to 5-fold increase in Hg accumulation (Fig. 2.3), and occurs during a period of stable sedimentation with respect to both organic and inorganic sediment fractions (Figs. A.2 and A.3). Consequently, these increases cannot be explained by a rapid influx of catchment material or enhanced Hg scavenging by organic matter. Moreover, lake sediment burdens of total Hg are largely unaffected by diagenetic processes (Lockhart et al., 2000; Rydberg et al., 2008), and represent minimum estimates of total Hg deposited to a lake surface because of reductive losses prior to final burial (Southworth et al., 2007). Because we know of no natural mechanism capable of replicating such large and synchronized increases in Hg deposition in two adjacent lakes, and given their proximity to a major cinnabar deposit, we attribute with confidence the early increases of Hg observed at LY1 and LY2 to the emergence of regional-scale cinnabar mining at Huancavelica.

Less than 20 km from Huancavelica, the archaeological site of Atalla is the earliest example of large-scale ceremonial architecture in the central Andes. While Atalla lacks direct dating and excavation, surface remains suggest the site served as a regional centre for procuring and distributing cinnabar (Burger and Matos, 2002). Ceramics suggest Atalla dates to the Early Horizon (~800-300 BC), and was actively engaged in trade with Chavín de Huántar in the Cordillera Blanca (Burger and Matos, 2002) (Fig. 2.1). Chavín influenced much of the Peruvian

Andes at its apogee, and represents the cradle of complex Andean culture (Burger, 2008; Rick, 2004). High-status burials at Chavín de Huántar, as well as other Early Horizon sites, commonly contain prestigious materials including gold adorned with vermillion (Burger, 2008; Onuki and Kato, 1993). However, cinnabar mining at Huancavelica precedes even the earliest radiocarbon dates for Chavín (Burger, 1992), and therefore must predate the rise and expansion of Chavín culture.

The rate of Hg accumulation at both LY1 and LY2 declined during the subsequent Early Intermediate Period (~200 BC to 500 AD; Fig. 2.3). At LY1, Hg flux ratios briefly return to background ~200 AD; however, no parallel return to background is evident at LY2. This discrepancy likely indicates that watershed-scale Hg retention times vary between the two lakes. The steady export of legacy Hg from the catchment of LY2 may be therefore partially responsible for the maintenance of elevated Hg accumulation during this period. In any case, cinnabar mining does appear to have continued during the Early Intermediate Period, though at reduced intensity. While the collapse of Chavín likely curtailed the demand for exotic goods including cinnabar, highly stratified cultures from the north coast of Peru, such as the Moche (~100-700 AD) and Sicán (~700-1200 AD), may have sustained some level of imperial demand for cinnabar. Burials of Moche and Sicán nobles are some of the richest yet excavated in Peru, and vermillion is ubiquitous (Shimada et al., 2004). Huancavelica is the likely source, given the scarcity of other cinnabar deposits in the Andes (Petersen, 1989).

By 800 AD, a brief renewal in cinnabar mining is indicated as Hg flux ratios increase to 3.5 and 5.5 at LY1 and LY2, respectively (Fig. 2.3). This increase occurs during the Middle Horizon (~500 to 1000 AD), and is followed by larger increases in Hg deposition at LY1 during the Late Intermediate Period (~1000 to 1400 AD). The Middle Horizon and the Late Intermediate Period

witnessed the rapid development and expansion of mining and metallurgy in the Andes (Cooke et al., 2008; Shimada et al., 1982). During the Late Intermediate Period, the archaeological site of Attalla appears to have been reoccupied (Burger and Matos, 2002), suggesting continuation, if not intensification, of local cinnabar processing. Inca expansion into the central Andes occurred ~1450 AD, and cinnabar production appears to have increased dramatically under Inca control. Hg accumulation at LY1 increases rapidly, (>55-fold), and is matched by the first increase in Hg at Negrilla, which exceeds background by ~30-fold (Fig. 2.3). The appearance of Hg pollution at Negrilla indicates Inca exploitation of the Huancavelica cinnabar deposits exceeded all previous cultures, producing a broadly dispersed legacy of Hg pollution captured by all three study lakes.

Inca mining continued until 1564 AD when the Spanish crown assumed control, at which time the Santa Bárbara mine was established. In contrast to cinnabar extraction for vermillion, Spanish efforts concentrated on supplying elemental Hg ($Hg^0$) to Colonial silver mines for use in Hg amalgamation. Hg amalgamation was invented in 1554 AD by Bartolomé de Medina in Mexico, and is considered one of the most remarkable technological advances of Ibero-America (Nriagu, 1994). Cinnabar ores from Huancavelica were smelted in grass-fired, clay-lined retorts (*hornos*; Fig. 2.1), until vaporization yielded gaseous $Hg^0$, a portion of which was trapped in a crude condenser and cooled, yielding liquid $Hg^0$. Emissions of Hg thus occurred both during mining, as cinnabar dust, but also during cinnabar smelting, as gaseous $Hg^0$. Historical records of Hg production at Huancavelica indicate declining Hg output while under Colonial control, and into the 20$^{th}$ Century (Wise and Féraud, 2005). At LY1 and Negrilla, Hg accumulation decreases through the Colonial period, while increasing at LY2 (Fig. 2.3). The apparent discordance between the Hg profiles appears to support the suggestion that the watershed of LY2 continued to export legacy Hg to the

lake during periods of declining atmospheric deposition, a mechanism which has also been observed in modern lake systems (Harris et al., 2007). The mine was permanently closed in 1975 AD, and currently the only mining of Hg at Huancavelica is artisanal. In response, Hg flux ratios at Negrilla have declined, and are currently ~4.6 times background in the uppermost sediments (Fig. 2.3). This level of relative Hg enrichment is in agreement with the vast majority of sediment-core studies from remote lakes, which collectively suggest an average increase in global Hg deposition rates of 3-5x background values (Biester et al., 2007). In contrast, Hg flux ratios at both LY1 and LY2 in 1975 AD were 105 times background. While modern flux ratios at LY1 have declined by ~60% (to 42 times background), no such decline is recorded at LY2. The elevated Hg accumulation rates still present at these lakes likely reflect the legacy of over 3,500 years of regional Hg pollution residing within their catchments.

The mercuric species emitted during Colonial and pre-Colonial mining activities have direct implications for the size of the impacted airshed. Atmospheric $Hg^0$ has long atmospheric residence times (~0.5-1.5 years), and is the most important Hg species at the global scale (Lindberg et al., 2007). In contrast, oxidized reactive species of mercury can be rapidly scavenged from the atmosphere, while coarse particulate forms (including cinnabar dust) predominate in direct proximity to Hg point-sources (Fitzgerald and Lamborg, 2005). Measurements of Hg speciation within LY2 sediments confirm that major changes in Hg extractive technology occurred at Huancavelica (Fig. A.1). Solid-phase thermal desorption reveals two predominant Hg phases: cinnabar and non-cinnabar (i.e. matrix-bound), which are variably expressed down-core (Fig. 2.4). During the pre-Inca era, cinnabar was the dominant Hg species in all sediment samples, averaging 78% of the total sediment Hg inventory. While not precluding the emission of other species of Hg, these results suggests that pre-Inca Hg

pollution, while important locally, exerted little influence beyond the range of particulate dust transport, a conclusion supported by the apparent lack of any pre-Inca Hg pollution at Negrilla. A progressive decline in the cinnabar fraction is noted in sediments that post-date ~1450 AD, and the majority of sediment Hg burdens remain matrix-bound through the remainder of the LY2 sediment record. This is despite absolute increases in the concentration of total Hg (Fig. A.3) and of the fraction that is cinnabar (Fig. 2.4). The onset of long-range transport of Hg during the Inca hegemony suggests a shift in Hg extractive technology and associated Hg emissions. Indeed, to transport Hg the ~225 km to Negrilla, at least some emissions must have been in the form of gaseous $Hg^0$ (or possibly reactive $Hg^{2+}$). In contrast to coarse particulate cinnabar dust, gaseous atmospheric Hg species can be broadcast atmospherically over far greater distances, can undergo atmospheric oxidation/reduction cycling, and $Hg^{2+}$ can be methylated once delivered to aquatic systems.

A growing number of cores from remote lakes suggest an approximately three-fold increase in Hg deposition over the last ~100-150 years (Biester et al., 2007; Lindberg et al., 2007). These records are predominantly from the northern hemisphere, and do not reveal any significant pre-industrial Hg enrichment. In contrast, our results suggest that considerable pre-industrial Hg pollution occurred in the Andes. The onset of cinnabar mining at Huancavelica ~1400 BC places our lake-sediment records among the earliest evidence for mining and metallurgy in the Andes, of comparable antiquity to the oldest known hammered and annealed objects from well-dated contexts (Aldenderfer et al., 2008). Prior to Inca control of the mine, Hg emissions appear to have been restricted to the environment surrounding Huancavelica. Over the past ~550 years however, emissions of Hg have been transported long distances.

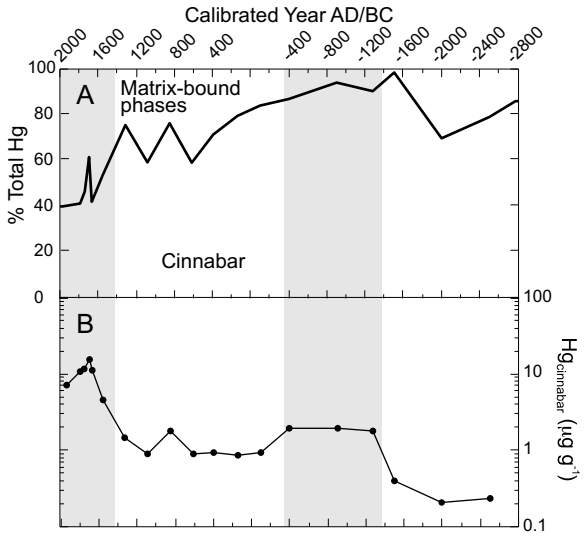


**Fig. 2.4.** Measurements of Hg speciation within LY2 sediment. (A) Plot of relative percent cinnabar and matrix-bound phases of Hg, and (B) concentration of Hg as cinnabar down-core. Prior to anthropogenic enrichment a combination of cinnabar dust and matrix-bound Hg make up the sediment Hg record. During the height of Chavín mining (~400-800 BC), cinnabar dust was the vast majority of sediment Hg. Following Inca control of the mine (~1450 AD), matrix-bound phases of Hg predominate, despite a synchronous rise in the concentration of Hg as cinnabar. This relationship suggests a shift in the phase of Hg emitted, from cinnabar dust to $Hg^0$ (or possibly $Hg^{2+}$). Both would subsequently be available for oxidation/reduction cycling within the atmosphere, sorption by organic matter, methylation, and subsequent bioaccumulation within aquatic food-webs.

**References**


Aldenderfer, M., Craig, N. M., Speakman, R. J. & Popelka-Filcoff, R. (2008) Four-thousand-year-old gold artifacts from the Lake Titicaca basin, Southern Peru. *Proceedings of the National Academy of Sciences,* 105**,** 5002-5005.

Biester, H., Bindler, R., Martínez-Cortizas, A. & Engstrom, D. R. (2007) Modeling the past atmospheric deposition of mercury using natural archives. *Environmental Science & Technology,* 41**,** 4851-4860.

Biester, H., Gosar, M. & Covelli, S. (2000) Mercury speciation in sediments affected by dumped mining residues in the drainage area of the Idrija mercury mine, Slovenia. *Environmental Science & Technology,* 34**,** 3330-3336.

Biester, H. & Scholz, C. (1997) Determination of mercury binding forms in contaminated soils: mercury pyrolysis versus sequential extractions. *Environmental Science & Technology,* 31**,** 233-239.

Brown, K. W. (2001) Workers' health and Colonial mercury mining at Huancavelica, Peru. *The Americas,* 57**,** 467-496.

Burger, R. L. (1992) *Chavín and the origins of Andean civilization,* London, Thames and Hudson.

Burger, R. L. (2008) Chavín de Huántar and its sphere of influence. IN Silverman, H. & Isbell, W. (Eds.) *Handbook of South American Archaeology.* New York, Springer.

Burger, R. L. & Matos, R. (2002) Atalla: a center on the periphery of the Chavín horizon. *Latin American Antiquity,* 13**,** 153-177.

Cooke, C. A., Abbott, M. B. & Wolfe, A. P. (2008) Late-Holocene atmospheric lead deposition in the Peruvian and Bolivian Andes. *The Holocene,* 18**,**

353-359.

Engstrom, D. R., Balogh, S. J. & Swain, E. B. (2007) History of mercury inputs to Minnesota lakes: influences of watershed disturbance and localized atmospheric deposition. *Limnology & Oceanography,* 52**,** 2467.

Fitzgerald, W. F. & Lamborg, C. H. (2005) Geochemistry of mercury in the environment. *Treatise on Geochemistry,* 9**,** 107–148.

Harris, R. C., Rudd, J. W. M., Amyot, M., Babiarz, C. L., Beaty, K. G., et al. (2007) Whole-ecosystem study shows rapid fish-mercury response to changes in mercury deposition. *Proceedings of the National Academy of Sciences,* 104**,** 16586-16591.

Heiri, O., Lotter, A. F. & Lemcke, G. (2001) Loss on ignition as a method for estimating organic and carbonate content in sediments: reproducibility and comparability of results. *Journal of Paleolimnology,* 25**,** 101-110.

Lindberg, S., Bullock, R., Ebinghaus, R., Engstrom, D., Feng, X., et al. (2007) A synthesis of progress and uncertainties in attributing the sources of mercury in deposition. *Ambio: A Journal of the Human Environment,* 36**,** 19-33.

Lockhart, W. L., Macdonald, R. W., Outridge, P. M., Wilkinson, P., DeLaronde, J. B., et al. (2000) Tests of the fidelity of lake sediment core records of mercury deposition to known histories of mercury contamination. *The Science of the Total Environment,* 260**,** 171-180.

McCormac, F. G., Hogg, A. G., Blackwell, P. G., Buck, C. E., Higham, T. F. G., et al. (2004) ShCal04 Southern Hemisphere calibration, 0-11.0 cal kyr BP. *Radiocarbon,* 46**,** 1087-1092.

Nriagu, J. O. (1993) Legacy of mercury pollution. *Nature,* 363**,** 589.

Nriagu, J. O. (1994) Mercury pollution from the past mining of gold and silver in the Americas. *The Science of the Total Environment,* 149**,** 167-181.

Onuki, Y. & Kato, Y. (1993) *Excavations at Kuntur Wasi, Peru: the first stage 1988-1990 (Spanish translation),* Tokyo, University of Tokyo.

Petersen, U. (1989) Geological Framework of Andean Mineral Resources. IN Ericksen, G. E., Theresa Cañas P., M. & Reinemund, J. A. (Eds.) *Geology of the Andes and its relation to hydrocarbon and mineral resources.* Houston, Circum-Pacific Council for Energy and Mineral Resources.

Rick, J. W. (2004) The evolution of authority and power at Chavín de Huántar, Peru. *Archeological Papers of the American Anthropological Association,* 14**,** 71-89.

Rydberg, J., Gälman, V., Renberg, I., Bindler, R., Lambertsson, L., et al. (2008) Assessing the stability of mercury and methylmercury in a varved lake sediment deposit. *Environmental Science & Technology,* 42**,** 4391-4396.

Shimada, I., Epstein, S. & Craig, A. K. (1982) Batán Grande: a prehistoric metallurgical center in Peru. *Science,* 216**,** 952-959.

Shimada, I., Shinoda, K., Farnum, J., Corruccini, R., Watanabe, H., et al. (2004) An integrated analysis of pre-Hispanic mortuary practices. *Current Anthropology,* 45**,** 369-402.

Southworth, G., Lindberg, S., Hintelmann, H., Amyot, M., Poulain, A., et al. (2007) Evasion of added isotopic mercury from a northern temperate lake. *Environmental Toxicology and Chemistry,* 26**,** 53-60.

Stuiver, M. & Reimer, P. J. (1993) Extended $^{14}C$ database and revised CALIB radiocarbon calibration program. *Radiocarbon,* 35**,** 215-230.

Wise, J. M. & Féraud, J. (2005) Historic maps used in new geological and engineering evaluation of the Santa Bárbara Mine, Huancavelica mercury district, Peru. *De Re Metallica,* 4**,** 15-24.

Wolfe, A. P., Vinebrooke, R., Michelutti, N., Rivard, B. & Das, B. (2006) Experimental calibration of lake-sediment spectral reflectance to

chlorophyll *a* concentrations: methodology and paleolimnological validation. *Journal of Paleolimnology,* 36**,** 91-100.

Wu, Y., Wang, S., Streets, D. G., Hao, J., Chan, M., et al. (2006) Trends in anthropogenic mercury emissions in China from 1995 to 2003. *Environmental Science & Technology,* 40**,** 5312-5318.

# CHAPTER 3: LAKE-SEDIMENT GEOCHEMISTRY REVEALS 1400 YEARS OF EVOLVING EXTRACTIVE METALLURGY AT CERRO DE PASCO, PERUVIAN ANDES

## Introduction

Lake sediments offer the potential to preserve interpretable records of pre-industrial metallurgical activities. In Europe, lake-sediment geochemistry has been used to address archaeological questions of metallurgical evolution (Brännvall et al., 2001; Renberg et al., 1994), while similar efforts are just beginning for the Andes (Abbott and Wolfe, 2003; Cooke et al., 2008). Our knowledge of the timing and evolution of Andean metallurgy remains incomplete because of extensive looting, and over 400 years of mine-site degradation associated with Colonial and industrial mineral extraction. Lake-sediment archives may potentially contribute not only to our understanding of the environmental legacy of archaeometallurgical activities, but also toward identifying patterns associated with the technological evolution of Andean metallurgy. Cerro de Pasco in the central Peruvian Andes contains one the most intensively exploited silver deposits in the world. Although Colonial silver mining in the region is well-known from historical accounts (e.g. Fisher, 1977), pre-Colonial exploitation patterns remain cryptic at best. Large-scale Hg mining began in the late 16$^{th}$ century with the development of Hg amalgamation, a process which facilitated the extraction of silver from low-grade ores and stimulated large-scale silver production in the New World. Historical records of Hg production and sale, coupled to known losses associated

---

* Previously published material: Cooke C. A., Wolfe, A. P., & Hobbs, W. O. (2009) Lake-sediment geochemistry reveals 1400 years of evolving extractive metallurgy at Cerro de Pasco, Peruvian Andes. *Geology*, **37**, 1019-1022.

with amalgamation, suggest that New World Colonial Hg emissions totaled 196,000 tons, averaging ~612 tons/year (Nriagu, 1993, 1994). However, the very existence of Colonial Hg pollution remains equivocal because natural archives collected outside the Andes, but in the Southern Hemisphere, show no evidence for pre-industrial Hg pollution (Biester et al., 2007; Lamborg et al., 2002). The Andean region itself has not been investigated systematically. Thus, lake-sediment archives recovered proximal to major amalgamation centers afford a unique opportunity to not only shed light on the evolution of New World metallurgy, but also to address long-standing questions regarding the pre-industrial global cycle of Hg. Here, we utilize a lake sediment core to reconstruct the history of mining and metallurgy around Cerro de Pasco, which was once the world's largest silver mine.

## Methods

### *Study site*

Cerro de Pasco is located on the Junín plain in central Peru (Fig. 3.1). Following Colonial discovery ~1630 AD, it quickly became one of the world's foremost producers of silver (Fisher, 1977). Cerro de Pasco, and the numerous nearby smaller mines surrounding it, exploit rich polymetallic (Pb-Zn-Cu-Ag) ore deposits, the primary minerals being enargite ($Cu_3AsS_4$), arsenopyrite (FeAsS), aramayoite [$Ag(Sb, Bi)S_2$], argentiferous galena [(Ag, Pb)S], argentiferous tennantite [$(Ag, Cu, Fe)_{12}(Sb, As)_4S_{13}$], grantonite ($Pb_9As_4S_{15}$), sphalerite [(Zn, Fe) S], bismuthinite ($Bi_2S_3$) and native silver (Einaudi, 1977; Ward, 1961). Orebodies at Cerro de Pasco are estimated to have contained over $2x10^4$ tons of silver, $2x10^6$ tons of lead and $4x10^6$ tons of zinc, with lesser amounts of gold and bismuth (Peterson, 1965).

This study is based on a 100 cm sediment core recovered from Llamacocha (*cocha* meaning lake in the native Quechua). Llamacocha (11° 4' S; 75° 48' W; 4190 m elevation) is small (0.08 km$^2$), 14 m deep, and lies within a pristine, granitic catchment of 1.31 km$^2$. At a distance of ~60 km southeast from Cerro de Pasco – distal to any known past and present mining activities – Llamacocha is strategically located to record regional-scale atmospheric deposition of metals associated with smelting and amalgamation in the Cerro de Pasco region (Fig. 3.1).

*Core Collection and Chronology*

A sediment core containing an intact sediment-water interface was recovered using a percussion corer fitted with a 7 cm diameter polycarbonate tube (Blomqvist, 1991). The core was extruded into continuous 1-cm intervals in the field, and the upper sediments were dated using $^{210}$Pb activities measured by α-spectroscopy. The lower-portion of the core was dated using accelerator mass spectrometry (AMS) $^{14}$C age determinations obtained from

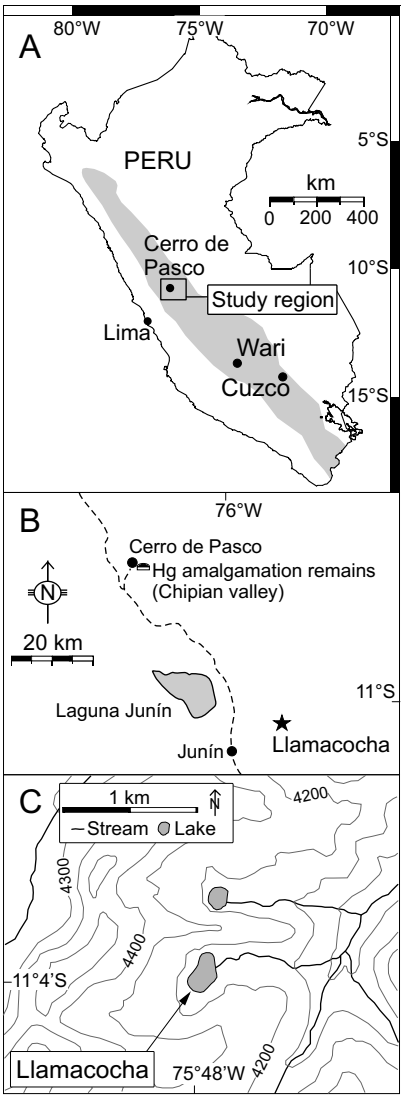


**Fig. 3.1.** (A) Location map of the study region within Peru. The shaded area indicates the zone of Cu-Pb-Zn-Ag polymetallic ores, which broadly corresponds to the crest of the Andean cordillera. (B) Location of the study lake in relation to Cerro de Pasco. (C) Detail of the study lake and surrounding area.

macroscopic charcoal (from grasses) and calibrated using SHCal (McCormac et al., 2004) within Calib 5.0 (Stuiver and Reimer, 1993).

*Sediment Geochemistry*

To assess the history of regional mining and smelting activity we analyzed the concentration of 16 elements using a Perkin Elmer Elan 6000 quadrupole inductively coupled plasma mass spectrometer (ICP-MS). To ascertain changes in Pb provenance, stable Pb isotopic ratios were determined using a Nu Plasma multicollector ICP-MS coupled to DSN-100 introduction system; Tl was used to correct for mass bias. The relative standard deviation of all Pb isotopic ratios was <0.1%. Elements were extracted using 1 M $HNO_3$ overnight; a standard extractive method for lake sediments (Graney et al., 1995). Duplicates were run every $10^{th}$ sample and were within 5% of each other. Concentrations of total Hg were determined on a Milestone Inc. DMA80 direct mercury analyzer. Blanks, duplicates, and standard reference materials were run every $10^{th}$ sample. Blanks averaged 0.16 ng $g^{-1}$; relative percent difference between duplicates was 11%; and standard reference materials were within 1% of certified values. To explore any underlying relationships between the analyzed elements, a correlation matrix of the centered and standardized sediment geochemical data (21 elements) was subjected to principle components analysis (PCA) using CANOCO ver. 4.5 software (ter Braak and Šmilauer, 1998).

**Results**

*Core Chronology*

Unsupported $^{210}Pb$ activity declines in near exponential fashion to a depth of ~35 cm (Table B.1; Fig. B.1). The constant rate-of-supply (CRS) model was applied

to calculate sediment ages and sedimentation rates spanning the past ~100 yr (Appleby and Oldfield, 1978). CRS sedimentation rates are relatively constant averaging 74±8 g $m^{-2}$ $yr^{-1}$ (Table B.1; Fig. B.1). CRS ages were then combined with the calibrated $^{14}C$ dates (Table B.2) using the mixed-effects model of Heegaard et al. (2005), which incorporates the age-depth relationship of the dates while integrating both within-and between-sample uncertainties (Fig. 3.2). The resulting age-depth model provides a conservative interpretation of available dates incorporating the two sources of random variability (i.e., dating uncertainty and variable time elapsed between dated horizons). Accordingly, the age model has been used to derive metal fluxes from the concentration data, which compensates for variable rates of sedimentation and facilitates comparisons to other studies (Fig. 3.2).

*Geochemistry*

Of the elements measured, Pb and Hg are cornerstones of our interpretations (though down-core stratigraphies for all elements measured are shown in Fig. B.2). This is because both are relatively immobile in lake sediments (Gallon et al., 2004; Rydberg et al., 2008), and furthermore are uniquely representative of the two predominant ore processing techniques used in the Andes: Pb-based smelting and Hg amalgamation. Titanium (Ti) is used to represent catchment-derived lithogenic inputs (Fig. 3.2). For nearly a millennium prior to ~600 AD, the accumulation of Pb is stable and low, averaging 0.07±0.01 mg $m^{-2}$ $yr^{-1}$. This represents the accumulation of natural, non-pollution Pb accumulation to Llamacocha sediment. Indeed, prior to 600 AD, the deposition of Pb and Ti are significantly correlated ($r^2$=0.76; $n$=35; $p$<0.001), indicating weathering of local bedrock within the Llamacocha watershed largely controlled Pb delivery to the lake. After ~600 AD, the deposition of Pb increases, becomes completely

decoupled from Ti ($r^2$=0.02; $n$=63), and $^{206}Pb/^{207}Pb$ ratios markedly decrease (Fig. 3.2).

By ~1600 AD, Pb accumulation rates had risen to 0.6 mg $m^{-2}$ $yr^{-1}$. However, in contrast to Pb and the other trace metals, Hg fails to increase over this 1000 yr period, remaining constant ~1.5±0.2 μg $m^{-2}$ $yr^{-1}$ (Fig. 3.2). This likely reflects the absence of Hg within local ores, and the fact that Hg was not directly utilized during pre-Colonial smelting activities. The first clear increase of Hg within Llamacocha sediment occurs at 1600 AD. Hg flux more than doubles (Fig. B.2), rising to 3.9 μg $m^{-2}$ $yr^{-1}$ by 1650 AD (Fig. 3.2). The deposition of Pb also increases across this period, but to a lesser degree. We therefore suggest that this first appearance of Hg pollution represents the adoption of Hg amalgamation as the

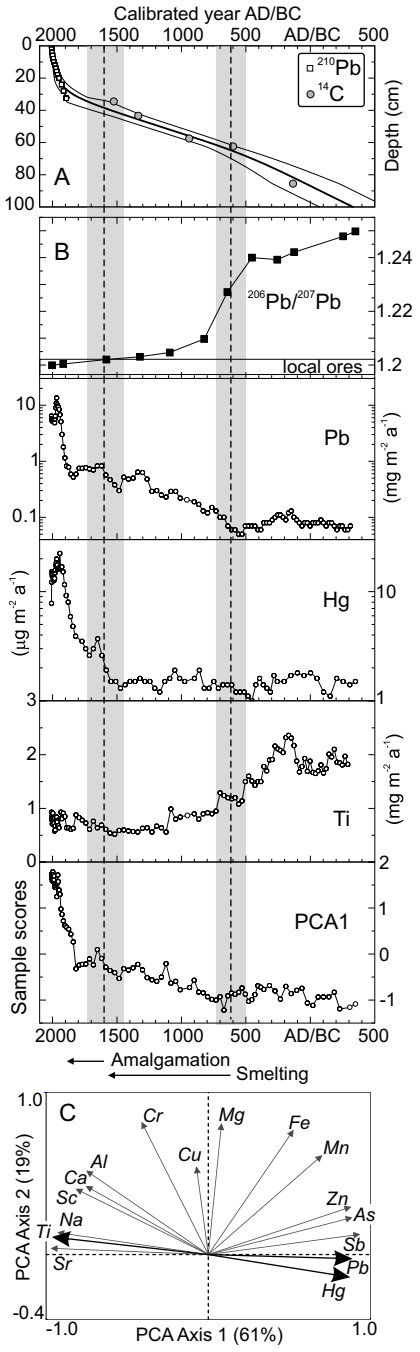


**Fig. 3.2.** (A) The composite age-depth model and 95% confidence interval (CI) integrating CRS dates (open squares) and calibrated $^{14}C$ median ages (shaded circles). (B) Stratigraphic profiles of $^{206}Pb/^{207}Pb$ ratios, Pb, Hg, Ti, and PCA axis 1 sample scores. The vertical dashed lines indicate the onset of smelting and amalgamation with 95% CI (shaded regions). Note Pb and Hg are plotted on a log scales. (C) Biplot of the PCA results for the leading two axes, showing loadings for each of the analyzed metals.

predominant silver-extractive technology at Cerro de Pasco, closely following Colonial take-over from indigenous metalsmiths (see discussion below).

Further increases in Pb and Hg are noted in Llamacocha sediment during the 19th century, and peak values for each metal are reached in 1968 AD and 1942 AD, respectively (Fig. 3.2). Twentieth-century Pb deposition peaks two orders of magnitude above background levels (Fig. B.2), representing massive enrichment associated with extensive local mining and smelting activity. This Pb enrichment is accompanied by sediment isotopic ratios that match closely those of Cerro de Pasco ores (Figs 3.2 and B.3) (Mukasa et al., 1990; Sangster et al., 2000).

Our interpretation of the geochemical data is supported by the PCA results (Fig. 3.2). The first PCA axis (hereafter PCA1) explains 61% of the variance observed within the geochemical data set. Those trace metals which are associated directly with metallurgical pollution (e.g., Hg, Pb, Sb, As, and Zn) all produce strong positive loadings on PCA1. In contrast, elements that are attributed to primarily lithogenic sources (e.g., Ti, Sr, Al, Sc, and Na) produce negative PCA1 loadings. These relationships imply that PCA1 defines a synthetic geochemical gradient that separates metals delivered to Llamacocha sediments by catchment processes from those associated with atmospheric deposition. Thus, when arranged stratigraphically (Fig. 3.2), increasing PCA1 sample scores record the relative importance of anthropogenic contributions from metallurgical sources to the overall geochemical record.

**Discussion and Conclusions**

Given Llamacocha's proximity to Cerro de Pasco, we attribute the initial increase of sedimentary Pb flux and the synchronous decline in $^{206}Pb/^{207}Pb$ ratios to the rise of smelting in the region. Our chronology suggests this occurred ~600 AD,

coinciding with the expansion of the Wari Empire out of the Ayacucho valley (Fig. 3.1). The Wari were the largest pre-Inca Empire in the Andes, and maintained both direct (i.e. occupation) and indirect (i.e. trade) control of the central Andes until ~1000 AD, when they abruptly collapsed (Isbell, 2008; Moseley et al., 2005). While there have been few Wari silver artifacts excavated archaeologically, there seems little doubt from the Llamacocha sediment record that smelting activity increased steadily during the ~400 yr of Wari influence. However, the collapse of Wari appears to have carried little consequence for smelting at Cerro de Pasco, as rates of Pb deposition increase across the cultural transition (Fig. 3.2). This observation suggests that while metallurgy at Cerro de Pasco was perhaps initiated by the initial expansion of Wari, it was decoupled from the Empire's demise.

This subsequent interval covers the expansion and apogee of the Inca civilization (ca. 1450–1532 AD), the largest pre-Colonial Empire of the New World. Due to the low sedimentation rates within Llamacocha at this time (Fig. B.1), the Inca period is poorly resolved in the record. However, it is during this interval that $^{206}Pb/^{207}Pb$ isotopic ratios first fall within the range of Cerro de Pasco ores (Fig. 3.2). A simple two-component mixing model between end-member $^{206}Pb/^{207}Pb$ ratios (1.245 for local bedrock and 1.200 for Cerro de Pasco ore) suggests that ~95% of the Pb within Llamacocha sediment was derived from atmospheric pollution from Inca time onwards. Indeed, archaeological research suggests regional silver production increased under Inca authority, likely driven by demand from Inca nobility for precious metals as a tribute tax (Costin et al., 1989). The geochemical record therefore suggests that smelting at Cerro de Pasco not only occurred continuously, but likely increased progressively, over the entire pre-Colonial interval captured. Although knowledge of early extractive technologies remains fragmentary, the Inca are known to have exploited

argentiferous galena (locally known as *soroche*) as a flux during smelting, which was conducted in clay-lined, wind-drafted furnaces called *huayras* (Bakewell, 1984). The use of *soroche* is unquestionably associated with increased atmospheric Pb emission and recruitment to down-wind lakes (Abbott and Wolfe, 2003), and likely manifested in Pb stable isotopic signatures (Cooke et al., 2007). The results from Llamacocha therefore suggest that similar technologies may have been known to metalsmiths from considerably earlier stages of Andean cultural development.

European discovery of the Cerro de Pasco silver deposit occurred ~1600 AD (Fisher, 1977; Purser, 1971). A large collection of unexcavated Colonial smelters and grinding wheels – presumably used during Hg amalgamation and the smelting of Ag-bearing ores – is located in the Chipian valley, <10 km east of Cerro de Pasco and ~60 km northwest of Llamacocha (Fig. 3.1; Cooke and Abbott, 2008). The process of Hg amalgamation dominated metallurgy in the Andes for the next ~400 yr. However, the environmental legacy of this Hg use has remained, until now, elusive. Nriagu (1993, 1994) estimated that Hg amalgamation resulted in annual atmospheric Hg emissions on the order of 400–1200 tons. If disseminated globally, these emissions would have resulted in an average increase in Hg deposition rates between 0.8 and 2.4 $\mu g\ m^{-2}\ yr^{-1}$. Remarkably, the Llamacocha record registers a ~2.3 $\mu g\ m^{-2}\ yr^{-1}$ increase in Hg accumulation at the onset of amalgamation, very near to the upper end of Nriagu's (1994) estimate. The majority of these emissions likely occurred during the heating of the Ag-Hg amalgam, and thus was most likely in the form of gaseous elemental Hg ($Hg^0$). $Hg^0$ has an atmospheric residence time of 0.5–2.0 yr, and is circulated hemispherically (and potentially also globally) (Lin and Pehkonen, 1999). However, lake-sediment archives collected outside the Andes have shown little evidence for pre-industrial Hg pollution (Biester et al., 2002; Lamborg et

al., 2002). While resolving this discrepancy will require additional records – especially from the southern Hemisphere – it is evident from this study that the Hg amalgamation generated regional-scale Hg pollution.

Around 1800 AD, atmospheric emissions increased dramatically, as indicated by both Hg and Pb flux data, and the trend of PCA1 (Fig. 3.2). During the 19$^{th}$ century, Cerro de Pasco was producing in excess of 60 tons yr$^{-1}$ of pure silver (Brading and Cross, 1972; Purser, 1971), and during the early 20$^{th}$ century construction was completed on the central Peruvian railway. The railway led to the rapid expansion of mining activities within the Cerro de Pasco region, and the central Andes in general. The Cerro de Pasco Corporation was founded in 1901 AD, initiating a shift from silver to copper production. By 1905 AD two copper smelters were in operation (Purser, 1971). Accumulation rates associated with 20$^{th}$ century mining operations greatly exceed those achieved under Colonial or pre-Colonial intervals, and Pb stable isotopes indicate virtually all of the sediment-Pb burden at this time can be attributed to atmospheric pollution (Fig. 3.2). Despite recent declines, modern accumulation rates of Pb remain 94 times greater than background Pb accumulation rates. In contrast, recent rates of Hg accumulation are six times background Hg accumulation rates (Fig. B.2), which falls in line with remote regions from around northern hemisphere (Biester et al., 2007).

While the silver deposits at Cerro de Pasco are generally believed to have been discovered by Colonial metallurgists ~1600 AD, the record presented here documents over a millennium of prior mining activity, at levels sufficient to deliver air-borne metal pollution ~60 km from the mine site. Given the paucity of intact pre-Colonial smelting facilities in the archaeological record, lake-sediment records associated with smelting are of considerable value in reconstructing ancient metallurgical histories. Furthermore, the sediment record is sensitive to evolving ore processing technologies, recording the switch from reductive

smelting in traditional *huayras* to Colonial Hg amalgamation. Finally, our data confirm the hypothesis, first proposed by Nriagu (1993, 1994), that Colonial amalgamation resulted in widespread Hg pollution.

**References**


Abbott, M. B. & Wolfe, A. P. (2003) Intensive pre-Incan metallurgy recorded by lake sediments from the Bolivian Andes. *Science,* 301**,** 1893-1895.

Appleby, P. G. & Oldfield, F. (1978) The calculation of lead-210 dates assuming a constant rate of supply of unsupported $^{210}$Pb to the sediment. *Catena,* 5**,** 1-18.

Bakewell, P. (1984) *Miners of the red mountain: Indian labor at Potosí, 1545-1650,* Albuquerque, University of New Mexico Press.

Biester, H., Bindler, R., Martínez-Cortizas, A. & Engstrom, D. R. (2007) Modeling the past atmospheric deposition of mercury using natural archives. *Environmental Science & Technology,* 41**,** 4851-4860.

Biester, H., Kilian, R., Franzen, C., Woda, C., Mangini, A., et al. (2002) Elevated mercury accumulation in a peat bog of the Magellanic Moorlands, Chile (53°S) - an anthropogenic signal from the Southern Hemisphere. *Earth and Planetary Science Letters,* 201**,** 609-620.

Blomqvist, S. (1991) Quantitative sampling of soft-bottom sediments: problems and solutions. *Marine Ecology Progress Series,* 72**,** 295-304.

Brading, D. A. & Cross, H. E. (1972) Colonial Silver Mining: Mexico and Peru. *The Hispanic American Historical Review,* 52**,** 545-579.

Brännvall, M.-L., Bindler, R., Emteryd, O. & Renberg, I. (2001) Four thousand years of atmospheric lead pollution in northern Europe: a summary from Swedish lake sediments. *Journal of Paleolimnology,* 25**,** 421-435.

Cooke, C. A. & Abbott, M. B. (2008) A paleolimnological perspective on industrial-era metal pollution in the Central Andes, Peru. *Science of the Total Environment,* 393**,** 262-272.

Cooke, C. A., Abbott, M. B. & Wolfe, A. P. (2008) Late-Holocene atmospheric

lead deposition in the Peruvian and Bolivian Andes. *The Holocene,* 18**,** 353-359.

Cooke, C. A., Abbott, M. B., Wolfe, A. P. & Kittleson, J. L. (2007) A millennium of metallurgy recorded by lake sediments from Morococha, Peruvian Andes. *Environmental Science & Technology,* 41**,** 3469-3474.

Costin, C., Earle, T., Owen, B. & Russell, G. (1989) The impact of Inca conquest on local technology in the Upper Mantaro Valley, Perú. IN van der Leeuw, S. E. & Torrence, R. (Eds.) *What's New? A Closer Look at the Process of Innovation.* London, Unwin Hyman.

Einaudi, M. T. (1977) Environment of ore deposition at Cerro de Pasco, Peru. *Economic Geology,* 72**,** 893-924.

Fisher, J. R. (1977) *Silver mines and silver miners in colonial Peru, 1776-1824,* Liverpool, Centre for Latin American Studies, University of Liverpool.

Gallon, C., Tessier, A., Gobeil, C. & Alfaro-De La Torre, M. C. (2004) Modeling diagenesis of lead in sediments of a Canadian Shield lake. *Geochimica et Cosmochimica Acta,* 69**,** 3531-3545.

Graney, J. R., Halliday, A. N., Keeler, G. J., Nriagu, J. O., Robbins, J. A., et al. (1995) Isotopic record of lead pollution in lake sediments from the Northeastern United States. *Geochimica et Cosmochimica Acta,* 59**,** 1715-1728.

Heegaard, E., Birks, H. J. B. & Telford, R. J. (2005) Relationships between calibrated ages and depth in stratigraphical sequences: An estimation procedure by mixed-effect regression. *The Holocene,* 15**,** 612-618.

Isbell, W. (2008) Wari and Tiwanaku: international identities in the Central Andean Middle Horizon. IN Silverman, H. & Isbell, W. (Eds.) *Handbook of South American Archaeology.* New York, Springer.

Lamborg, C. H., Fitzgerald, W. F., Damman, A. W. H., Benoit, J. M., Balcom, P.

H., et al. (2002) Modern and historic atmospheric mercury fluxes in both hemispheres: Global and regional mercury cycling implications. *Global Biogeochemical Cycles,* 16**,** 1104.

Lin, C. J. & Pehkonen, S. O. (1999) The chemistry of atmospheric mercury: a review. *Atmospheric Environment,* 33**,** 2067-2079.

McCormac, F. G., Hogg, A. G., Blackwell, P. G., Buck, C. E., Higham, T. F. G., et al. (2004) ShCal04 Southern Hemisphere calibration, 0-11.0 cal kyr BP. *Radiocarbon,* 46**,** 1087-1092.

Moseley, M. E., Nash, D. J., Williams, P. R., deFrance, S. D., Miranda, A., et al. (2005) Burning down the brewery: establishing and evacuating an ancient imperial colony at Cerro Baul, Peru. *Proceedings of the National Academy of Sciences,* 102**,** 17264-17271.

Mukasa, S. B., Vidal C., C. E. & Injoque-Espinoza, J. (1990) Pb isotope bearing on the metallogenesis of sulfide ore deposits in Central and Southern Peru. *Economic Geology,* 85**,** 1438-1446.

Nriagu, J. O. (1993) Legacy of mercury pollution. *Nature,* 363**,** 589.

Nriagu, J. O. (1994) Mercury pollution from the past mining of gold and silver in the Americas. *The Science of the Total Environment,* 149**,** 167-181.

Peterson, U. (1965) Regional geology and major ore deposits of Central Peru. *Economic Geology,* 85**,** 1287-95.

Purser, W. F. C. (1971) *Metal-mining in Peru, past and present,* New York, Praeger Publishers.

Renberg, I., Persson, M. W. & Emteryd, O. (1994) Pre-industrial atmospheric lead contamination detected in Swedish lake sediments. *Nature,* 368**,** 323-326.

Rydberg, J., Gälman, V., Renberg, I., Bindler, R., Lambertsson, L., et al. (2008) Assessing the stability of mercury and methylmercury in a varved lake sediment deposit. *Environmental Science & Technology,* 42**,** 4391-4396.

Sangster, D. F., Outridge, P. M. & Davis, W. J. (2000) Stable lead isotope characteristics of lead ore deposits of environmental significance. *Environmental Reviews,* 8**,** 115-147.

Stuiver, M. & Reimer, P. J. (1993) Extended $^{14}C$ database and revised CALIB radiocarbon calibration program. *Radiocarbon,* 35**,** 215-230.

ter Braak, C. J. F. & Šmilauer, P. (1998) CANOCO Reference Manual and User's Guide to Canoco for Windows: Software for Canonical Community Ordination (version 4).

Ward, H. J. (1961) The pyrite body and copper orebodies, Cerro de Pasco Mine, central Peru. *Economic Geology,* 56**,** 402-422.

# CHAPTER 4: PRE-COLONIAL MERCURY POLLUTION ASSOCIATED WITH THE SMELTING OF ARGENTIFEROUS ORES IN THE BOLIVIAN ANDES

## Introduction

The global mercury (Hg) cycle has been demonstrably impacted by humans. Emissions of Hg are of worldwide concern because of the long atmospheric residence time (6-24 months) of atmospheric elemental Hg ($Hg^0$), which favours homogenization of atmospheric Hg on a hemispheric scale. Importantly, linkages between inputs of anthropogenic Hg, especially from the atmosphere, and the formation of monomethylmercury ($CH_3Hg$) have not been firmly established, and methylated species of Hg can bioaccumulate through food chains to concentrations that are potentially dangerous for top-level consumers. Natural and anthropogenic sources release approximately 5200 and 2900 Mg of Hg annually to the atmosphere, though natural emissions include the recycling of some (largely unknown) amount of Hg that was deposited historically. The most important anthropogenic sources of Hg emissions are thought to include: fossil-fuel consumption (1422 Mg $yr^{-1}$), artisanal small-scale gold mining and processing (400 Mg $yr^{-1}$), waste disposal (187 Mg $yr^{-1}$), cement production (236 Mg $yr^{-1}$), and non-ferrous metal manufacturing (310 Mg $yr^{-1}$), though considerable uncertainty about the absolute magnitude of these emissions exists. Two of these extractive activities, artisanal gold mining and non-ferrous metal production, have long histories predating the industrial revolution, raising the possibility that pre-

---

*Submitted for publication: Cooke C. A., Balcom, P. H., Kerfoot, C., Abbott, M. B., & Wolfe, A. P. Pre-Colonial mercury pollution in the Bolivian Andes. *Ambio: A journal of the human environment*.

industrial activities generated large-scale Hg emissions.

Pre-industrial emissions of heavy-metals associated with mineral extraction have been convincingly demonstrated in both the New and Old Worlds. In Europe, the earliest indications of atmospheric lead (Pb) pollution date ~500 BC. These early Pb emissions were transported atmospherically across the Northern Hemisphere, and are registered within ice cores from Greenland (Hong et al., 1994), lake sediments from Northern Fennoscandia (Renberg et al., 1994), and peat cores from North-Western Spain (Martínez-Cortizas et al., 2002). Similarly early pollution signatures have been reported from central China associated with metal production during the early Han Dynasty (206 BC - 220 AD) (Lee et al., 2008). In the New World, early metal pollution appears to be limited to the South American Andes, where argentiferous galena [(Pb, Ag)S] was heavily utilized during smelting as a flux during silver production (400-1000 AD) (Abbott and Wolfe, 2003; Cooke et al., 2008).

Despite this extensive history of Pb pollution, there is no evidence for Hg emissions associated with early smelting of non-ferrous ores. Non-ferrous ores contain Hg as an impurity (Schwartz, 1997; Kerfoot et al., 2002), and the smelting of non-ferrous ores today constitutes a major source of atmospheric Hg emissions. The hypothesis therefore emerges that, analogous to Pb, artisanal mining and smelting of non-ferrous ores may have been a significant source of Hg to the preindustrial atmosphere. Testing this hypothesis is difficult however, because (i) the Hg content of non-ferrous ore deposits is poorly constrained, and (ii) many of the world's richest ore deposits were exhausted decades, centuries, or even millennia ago. Here, we address these limitations using lake-sediment geochemical archives obtained downwind from Cerro Rico de Potosí in the Bolivian Andes, historically the world's largest silver deposit. By exploiting the environmental archive preserved within lake sediments, we infer a temporally

continuous regional history of Hg emissions associated with the smelting of world's richest silver ores. We also present a suite of measurements of [Hg] within global ore deposits, suggesting that Hg occurs as a persistent trace contaminant in massive metal deposits. Collectively, our results indicate that smelting of metal-bearing ores constitute a hitherto now unrecognized and potentially significant source of pre-industrial Hg emissions to the global atmosphere.

## Methods and materials

*Study site*

Cerro Rico de Potosí (Fig. 4.1) was first exploited by pre-Incan metalsmiths a millennium ago (Abbott and Wolfe, 2003). Smelting of argentiferous ores was initially conducted in artisanal wind-drafted kilns called *huyaras* (Fig. 4.2a), culminating with the silver riches of the Incan empire. Between initial Colonial control of the mine in 1545 AD and the introduction of Hg amalgamation in 1574 AD, various phases of metallurgical experimentation occurred, typically involving the enslavement of indigenous miners and metallurgists by the Spanish crown. Potosí became the largest consumer of Hg globally in 1574 AD when Hg amalgamation was adopted at the mine (Fig. 4.2b), a distinction it retained for the next ~300 years. By the mid

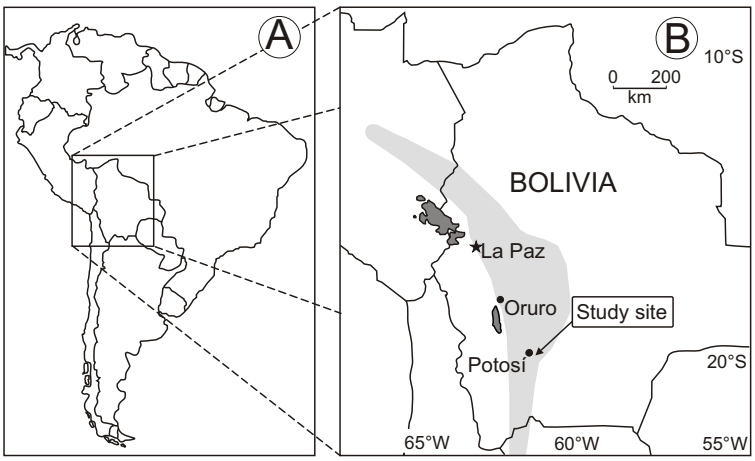


**Fig. 4.1.** Maps of South America (A) and Bolivia (B) showing the location of Potosí. The shaded region represents the extent of the Bolivian tin belt.

17th -century, the population of Potosí exceeded 160,000 people, making it one of the largest and most economically important cities in the world. Silver production at Potosí declined until its eventual abandonment in 1930 AD. As the supply of silver progressively declined over the 18th and 19th centuries, tin production became increasingly important, and peak tin production, driven by heightened demand during WWI, was reached during the early 20th century. Mining of silver-rich alluvium at the base of Cerro Rico, known as *pallacos* (Bartos, 2000), has recently been initiated by the Coeur d'Alene Mines Corporation.

*Core chronology*

In order to assess the history of Hg pollution associated with each stage of metallurgical development at Potosí, we exploited the well-dated geochemical record preserved in a nearby lake, Laguna Lobato, situated 6 km east of Cerro Rico. The Laguna Lobato core preserves a continuous record of sedimentation spanning the Holocene, and both the core and the age model used here have been described in detail previously along with geochemical stratigraphies for lead (Pb), silver (Ag), antimony (Sb), bismuth (Bi), and tin (Sn) (Abbott and Wolfe, 2003). The chronology for the Laguna Lobato sediment core was developed using $^{210}$Pb, $^{137}$Cs, and $^{14}$C radioisotopes.

*Sediment geochemistry*

New measurements of total [Hg] were determined on each interval in which sufficient sediment remained from previous analyses. Sediment Hg burdens were quantified using a DMA80 direct mercury analyzer (Milestone Inc.) at the University of Connecticut, Department of Marine Sciences (EPA, 1998). Blank values averaged 0.31±0.25 ng g$^{-1}$ ($n$=22); recoveries of standard reference material MESS-3 (marine sediment) averaged 90±2 ng g$^{-1}$ ($n$=18) and were in agreement

with certified values (91±9 ng $g^{-1}$); and the relative percent difference between duplicate measurements of the same sample averaged 5.30±0.03% (*n*=19).

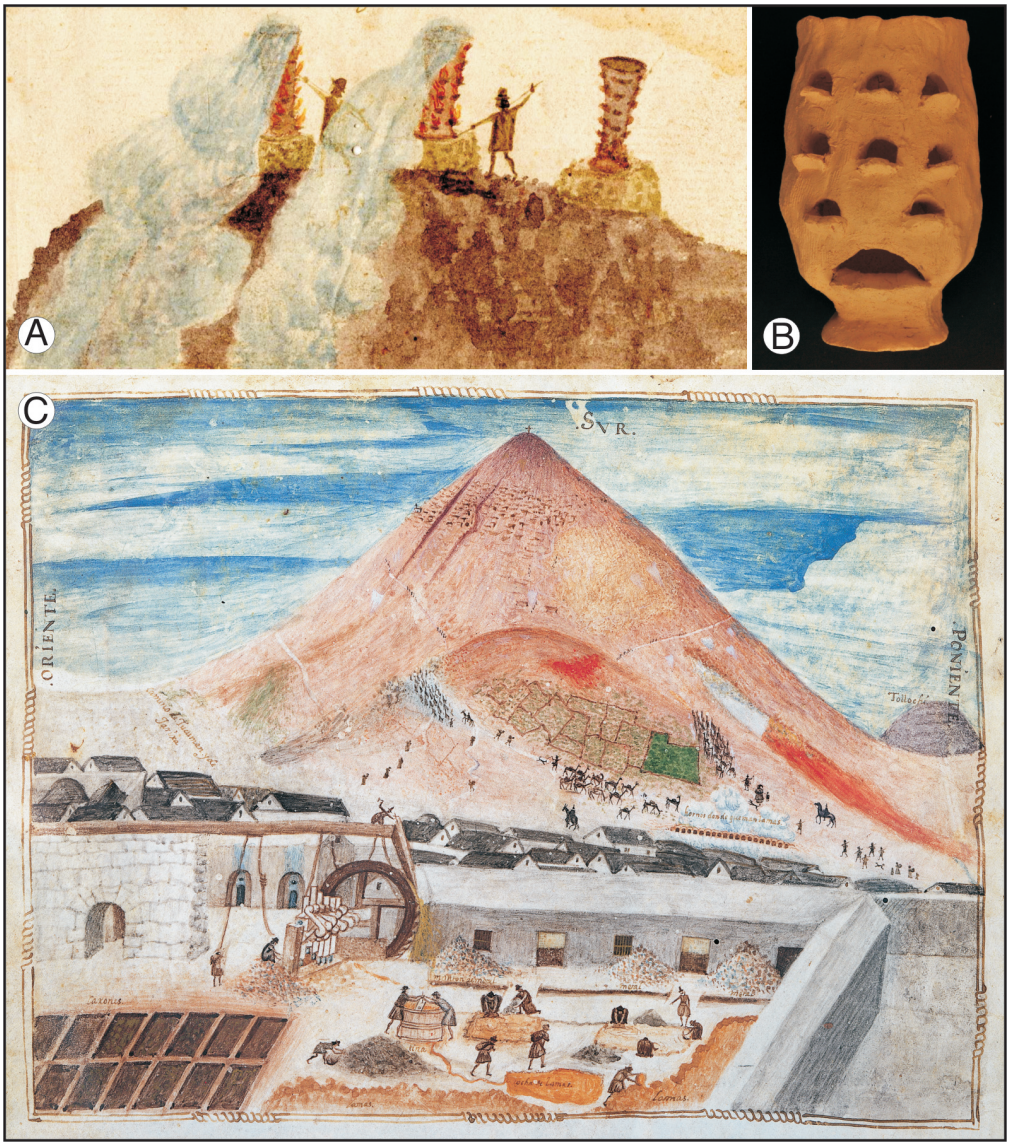


**Fig. 4.2.** (A) Painting from the Colonial era of smelting operations at Cerro Rico de Potosí using Incan huyaras (artist unknown). (B) Model of a clay huyara used to smelt argentiferous ores at the time of Colonial contact. The small slots vented the kiln, whereas the molten metal was retrieved from the large basal opening. Ore was introduced from above, onto the fuel. The model was created by the late Jeanne M. Wolfe (McGill University). (C) A 1584 painting by an unknown artist of Cerro Rico de Potosi, with trains of llamas transporting ore from the mountain to one of the amalgamation facilities built to process the ore. The paintings are courtesy of *The Hispanic Society of America*.

Total Hg pollution burdens for the core were calculated as the product of sediment dry mass (g $m^{-2}$) and Hg concentration (mg $g^{-1}$). Core intervals lacking [Hg] data were estimated using linear interpolation between measurements, and intervals within each cultural period (i.e. Colonial, pre-Colonial, industrial) were summed.

*Global ore geochemistry*

Mercury is known to occur in trace amounts in sulfide ores (e.g., PbS), and can form natural minerals with silver (including arquerite ($Ag_{12}Hg$), kongspergite [α-(Ag,Hg)] and moschellandsbergite [γ-(Ag,Hg)]). However, direct measurements of Hg content in non-ferrous ores are limited. To assess the possible larger implications of our results, we measured the Hg content in a suite of ore samples collected from mines around the world. Ores were grouped into five broad categories based on primary ore mineralogy: native copper ores, silver ores, copper-silver ores, zinc ores, and native silver ores.

For world ore comparisons, samples from the Seaman Mineral Museum (Michigan Technological University) were digested in a Milestone Thos 900 microwave digestor, and analyzed for total mercury by the cold vapour technique using a Perkin-Elmer Model 5000 and a Perkin-Elmer MHS-10 mercury-hydride system. For every set of 10 samples, a minimum of two sets of standards were analyzed, in addition to two procedural blanks and one duplicate sample. Natural matrix certified reference materials included: Metals of soil/sediment #4 (Ultra Scientific; SRM 2704a) and Buffalo River sediment (National Bureau of Standards, NIST 1990). Mercury recovery from these reference materials was 96.7±9.0% ($n$=35).

## Results

*Core chronology*

The chronology of the Laguna Lobato sediment core has been published and described previously (Abbott and Wolfe, 2003) and therefore is only summarized here (Fig. 4.3a). The upper 23.5 cm of the Laguna Lobato sediment core contained inventories of unsupported $^{210}$Pb, to which the constant rate of supply (CRS) model was applied. The resultant $^{210}$Pb age model was verified by matching peak sediment $^{137}$Cs activity with the CRS model year for 1963 A.D. Of the nine calibrated $^{14}$C dates obtained on plant macrofossils at Laguna Lobato only the uppermost two are shown here, as they encapsulate the period of interest (the last ~1000 years). Sedimentation rates for the core were calculated as the product of linear sediment accumulation rates between dated horizons (cm yr$^{-1}$) and dry bulk density (g cm$^{-3}$) (Fig. 4.3b).

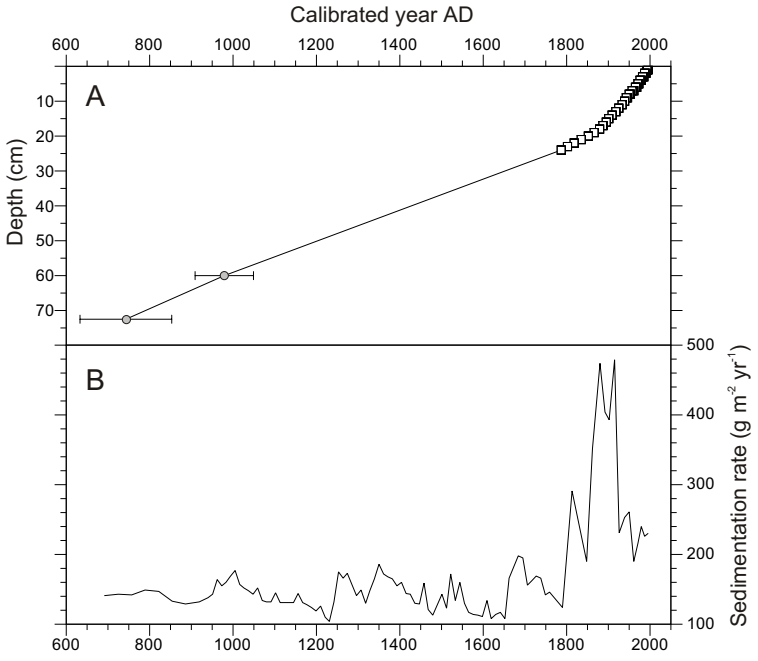


**Fig. 4.3.** (A) Composite age depth model for the Laguna Lobato sediment core. Squares represent CRS $^{210}$Pb dates whereas circles are calibrated AMS $^{14}$C dates with associated 2σ error ranges. (B) Down-core sedimentation rate for the Laguna Lobato sediment core.

*Sediment geochemistry*

Laguna Lobato sediment [Hg] rises dramatically above background ~1100 AD, in concert with a similar rise in [Ag], and following the initial rise in [Pb] (~1000 AD; Fig. 4.4). These features are not artefacts of variable sedimentation, and are expressed whether the data is presented as metal concentrations or fluxes. By 1250 AD, sediment [Hg] and Hg flux attain peak values of 2000 ppb, and 325 μg $m^{-2}$ $yr^{-1}$, respectively. After 1300 AD, and into the Colonial era (1554-1900 AD), Hg steadily decreases, whereas Pb increases and Ag remains relatively constant at ~100 ppb. While both Hg concentration and flux are characterized by a declining trend through the Colonial era, both remain elevated relative to background values ([Hg]: >300 ppb; Hg flux: 80 μg $m^{-2}$ $y^{-1}$).

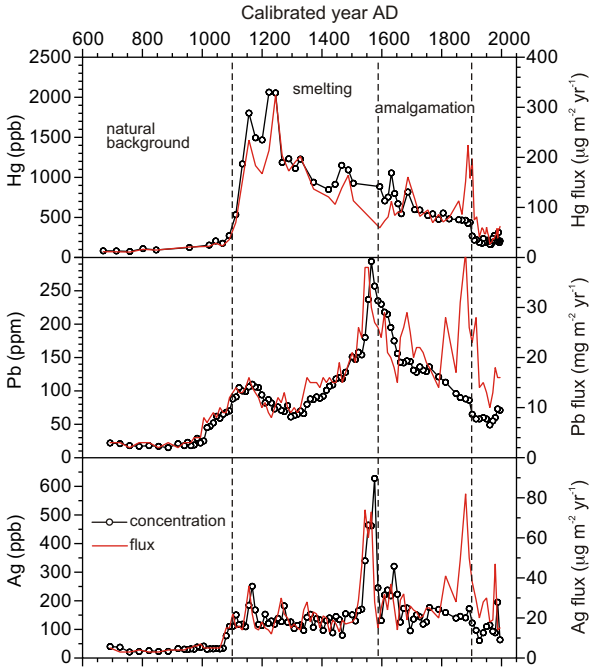


**Fig. 4.4.** Stratigraphic profiles of concentrations (circles) and fluxes (red line) for Hg, Pb and Ag in Laguna Lobato sediment. Note the different units between Pb (ppm; mg $m^{-2}$ $yr^{-1}$) and Ag and Hg (ppb; μg $m^{-2}$ $yr^{-1}$).

Flux rates for all three metals experience a brief increase during the late 19th century, which is attributable to an increase in sedimentation rates at this time (Fig. 4.4). During the 20th century, concentrations and fluxes for all three metals

decline to their lowest values since enrichment first appeared ~1000 years before present.

*World ore geochemistry*

Figure 4.5 and Table 4.1 summarize the [Hg] results for the 109 ore samples analyzed. There is considerable heterogeneity in [Hg] both between and among the four groups of ores. Native copper ores and silver ores contain the lowest Hg concentrations, but span nearly three orders of magnitude in [Hg]. Native silver ores contain on average the highest concentrations of Hg and are characterized by the greatest variability in [Hg] spanning nearly four orders of magnitude (0.3-2548 ppm). The second highest [Hg] measured was on a Ag-rich ore from San Pedro de Atacama, Chile, which is located <400 km from Potosí. While we lacked ore from Potosí or even Bolivia, the high [Hg] noted from northern Chile may suggest regional enrichment of Hg in silver ores from the Andean *altiplano*.

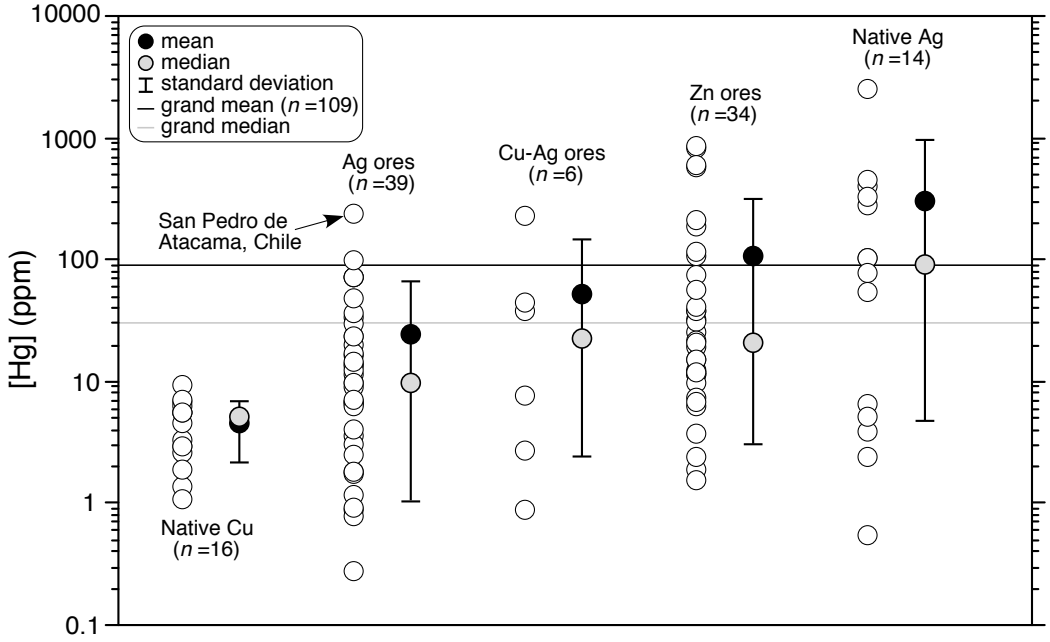


**Fig. 4.5.** Comparison of [Hg] for five types of ore deposits indicating both individual measurements and the mean, median, and standard deviation of each group and the grand mean and median for all samples combined.

**Table 4.1.** Summary statistics of Hg concentrations (ppm) within world-wide ore samples.

| Ore type | n | Max | Min | Mean | S.D. | Median |
|---|---|---|---|---|---|---|
| Native Ag | 14 | 2548.0 | 0.6 | 314.5 | 662.8 | 93.3 |
| Zn ores | 34 | 872.2 | 1.6 | 119.9 | 235.1 | 21.4 |
| Cu-Ag ores | 6 | 230.1 | 0.9 | 54.2 | 88.2 | 22.9 |
| Ag ores | 39 | 244.3 | 0.3 | 25.0 | 43.4 | 9.9 |
| Native Cu | 16 | 9.4 | 1.1 | 4.6 | 2.3 | 5.2 |
| All ores | 109 | 2548.0 | 0.3 | 90.4 | 11.9 | 283.3 |

**Discussion**

Pre-Columbian smelting at Cerro Rico de Potosí was conducted in wind-drafted clay furnaces called *huyaras*, in which galena (PbS) was used as a flux. The first Columbian conquistadors to visit Potosí recorded the use of both *huyaras* and Pb flux by Incan metalsmiths (Bakewell, 1984). The legacy of this technology is preserved in lake sediment archives surrounding several metallurgical centers in the Andes (Abbott and Wolfe, 2003; Cooke et al., 2007, 2008). Pb-based smelting continued to be relied upon to win silver throughout the pre-Colonial era. Surface ores at Potosí were depleted shortly after the Spanish took control of the mine in 1545 AD (Craig, 1989), and *huyara*-based smelting was largely replaced by mercury amalgamation, which facilitated extraction from lower-grade ores recovered from subterranean adits (Nriagu, 1994). Mercury amalgamation continued at Potosí until the early-20$^{th}$ century, when silver mining was largely abandoned.

The stratigraphies of Pb and Ag in Laguna Lobato sediment reflect volatile losses of these metals during the smelting of argentiferous galena (Abbott and Wolfe, 2003). However, [Hg] and Hg flux are highest during the pre-Colonial era. Enrichment factors (EFs) are unitless ratios in which metal concentrations

at each interval are normalized to the average background metal concentration, providing a relative measure of the increase in Hg, Pb, and Ag (Fig. 4.6). Background concentrations of Hg, Pb, and Ag are 95±19 ppb, 20±4 ppm, and 31±7 ppb, respectively. These background concentrations are comparable to the bulk composition of the upper continental crust (Wedepohl, 1995), suggesting little pre-industrial enrichment of these metals in catchment soils surrounding Laguna Lobato, despite its proximity to the world's largest silver deposit. Of the three metals presented here, Hg shows the greatest relative increase, with EFs exceeding 15 during the pre-Inca period of 1100-1250 AD (Fig. 4.6). In contrast, Pb and Ag EFs remain tightly coupled remaining between 5 and 15 throughout much of the record, despite the fact that they are characterized by very different absolute concentrations.

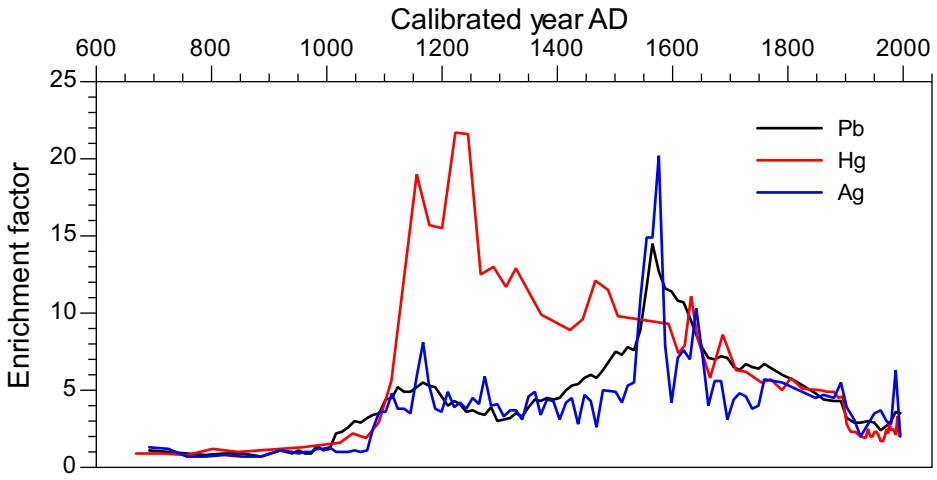


**Fig. 4.6.** Temporal evolution of metal enrichment factors (EFs) for Ag (blue), Hg (red) and Pb (black). Enrichment factors are unitless ratios calculated by normalizing concentrations from each interval to the average background metal concentration, taken here to be pre-1000 BC. Background concentrations of Hg, Pb, and Ag are 95±19 ppb, 20±4 ppm, and 31±7 ppb, respectively.

The relatively large pre-Colonial increase in Hg occurs despite the fact that Pb, not Hg, was involved in the smelting process. At Huancavelica in central Peru, Cinnabar (HgS) has been mined continuously since ~1400 BC (Cooke et al., 2009a). Indeed, the early onset of mining at Huancavelica suggests cinnabar was one of the first minerals to be exploited in the Andes. While the Inca may have experimented with the heating or retorting of cinnabar (Cooke et al., 2009a), the early use of cinnabar appears to have been limited to its use as a pigment (vermillion). We know of no documentary or archaeological evidence to suggest pre-Colonial use of Hg to facilitate silver extraction. Our preferred interpretation is therefore that the extensive pre-Colonial Hg pollution present in Laguna Lobato sediment represents native Hg within the silver ore at Potosí. Hg has a high vapour pressure and any Hg present as a trace-constituent in the ore would have been rapidly emitted to the atmosphere during smelting. The highest-grade surface ores may have exceeded 25% Ag (Craig, 1989), and apparently contained large amounts of Hg as well. Moreover, total [Hg] within the ore appears to have changed with time, as Hg EF gradually decreases throughout the pre-Colonial era (Fig. 4.6).

There is independent support for our suggestion that pre-Colonial smelting released large quantities of Hg to the regional environment. Cerro Rico de Potosí is drained by the Río Pilcomayo, which is the largest river system in southern Bolivia. To estimate the environmental impact of both modern and ancient mining activity on the Río Pilcomayo, Hudson-Edwards et al. (2001) measured the concentration of Pb, Ag, Hg, and other metals in contemporary and buried channel deposits and in modern and ancient terraces down the course of the Río Pilcomayo. Remarkably, these authors found elevated Hg burdens (but not Pb, Ag or any other metals) in organic-rich terrace deposits that $^{14}C$ date to 1220-1435 AD, thus predating the adoption of Hg amalgamation at Potosí. The concentration

of Hg in these ancient organic-rich units exceeded 5000 ppb, and they contained the highest Hg levels measured along the Río Pilcomayo. However, Hudson-Edwards et al. (2001) were unaware of the long pre-Colonial mining history at Potosí and therefore lacked an explanation for the pre-Colonial Hg enrichment. Our new data reconcile these data by suggesting that pre-Colonial mining activities were a vector for both atmospheric Hg emissions and increased Hg supply to the Rio Pilcomayo.

The Spanish arrived at Potosí in 1545 AD and immediately took control of mining at Potosí (Bakewell, 1984). Soon after silver-rich surface ores were depleted and mercury amalgamation was adopted as the predominate ore-processing method. Mercury amalgamation was preformed in large open-air patios and was thus known as patio amalgamation. The patio process allowed for large amounts of ore, containing as little as 400 g Ag per 1 Mg of ore to be extracted profitably (Nriagu, 1994). In modern mercury amalgamation operations, the ratio of mercury lost to silver produced ($R_{Hg/Ag}$) is commonly between 1.0 and 1.5 (Pfeiffer and Lacerda, 1988; van Straaten, 2000; Lacerda, 2003). In Tanzania and Zimbabwe, 70-80% of the Hg lost is emitted to the atmosphere whereas only 20-30% is lost to tailings, soils, stream sediments and water (van Straaten, 2000). Similar results have been reported from Brazil (Lacerda, 1997). During the Colonial era, Nriagu (1994) suggested a similar average $R_{Hg/Ag}$ of 1.5, and that 60-65% of the mercury lost was released to the atmosphere. This suggests New World amalgamation activities released 156,000 Mg of mercury to the atmosphere and over 250,000 Mg of mercury to the environment Nriagu (1993; 1994). During the Colonial era, Potosí accounted for 25-50% of the total silver produced globally (Fisher, 1977), and therefore likely emitted between 50,000 and 100,000 Mg of mercury to the atmosphere. These estimates remain highly conservative because (i) patio amalgamation likely had a higher $R_{Hg/Ag}$ than modern-day

mining operations, and (ii) some of the silver mined during the Colonial era went unregistered.

To estimate atmospheric Hg emissions associated with pre-Colonial smelting we calculated sediment Hg pollution burdens for pre-Colonial, Colonial, and industrial time periods (Table 4.2). The excess Hg pollution burden represents the difference between the total inventory of Hg on the lake bottom and the expected natural inventory, if no anthropogenic Hg enrichment had occurred. Approximately 70% of the total Hg pollution inventory in Laguna Lobato sediment predates the adoption of amalgamation. As Hg amalgamation at Cerro Rico generated a minimum of 50,000 Mg of atmospheric mercury emissions, our sedimentary Hg record suggests that at least 125,000 Mg were emitted to the atmosphere during pre-Colonial smelting. While this estimate possesses several caveats, the largest being that Hg pollution burdens within Laguna Lobato sediment can be directly related to mercury emissions at Potosí through time, it remains a conservative estimate because a greater fraction of ore-hosted mercury would have been emitted relative to amalgamation, where some mercury was recaptured.

**Table 4.2.** Average [Hg], Hg enrichment factors (EF), Hg flux, and Hg pollution burdens for different temporal intervals including: Inca and pre-Inca smelting, Colonial amalgamatioon, and industrial mining.

| Period | [Hg] | Hg EF | Hg flux | Hg pollution burdens (mg $cm^{-2}$) | n |
|---|---|---|---|---|---|
| Pre-pollution (pre-1100 AD) | 95 | 1 | 14 | - | 6 |
| Inca & pre-Inca (1100-1550 AD) | 1049 | 11 | 143 | 69 | 21 |
| Colonial amalgamation (1575-1900 AD) | 613 | 6 | 104 | 27 | 20 |
| Industrial (post-1900) | 214 | 2 | 55 | 4 | 24 |

*Mercury in global ores*

Measurements of [Hg] within ores suggest that Hg enrichment in non-ferrous ores is widespread (Table 4.1; Fig. 4.5). Hg concentrations in the sampled ores ($n$=109) average 90.4±11.9 ppm, which is ~1500 times the lithospheric average of 0.06 ppm (Wedepohl, 1995). However, considerable heterogeneity exists both within and among ore types, because [Hg] is frequently controlled by mineralogical variability or local depositional conditions. In a detailed study of the Hg content of Zn deposits, Schwartz (1997) suggested that the Hg content of Zn ores also depends on ore type and age. For example, sphalerites (ZnS) from Proterozoic exhalative deposits contain more Hg than those from Phanerozoic deposits. However, concentrations of Hg are high in many types of ore (Fig. 4.5), and Hg occurrences in copper, silver, and gold ores are only beginning to be fully appreciated (Kerfoot et al., 2002, 2004, 2009). Nonetheless, the existing data is sufficient to identify a number of consistent trends, such as the consistently elevated [Hg] of native Ag deposits relative to other ore types (Table 4.1). The results of [Hg] in global ores suggest that non-ferrous metal smelters may serve as important point sources for Hg emissions that have, until now, been severely underestimated in both pre- and post-industrial contexts.

## Conclusions

The sediment record from Laguna Lobato near Potosí demonstrates a long history of New World metal pollution extending back over one thousand years. Most previous studies have focused on lead, largely because of its immobility in lake, peat, and ice core deposits, and the utility of lead stable isotopes for fingerprinting anthropogenic emissions. However, a growing body of evidence suggests significant and widespread mercury pollution beginning as early as ~1400 BC

(Cooke et al., 2009a). Early mercury pollution resulted from both the mining of cinnabar (Cooke et al., 2009a) and the use of mercury in amalgamation (Cooke et al., 2009b). The results from this study demonstrate that pre-Colonial silver smelting was potentially a major source of Hg pollution in the Andes. If these results apply to early silver, copper, and gold extraction elsewhere, as is suggested by elevated [Hg] in many economic ore types, extensive pre-industrial mercury pollution may be similarly encountered elsewhere, for example in association with the Roman Empire in Europe. Consequently, the possibility exists that pre-industrial anthropogenic mercury pollution inventories have been grossly and systematically underestimated.

**References**


Abbott, M. B. & Wolfe, A. P. (2003) Intensive pre-Incan metallurgy recorded by lake sediments from the Bolivian Andes. *Science,* 301**,** 1893-1895.

Bakewell, P. (1984) *Miners of the red mountain: Indian labor at Potosí, 1545-1650,* Albuquerque, University of New Mexico Press.

Bartos, P. J. (2000) The pallacos of Cerro Rico de Potosi, Bolivia: a new deposit type. *Economic Geology,* 95**,** 645-654.

Cooke, C. A., Abbott, M. B. & Wolfe, A. P. (2008) Late-Holocene atmospheric lead deposition in the Peruvian and Bolivian Andes. *The Holocene,* 18**,** 353-359.

Cooke, C. A., Abbott, M. B., Wolfe, A. P. & Kittleson, J. L. (2007) A millennium of metallurgy recorded by lake sediments from Morococha, Peruvian Andes. *Environmental Science & Technology,* 41**,** 3469-3474.

Cooke, C. A., Balcom, P. H., Biester, H. & Wolfe, A. P. (2009a) Over three millennia of mercury pollution in the Peruvian Andes. *Proceedings of the National Academy of Sciences,* 106**,** 8830-8834.

Cooke, C. A., Wolfe, A. P. & Hobbs, W. O. (2009b) Lake-sediment geochemistry reveals 1400 years of evolving extractive metallurgy at Cerro de Pasco, Peruvian Andes. *Geology,* 37**,** 1019-1022.

Craig, A. K. (1989) Mining ordenanzas and silver production at Potosí: the Toledo reforms. IN Van Cauwenberghe, E. (Ed.) *Precious metals, coinage, and the changes in monetary structures in Latin America, Europe, and Asia.* Leuven, Netherlands, Leuven University Press.

Epa (1998) Mercury in solids and solutions by thermal decomposition, amalgamation, and atomic absorption spectrophotometry. *EPA Method 7473 Report.* Washington, DC, Environmental Protection Agency.

Fisher, J. R. (1977) *Silver mines and silver miners in colonial Peru, 1776-1824,* Liverpool, Centre for Latin American Studies, University of Liverpool.

Hong, S., Candelone, J.-P., Patterson, C. C. & Boutron, C. F. (1994) Greenland ice evidence of hemispheric lead pollution two millennia ago by Greek and Roman Civilizations. *Science,* 265**,** 1841-1843.

Hudson-Edwards, K. A., Macklin, M. G., Miller, J. R. & Lechler, P. J. (2001) Sources, distribution and storage of heavy metals in the Río Pilcomayo, Bolivia. *Journal of Geochemical Exploration,* 72**,** 229-250.

Kerfoot, W. C., Harting, S. L., Jeong, J., Robbins, J. A. & Rossmann, R. (2004) Local, regional, and global Implications of elemental mercury in metal (copper, silver, gold, and zinc) ores: Insights from Lake Superior sediments. *Journal of Great Lakes Research,* 30**,** 162-184.

Kerfoot, W. C., Harting, S. L., Rossmann, R. & Robbins, J. A. (2002) Elemental mercury in copper, silver and gold ores: an unexpected contribution to Lake Superior sediments with global implications. *Geochemistry: Exploration, Environment, Analysis,* 2**,** 185-202.

Kerfoot, W. C., Jeong, J. & Robbins, J. A. (2009) Lake Superior mining and the proposed mercury zero-discharge region. IN Munawar, M. & Munawar, I. F. (Eds.) *State of Lake Superior.* Burlington, Canada, Ecovision World Monograph Series, Aquatic Ecosystem Health & Management Society, 153-216.

Lacerda, L. D. (1997) Global mercury emissions from gold and silver mining. *Water, Air, & Soil Pollution,* 97**,** 209-221.

Lacerda, L. D. (2003) Updating global Hg emissions from small-scale gold mining and assessing its environmental impacts. *Environmental Geology,* 43**,** 308-314.

Lee, C. S. L., Qi, S.-H., Zhang, G., Luo, C.-L., Zhao, L. Y. L. & Li, X.-D.

(2008) Seven thousand years of records on the mining and utilization of metals from lake sediments in central China. *Environmental Science & Technology,* 42**,** 4732-4738.

Martínez-Cortizas, A., García-Rodeja, E., Pontevedra Pombal, X., Nóvoa Muñoz, J. C., Weiss, D. & Cheburkin, A. (2002) Atmospheric Pb deposition in Spain during the last 4600 years recorded by two ombrotrophic peat bogs and implications for the use of peat as archive. *The Science of the Total Environment,* 292**,** 33-44.

Nriagu, J. O. (1993) Legacy of mercury pollution. *Nature,* 363**,** 589.

Nriagu, J. O. (1994) Mercury pollution from the past mining of gold and silver in the Americas. *The Science of the Total Environment,* 149**,** 167-181.

Pfeiffer, W. C. & Lacerda, L. D. (1988) Mercury inputs into the Amazon region, Brazil. *Environmental Technology Letters,* 9**,** 325-330.

Renberg, I., Persson, M. W. & Emteryd, O. (1994) Pre-industrial atmospheric lead contamination detected in Swedish lake sediments. *Nature,* 368**,** 323-326.

Schwartz, M. O. (1997) Mercury in zinc deposits: economic geology of a pollution element. *International Geology Review,* 39**,** 905-923.

Van Straaten, P. (2000) Mercury contamination associated with small-scale gold mining in Tanzania and Zimbabwe. *The Science of the Total Environment,* 259**,** 105-113.

Wedepohl, K. H. (1995) The composition of the continental crust. *Geochimica et Cosmochimica Acta,* 59**,** 1217-1232.

# CHAPTER 5: RELIANCE ON $^{210}$Pb CHRONOLOGY CAN COMPROMISE THE INFERENCE OF PRE-INDUSTRIAL Hg FLUX TO LAKE SEDIMENTS

## Introduction

Human activities have profoundly altered the global cycle of mercury (Hg) (Lindberg et al., 2007). However, the lack of long-term monitoring of Hg deposition limits the ability to quantify anthropogenic disruptions to the Hg cycle. Natural archives, including lake sediment cores, ice cores, and peat bogs, can provide continuous records of Hg deposition through time (Biester et al., 2007; Schuster et al., 2002). Lake sediments are thought to be the most reliable archive of past Hg deposition (Biester et al., 2007), and a growing number of cores record an approximately 3-fold increase in Hg deposition rates since 1850-1900 AD (Biester et al., 2007; Muir et al., 2009).

Estimating past Hg fluxes (also known as Hg accumulation rates; typically $\mu g\ m^{-2}\ yr^{-1}$) requires two independently derived measurements: Hg concentration ($\mu g\ g^{-1}$) and dry mass sedimentation rate ($g\ m^{-2}\ yr^{-1}$). Quantifying [Hg] in natural media is well developed and can be crosschecked with standard reference materials. However, sedimentation rates must be estimated using models of core chronology, for which uncertainties are propagated to the estimate of Hg flux. Accurate dating of lake sediments is thus paramount for estimating past Hg flux.

For Hg studies, sedimentation rates are most often estimated using $^{210}$Pb geochronology (e.g. Biester et al., 2007; Muir et al., 2009). $^{210}$Pb has a half-life of 22.3 years, and its usefulness as a geochronological tool in paleolimnology

---

*Previously published material: Cooke C. A., Hobbs, W. O., Michelutti, N., & Wolfe, A. P. (2010) Reliance on $^{210}$Pb chronology can compromise the inference of pre-industrial Hg flux to lake sediments. *Environmental Science & Technology*, 44, 1998-2003.

is limited to the past 100-150 years (Appleby, 2001). $^{210}$Pb-derived ages and sedimentation rates for each core interval are typically calculated using either the constant flux:constant sedimentation (CF:CS) or constant rate of supply (CRS) models, and the chronology derived depends (at least in part) on the model selected (Appleby, 2001). The estimate of sediment ages (and sedimentation rates) beyond the range of $^{210}$Pb requires either an extrapolation of the $^{210}$Pb-derived chronology, or the incorporation of additional geochronological tools.

Radiocarbon ($^{14}$C) dating is the most widely applied geochronometer for reconstructing environmental change over the Holocene. Accelerator Mass Spectrometry (AMS) $^{14}$C dating allows for precise measurements on even very small sample sizes (~0.05 mg C), and offers the opportunity to target discrete fractions within sediment horizons (Jull and Scott, 2007). However, AMS $^{14}$C dating has been rarely included in paleolimnological reconstructions of past Hg deposition (see Biester et al., 2007 and references therein), despite the potential for improving the assessment of sedimentation rates beyond the limit of $^{210}$Pb dating. Here, we demonstrate that relying solely on $^{210}$Pb chronologies risks overestimating the rate of natural, pre-anthropogenic Hg accumulation. This in turn has ramifications for understanding the legacy of anthropogenic Hg pollution.

## Methods and materials

### *Study site*

We selected four remote study lakes representing different end members in their environmental setting and in potential exposure to anthropogenic Hg emissions (Fig. C.1; Table C.1). The first two lakes, Lagunas Yanacocha 2 (hereafter LY2) and Negrilla, are located in the central Peruvian Andes. Both lakes were exposed to pre-industrial Hg pollution generated by the mining and processing of cinnabar

(HgS) ore at Huancavelica, Peru (Cooke et al., 2009). A detailed examination of the pre-industrial mining legacy preserved in both LY2 and Negrilla sediments has been presented in detail previously, showing an initial rise in Hg pollution beginning ~1400 BC (Cooke et al., 2009). These are contrasted with two lakes from the east coast of Baffin Island, Arctic Canada: Lost Pack and CF8. Surface cores from both lakes have been described in previous publications (Michelutti et al., 2005; Thomas et al., 2008). In contrast to the Peruvian lakes, the exposure of Lost Pack and CF8 to pre-industrial Hg pollution should have been minimal, although arctic lakes record 20$^{th}$ century Hg pollution (Muir et al., 2009).

*Sediment geochemistry*

Total sediment Hg was quantified using a DMA80 direct mercury analyzer (Milestone Inc., CT), duplicates, and standard reference materials were run every 10$^{th}$ sample (EPA, 1998). Total organic matter content of the sediment was determined using loss on ignition (% LOI 550°C) (Heiri et al., 2001). Sediment [Hg] from LY2, Negrilla, and Lost Pack were determined at 0.5 cm intervals and 0.25 cm in the CF8 core.

*Core chronologies*

To constrain recent sedimentation, $^{210}$Pb activities were measured using $\alpha$-spectroscopy. Supported $^{210}$Pb was estimated from the asymptotic activity at depth (the mean of the lowermost samples in a core), and was subtracted from total $^{210}$Pb activity measured at each level to derive unsupported $^{210}$Pb inventories. The constant rate of supply (CRS) model was used to calculate sedimentation rates and the age of each dated interval. Errors associated with $^{210}$Pb dates were estimated from counting uncertainties (Appleby, 2001). To provide independent estimates of sediment age underlying excess $^{210}$Pb, AMS $^{14}$C dates were obtained

on all cores. In the Andes, carbonized grass macrofossils were dated. Charcoal is terrestrial in origin and is unlikely to experience long soil-residence times, and thus is a highly reliable dating target (Brown et al., 2005; Nelson et al., 2006). For the two arctic lakes, aquatic moss macrofossils were dated; these have been shown to be appropriate for $^{14}C$ dating in ecosystems containing little to no terrestrial vegetation (Wolfe et al., 2004). AMS $^{14}C$ dates were calibrated within Calib 5.0 using the SHCal (LY2 and Negrilla) (McCormac et al., 2004) and IntCal04 (Lost Pack and CF8) (Reimer et al., 2004) calibration curves and are unchanged from previous publications (Cooke et al., 2009; Michelutti et al., 2005; Thomas et al., 2008).

Two age-depth models were subsequently developed for each core. The first relied solely upon the $^{210}Pb$ chronologies and extrapolation to the core base. The extrapolation of $^{210}Pb$ dates assumes *a priori* that a single, long-term value of sedimentation rate can be derived from $^{210}Pb$ analysis of the upper core intervals (Appleby, 2001; Binford, 1990). This assumption is usually considered tenable if profiles of water content, organic matter, and sediment density remain relatively constant down-core (e.g. Lamborg et al., 2002). Extrapolated sediment ages were calculated following Binford (1990) using the equation:

$$t_e = t_b + [(m_x - m_b) \div s_e]$$

where $t_e$ is the extrapolated age at depth $x$ in years, $t_b$ is the age at the lowest depth with unsupported $^{210}Pb$, $m_x$ is the cumulative mass at depth $x$ in g $cm^{-2}$, $m_b$ is the cumulative mass at the lowest depth with unsupported $^{210}Pb$, and $s_e$ is the $^{210}Pb$-estimated sedimentation rate. If the sedimentation rate was variable over the period of unsupported $^{210}Pb$ activity, then the lowest sedimentation rate value was used for $s_e$. A second age-depth model was constructed for each core using a mixed-effects model (Heegaard et al., 2005). This composite age-depth model uses the $^{210}Pb$ CRS dates for the past 100 years, and provides a best-fit age

estimate for those intervals that are >100 years old. The composite age-depth model integrates the error associated with each individual date and between dates.

*Calculations of Hg fluxes*

CRS sedimentation rates and Hg concentrations were used to calculate Hg flux spanning the past ~100 years. Below the limit of $^{210}$Pb (i.e. below the lower-most CRS date), Hg flux was estimated using the two different age-depth models developed for each core. The first estimate of Hg flux was calculated by multiplying Hg concentrations by the same sedimentation rate used to extrapolate $^{210}$Pb dates. This remains the most common approach used to estimate pre-industrial Hg flux from lake sediment cores (e.g. Biester et al., 2007; Muir et al., 2009). A second estimate of Hg flux ($Hg_{flux}$) was calculated using:

$$Hg_{flux} = s \times d \times Hg_i$$

where $s$ is the sediment accumulation rate between core intervals derived from the combined $^{210}$Pb-$^{14}$C chronology (cm yr$^{-1}$), $d$ is the dry density (g cm$^{-3}$) at each core interval, and $Hg_i$ is the concentration of Hg within each core interval (μg g$^{-1}$).

**Results and Discussion**

*Sediment Hg concentrations and core stratigraphies*

At LY2, [Hg] is characterized by a relatively stable background of 0.34±0.06 μg g$^{-1}$ below ~85 cm depth (Fig. 5.1). Above this depth, [Hg] increases to >1 μg g$^{-1}$, fluctuating between 1 μg g$^{-1}$ and 5 μg g$^{-1}$ until ~20 cm when it increases abruptly again before subsequently declining towards the top of the core. At Negrilla, [Hg] is stable and low below ~50 cm, averaging 0.18±0.04 μg g$^{-1}$. [Hg] increases above ~50 cm to >1 μg g$^{-1}$, and gradually declines up-core, reaching background values by the uppermost intervals. In the two arctic lakes, [Hg] displays considerable

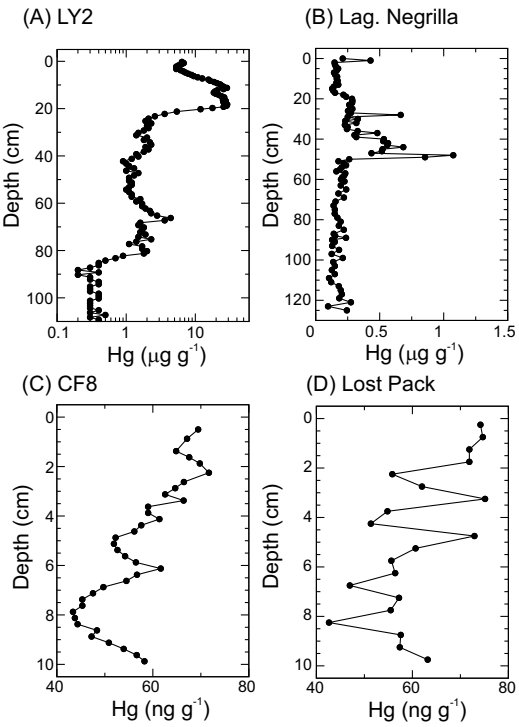


**Fig. 5.1.** Down-core profiles of Hg concentration for all four study lakes.

variability, superimposed on gradually increasing trends (Fig. 5.1). At CF8, [Hg] rises from a minimum value of 42 ng $g^{-1}$, to a surface concentration of 70 ng $g^{-1}$. At Lost Pack, [Hg] displays greater variability; however Hg concentrations are within the same range as at CF8 (40-80 ng $g^{-1}$). These [Hg] concentrations are directly comparable to other arctic lakes (Muir et al., 2009). Profiles of dry density and organic matter content are presented in Fig. C.2. None of the shifts in dry density are paralleled by shifts in organic content within the cores, suggesting that differences in density reflect variable water content and the effect of compaction, rather than changes in sediment composition. This is commonly thought to represent an ideal situation for the extrapolation of $^{210}$Pb dates (e.g. Lamborg et al., 2002).

*Core chronologies*

At all four study lakes, $^{210}$Pb activity declines to stable supported levels, and the CRS model was used to calculate sediment ages spanning the past century (Fig. 5.2) (Appleby, 2001). Below unsupported $^{210}$Pb intervals however, there are major discrepancies between the extrapolated and composite age models, the latter yielding much older basal dates in each case (Fig. 5.3). This discrepancy is greatest in the two arctic lake cores. The smallest offset is observed at

Negrilla, where the extrapolated $^{210}$Pb age model first overestimates and then underestimates the composite age model, reaching a $\Delta^{14}$C of ~1000 years at the core base. Thus, at all four of the study lakes presented here a difference exists between the extrapolated $^{210}$Pb model and the composite age-depth model suggesting changes in lake sedimentation rates with time.

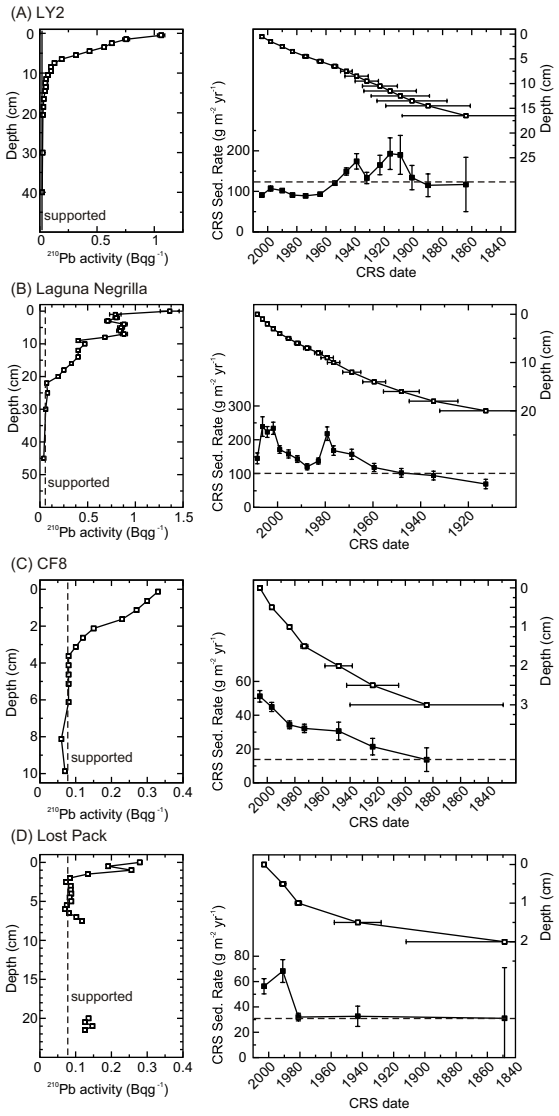


**Fig. 5.2.** Down-core profiles of total and supported (dashed line) $^{210}$Pb activities for all four study lakes. Also shown are the CRS dates and sedimentation rates for each lake. The dashed line indicates the extrapolated $^{210}$Pb sedimentation rates.

*Pre-industrial Hg flux estimates*

Pre-industrial Hg fluxes were calculated using both age-depth models (Table C.2). At all four lakes, pre-industrial Hg flux calculated using the extrapolated $^{210}$Pb age-depth model are consistently higher than those calculated using the composite age-depth model (Fig. 5.4). The differences between the two estimates of pre-industrial Hg flux reflect the incorporation of $^{14}$C dates into the core chronologies, and the attendant changes in pre-industrial sedimentation rates. The $^{14}$C dates from LY2, CF8 and Lost Pack suggest a decrease in lake sedimentation rates sometime between the uppermost

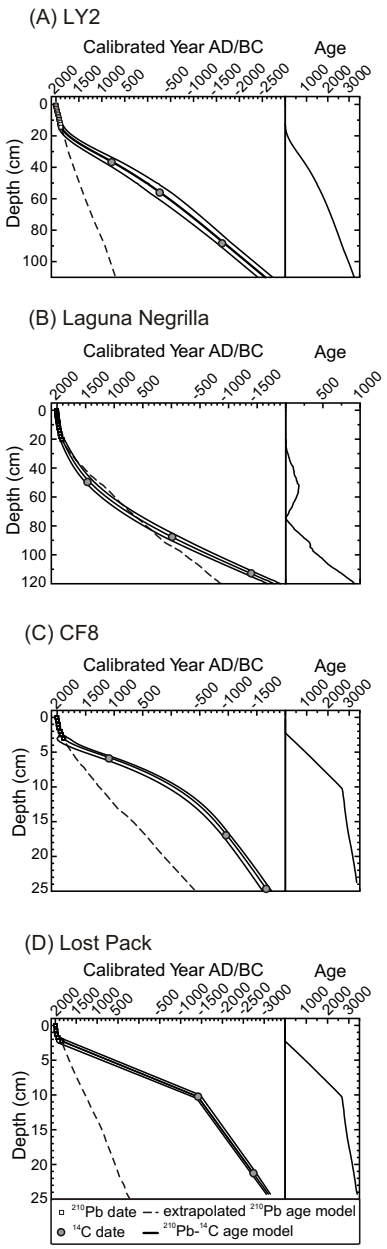


**Fig. 5.3.** Plots of both the extrapolated $^{210}$Pb age model (dashed line) and the composite $^{210}$Pb-$^{14}$C age model (heavy line) with 95% confidence intervals (thin lines) for all four study lakes.

---

$^{14}$C date and the lowermost $^{210}$Pb date. While constraining the exact timing of this decrease in sedimentation rates would require additional $^{14}$C dates, it remains nonetheless apparent that sedimentation rates were slower pre-1900 AD than post-1900AD.

*Implications for pre-industrial Hg exploitation*

Profiles of Hg flux from both LY2 and Negrilla demonstrate the presence of pre-industrial Hg pollution resulting from regional cinnabar mining at Huancavelica, Peru (Fig. 5.4) (Cooke et al., 2009). The earliest increase in Hg occurs in LY2 sediment at ~1400 BC (~80 cm depth). A subsequent increase in Hg is preserved ~1500 AD (~20 cm depth), suggesting an intensification of mining activities at this time. This latter rise in Hg is also preserved at Negrilla, reflecting the adoption of cinnabar smelting at Huancavelica and the long-range transport of Hg emissions (Cooke et al., 2009). The recovery of long sediment records, and the incorporation of $^{14}$C dates, is therefore critical towards providing an accurate history of Hg enrichment in regions exposed to pre-industrial Hg emissions from artisanal mining activities. Short sediment cores (e.g. a typical gravity core) that are only

$^{210}$Pb-dated will fail to capture the true antiquity of Hg pollution in these regions, and may overestimate pre-industrial Hg fluxes.

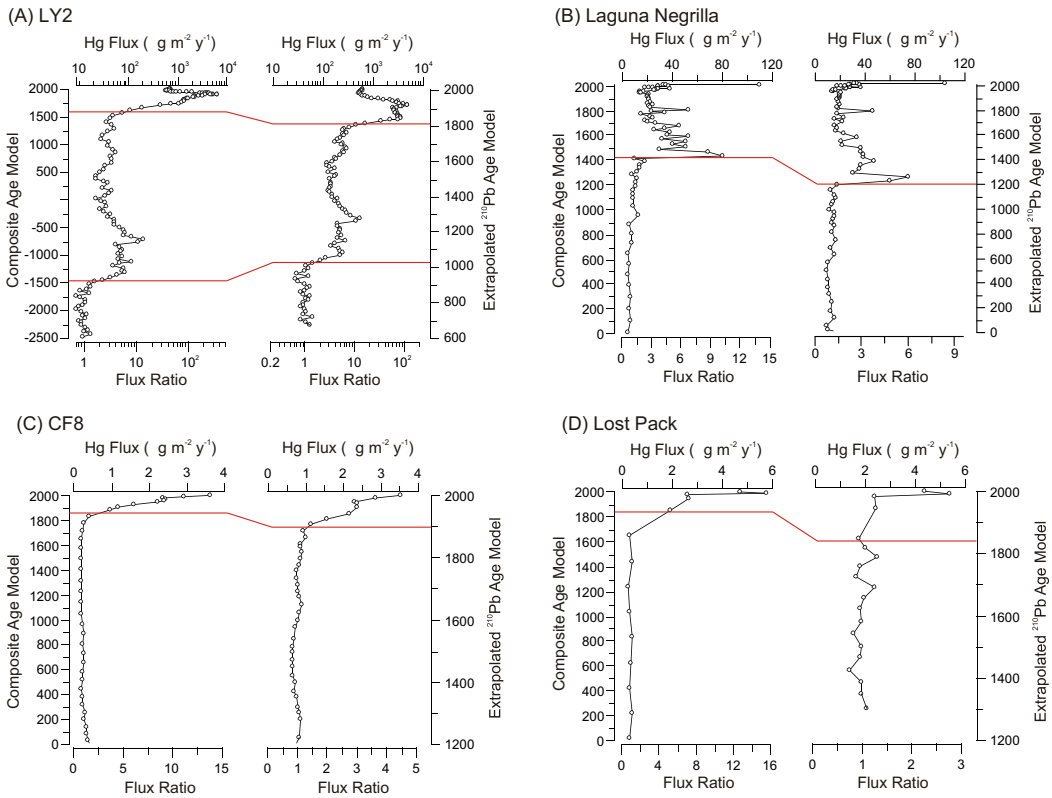


**Fig. 5.4.** Hg fluxes and flux ratios for all four study lakes. Fluxes and flux ratios were calculated using both the composite ($^{210}$Pb and $^{14}$C) age model and the extrapolated $^{210}$Pb age model for each core. Flux ratios are unitless (sample:background) and capture the relative increase in Hg flux at each study site. Background Hg fluxes were calculated as the average Hg flux prior to the earliest evidence for Hg enrichment. Red lines join the same sediment depths across both models, and highlight the age discrepancies between the two Hg flux estimates.

*Implications for Canadian arctic lakes*

In the two arctic lakes, extrapolating basal $^{210}$Pb dates yields pre-industrial fluxes of ~1 μg m$^{-2}$ yr$^{-1}$ and ~2 μg m$^{-2}$ yr$^{-1}$ at CF8 and Lost Pack, respectively (Fig. 5.4). While these $^{210}$Pb-based estimates are in general agreement with previous

estimates (Biester et al., 2007), none of these previous studies incorporated $^{14}C$ dating into their core chronologies. In contrast, the composite $^{210}Pb$-$^{14}C$ fluxes suggest pre-industrial Hg accumulation rates of <0.5 μg $m^{-2}$ $yr^{-1}$ for both lakes, well below the $^{210}Pb$-based estimates. Thus, the differences between the $^{14}C$ and $^{210}Pb$ estimates of pre-industrial Hg flux suggest that previous estimates of pre-industrial Hg accumulation in the Arctic may be over-estimated. Other studies have similarly concluded that sedimentation rates have increased across arctic lakes. In a recent study of 50 lakes spanning eastern and northern Canada, Muir et al. (2009) found that half of the arctic lakes studied had experienced an increase of 10% or greater in sedimentation rates over the $^{210}Pb$-dated portion of the core. Lakes across much of this region are undergoing profound hydrological and biological changes as a result of recent warming, including increased summer evaporation (Smol and Douglas, 2007), changes in algal community assemblages (Smol et al., 2005), and increases in both primary production (Michelutti et al., 2005) and inorganic sedimentation (Hughen et al., 2000; Thomas and Briner, 2009). It seems likely that similar processes have contributed to the sedimentation histories documented here.

*Hg flux ratios and the magnitude of anthropogenic Hg enrichment*

A critical assumption in using lake sediments to estimate past Hg deposition rates is that they provide a robust record of Hg delivery to lakes. The loading of Hg can be influenced by watershed size and characteristics (Mills et al., 2009), catchment:lake area ratios (Swain et al., 1992), sediment focusing (Van Metre and Fuller, 2009), and volatile losses of Hg prior to sequestration (Southworth et al., 2007). Nonetheless, a broad array of data supports the assertion that relative changes in Hg accumulation within an individual core can be attributed to relative changes in Hg loading (Engstrom et al., 1994). Assuming site-specific factors

remain constant over time, the relative change in Hg accumulation from modern to background times (Hg flux ratio) provides a comparable measure of increases in atmospheric Hg deposition (Biester et al., 2007). Hg flux ratios can facilitate comparisons between cores, and provide a relative measure on how Hg deposition has changed over time.

The modern Hg flux ratio at LY2 is ~45 when the $^{14}C$ age-depth model is used, but is only 15 when the extrapolated $^{210}Pb$ dates are used (Fig. 5.4; Table C.2). Even at Negrilla, where the extrapolated $^{210}Pb$ dates provide a reasonable approximation of the true age-depth relationship, the modern $^{14}C$-based Hg flux ratio is ~5, versus ~2.5 when the extrapolated $^{210}Pb$ chronology is used. As with our lake sediment records, the Hg record from the Upper Fremont Glacier also implies a larger Hg flux ratio (Schuster et al., 2002). The Upper Fremont Glacier suggests a Hg flux ratio of ~20 during the mid-1980's followed by a decrease ~11 during the early 1990's. Similarly, trends in [Hg] in hard tissues, including teeth, hair, and feathers from arctic animals suggest an order-of-magnitude increase in arctic marine foodweb-based animals over the industrial era (Dietz et al., 2009). Our results raise the possibility that discordance between lake sediment cores, the Upper Fremont Glacier, and arctic animal tissues may be attributable to a lack of chronological control beyond ~1850 AD in the lake records.

Both arctic lakes record an Hg flux ratio of ~12 when the $^{14}C$ age-depth model is used (Fig. 5.4; Table C.2). In contrast, if extrapolated $^{210}Pb$ dates are used, the flux ratio for both lakes is 2-3, at least four times lower than the Hg flux ratio implied by $^{14}C$ chronologies. These results suggest that Hg delivery to the Arctic may have increased to a much larger degree than has been suggested previously.

The roughly 12-fold increase in Hg accumulation at CF8 and Lost Pack is dramatically higher than any other reconstructions of past Hg accumulation from

the Arctic of which we are aware. In a survey of lakes from Alaska, Landers et al. (1998) found Hg flux had increased by a factor of ~1, while Engstrom and Swain (1997) reported flux ratios of ~2 for southeast Alaska. Fitzgerald et al. (2005) reported a 3-fold increase in Hg fluxes for the same region. Bindler et al. (2001) examined Hg fluxes from lakes along the west coast of Greenland, and the flux ratios were between 2 and 5. A recent summary by Muir et al. (2009) includes 18 lake records of Arctic Hg accumulation, which collectively suggest an average flux ratio of ~2.

While one must exercise care when interpreting only limited numbers of records, the CF8 and Lost Pack Hg flux ratios are consistently higher than any previously published Hg flux ratios for the Arctic. This raises the possibility that previous lake sediment core studies may have underestimated both pre-industrial Hg flux rates and, as a result, the degree to which anthropogenic activities have altered Hg deposition in the Arctic. Ideally, one would obtain $^{14}C$ dates at regular intervals down the length of a sediment core. While this is rarely possible due to the availability of good dating targets, even a single date below the limit of $^{210}Pb$ can offer some degree of additional chronological control if appropriate material exists. Whenever possible, dates on bulk sediments should be avoided, especially in regions containing carbonate rocks or clastic material derived from lignite, coal and carbonaceous shales (Grimm et al., 2009). New AMS $^{14}C$ dates on existing Hg data sets would provide a revised appraisal of Hg enrichment, and may identify spatial heterogeneity in Hg deposition over the Arctic.

*Future efforts*

The lake records presented here place provisions on the assumption that stable sedimentation rates are reached near the base of unsupported $^{210}Pb$ activity. At all four study lakes, pre-industrial Hg fluxes are lower when $^{14}C$ dates are

incorporated into the age model. In the Andes, incorporating other means of dating is critical if the full history of pre-industrial Hg emissions is to be captured. In the Arctic, our results suggest pre-industrial Hg fluxes were <1 μg $m^{-2}$ $yr^{-1}$, and the Hg flux ratio is >10. In many cases, even a rudimentary $^{14}C$ chronology may be sufficient to confirm or refute extrapolated $^{210}Pb$ ages, and offers the opportunity to better constrain pre-industrial Hg flux. While $^{210}Pb$ dates should continue to be employed whenever possible, they should be augmented with other dating techniques to provide more accurate estimates of pre-industrial sedimentation histories and hence Hg flux. If the recent increase in Hg deposition is to be considered in a long-term context, there is a need to develop regional AMS $^{14}C$ chronologies that can be applied to both new and existing data sets.

**References**


Appleby, P. G. (2001) Chronostratigraphic techniques in recent sediments. IN Last, W. M. & Smol, J. P. (Eds.) *Tracking Environmental Changes Using Lake Sediments.*

Biester, H., Bindler, R., Martínez-Cortizas, A. & Engstrom, D. R. (2007) Modeling the past atmospheric deposition of mercury using natural archives. *Environmental Science & Technology,* 41**,** 4851-4860.

Bindler, R., Renberg, I., Appleby, P. G., Anderson, N. J. & Rose, N. L. (2001) Mercury accumulation rates and spatial patterns in lake sediments from west Greenland: A coast to ice margin transect. *Environmental Science & Technology,* 35**,** 1736-1741.

Binford, M. W. (1990) Calculation and uncertainty analysis of $^{210}$Pb dates for PIRLA project lake sediment cores. *Journal of Paleolimnology,* 3**,** 253-267.

Brown, K. J., Clark, J. S., Grimm, E. C., Donovan, J. J., Mueller, P. G., et al. (2005) Fire cyces in North American interior grasslands and their relation to prairie drought. *Proceedings of the National Academy of Sciences USA,* 102**,** 8865-8870.

Cooke, C. A., Balcom, P. H., Biester, H. & Wolfe, A. P. (2009) Over three millennia of mercury pollution in the Peruvian Andes. *Proceedings of the National Academy of Sciences,* 106**,** 8830-8834.

Dietz, R., Outridge, P. M. & Hobson, K. A. (2009) Anthropogenic contributions to mercury levels in present-day Arctic animals-A review. *Science of the Total Environment,* 407**,** 6120-6131.

Engstrom, D. R. & Swain, E. B. (1997) Recent declines in atmospheric mercury deposition in the upper midwest. *Environmental Science & Technology,*

31, 960-967.

Engstrom, D. R., Swain, E. B., Henning, T. A., Brigham, M. E. & Brezonik, P. L. (1994) Atmospheric mercury deposition to lakes and watersheds-A quantitative reconstruction from multiple sediment cores. IN Baker, L. A. (Ed.) *Environmental Chemistry of Lakes and Reservoirs.* Washington, DC, American Chemical Society.

EPA (1998) Mercury in solids and solutions by thermal decomposition, amalgamation, and atomic absorption spectrophotometry. *EPA Method 7473 Report.* Washington, DC, Environmental Protection Agency.

Fitzgerald, W. F., Engstrom, D. R., Lamborg, C. H., Tseng, C. M., Balcom, P. H., et al. (2005) Modern and historic atmospheric mercury fluxes in northern Alaska: global sources and Arctic depletion. *Environmental Science & Technology,* 39, 557-568.

Grimm, E. C., Maher Jr, L. J. & Nelson, D. M. (2009) The magnitude of error in conventional bulk-sediment radiocarbon dates from central North America. *Quaternary Research,* 72, 301-308.

Heegaard, E., Birks, H. J. B. & Telford, R. J. (2005) Relationships between calibrated ages and depth in stratigraphical sequences: An estimation procedure by mixed-effect regression. *The Holocene,* 15, 612-618.

Heiri, O., Lotter, A. F. & Lemcke, G. (2001) Loss on ignition as a method for estimating organic and carbonate content in sediments: reproducibility and comparability of results. *Journal of Paleolimnology,* 25, 101-110.

Hughen, K. A., Overpeck, J. T. & Anderson, R. F. (2000) Recent warming in a 500-year palaeotemperature record from varved sediments, Upper Soper Lake, Baffin Island, Canada. *The Holocene,* 10, 9-19.

Jull, A. J. T. & Scott, A. E. (2007) Radiocarbon Dating: AMS Method. *Encyclopedia of Quaternary Science.* Oxford, Elsevier.

Lamborg, C. H., Fitzgerald, W. F., Damman, A. W. H., Benoit, J. M., Balcom, P. H., et al. (2002) Modern and historic atmospheric mercury fluxes in both hemispheres: global and regional mercury cycling implications. *Global Biogeochemical Cycles,* 16**,** 1104.

Landers, D. H., Gubala, C., Verta, M., Lucotte, M., Johansson, K., et al. (1998) Using lake sediment mercury flux ratios to evaluate the regional and continental dimensions of mercury deposition in arctic and boreal ecosystems. *Atmospheric Environment,* 32**,** 919-928.

Lindberg, S., Bullock, R., Ebinghaus, R., Engstrom, D., Feng, X., et al. (2007) A synthesis of progress and uncertainties in attributing the sources of mercury in deposition. *Ambio: A Journal of the Human Environment,* 36**,** 19-33.

McCormac, F. G., Hogg, A. G., Blackwell, P. G., Buck, C. E., Higham, T. F. G., et al. (2004) ShCal04 Southern Hemisphere calibration, 0-11.0 cal kyr BP. *Radiocarbon,* 46**,** 1087-1092.

Michelutti, N., Wolfe, A. P., Vinebrooke, R. D., Rivard, B. & Briner, J. P. (2005) Recent primary production increases in arctic lakes. *Geophysical Research Letters,* 32.

Mills, R. B., Paterson, A. M., Blais, J. M., Lean, D. R. S., Smol, J. P., et al. (2009) Factors influencing the achievement of steady state in mercury contamination among lakes and catchments of south-central Ontario. *Canadian Journal of Fisheries and Aquatic Sciences,* 66**,** 187-200.

Muir, D. C. G., Wang, X., Yang, F., Nguyen, N., Jackson, T. A., et al. (2009) Spatial trends and historical deposition of mercury in eastern and northern Canada inferred from lake sediment cores. *Environmental Science & Technology,* 43**,** 4802-4809.

Nelson, D. M., Hu, F. S., Grimm, E. C., Curry, B. B. & Slate, J. E. (2006) The

influence of aridity and fire on Holocene prairie communities in the eastern Prairie Peninsula. *Ecology,* 87**,** 2523-2536.

Reimer, P. J., Baillie, M. G. L., Bard, E., Bayliss, A., Beck, J. W., et al. (2004) IntCal04 terrestrial radiocarbon age calibration, 0–26 cal kyr BP *Radiocarbon,* 46**,** 1029-1058.

Schuster, P. F., Krabbenhoft, D. P., Naftz, D. L., Cecil, L. D., Olson, M. L., et al. (2002) Atmospheric mercury deposition during the last 270 years: a glacial ice core record of natural and anthropogenic sources. *Environmental Science & Technology,* 36**,** 2303-2310.

Smol, J. P. & Douglas, M. S. V. (2007) Crossing the final ecological threshold in high Arctic ponds. *Proceedings of the National Academy of Sciences,* 104**,** 12395-12397.

Smol, J. P., Wolfe, A. P., Birks, H. J. B., Douglas, M. S. V., Jones, V. J., et al. (2005) Climate-driven regime shifts in the biological communities of arctic lakes. *Proceedings of the National Academy of Sciences USA,* 102**,** 4397-4402.

Southworth, G., Lindberg, S., Hintelmann, H., Amyot, M., Poulain, A., et al. (2007) Evasion of added isotopic mercury from a northern temperate lake. *Environmental Toxicology and Chemistry,* 26**,** 53-60.

Swain, E. B., Engstrom, D. R., Brigham, M. E., Henning, T. A. & Brezonik, P. L. (1992) Increasing rates of atmospheric mercury deposition in midcontinental North America. *Science,* 257**,** 784-787.

Thomas, E. & Briner, J. (2009) Climate of the past millennium inferred from varved proglacial lake sediments on northeast Baffin Island, Arctic Canada. *Journal of Paleolimnology,* 41**,** 209-224.

Thomas, E. K., Axford, Y. & Briner, J. P. (2008) Rapid 20$^{th}$ century environmental change on northeastern Baffin Island, Arctic Canada inferred from a multi-

proxy lacustrine record. *Journal of Paleolimnology,* 40**,** 507-517.

Van Metre, P. C. & Fuller, C. C. (2009) Dual-core mass-balance approach for evaluating mercury and $^{210}$Pb atmospheric fallout and focusing to lakes. *Environmental Science & Technology,* 43**,** 26-32.

Wolfe, A. P., Miller, G. H., Olsen, C. A., Forman, S. L., Doran, P. T., et al. (2004) Geochronology of high latitude lake sediments. IN Pienitz, R., Douglas, M. S. V. & Smol, J. P. (Eds.) *Long-term Environmental Change in Arctic and Antarctic Lakes.* Dordrecht, The Netherlands, Kluwer Academic Publishers.

# CHAPTER 6: PLACING RECENT ARCTIC MERCURY ACCUMULATION IN THE TEMPORAL CONTEXT OF MULTIPLE INTERGLACIATIONS

## Introduction

There is increasing concern regarding mercury (Hg) burdens within arctic foodwebs and ecosystems (AMAP, 2002). Anthropogenic activities emit Hg to the atmosphere primarily as gaseous elemental Hg ($Hg^0$), which is globally dispersed. Lake-sediment cores collected from across the Arctic suggest a one- to four-fold increase in Hg deposition since 1850-1900 AD, and testify to the global nature of anthropogenic Hg emissions (Fitzgerald et al., 2005; Landers et al., 1998; Muir et al., 2009). However, Hg accumulation in arctic lake sediment has not previously been considered in the context of millennial-scale natural variability.

Coupled to recent increases in Hg deposition is a rapid warming of arctic climate. This warming is driven primarily by an increase in greenhouse gas concentrations, amplified by strong cysopheric and aerosol feedbacks (Shindell and Faluvegi, 2009). Yet the magnitude of recent warming in the Arctic may not exceed early-Holocene summer temperatures associated with peak summer insolation (Wolfe and Smith, 2004). The fourth assessment report from the IPCC (Intergovernmental Panel on Climate Change) (2007) hypothesizes that climate warming may accelerate the delivery of contaminants from soils to arctic freshwater systems. Indeed, previous studies exploiting lake sediments (Cannon et al., 2003), peat cores (Biester et al., 2006; Martínez-Cortizas et al., 1999, 2007) and ice cores (Jitaru et al., 2009; Vandal et al., 1993) suggest that Hg-climate

---

*In preperation for submission: Cooke C. A., Balcom, P. H., Briner, J., P., & Wolfe, A. P. Placing recent Arctic mercury accumulation in the temporal context of multiple interglaciations. *Global Biogeochemical Cycles*.

couplings exist at various timescales, and that the pre-industrial natural cycle of Hg is dynamic. In addition, it has been suggested that recent climate warming may amplify Hg sequestration to arctic lake sediments via warming-driven increases in within-lake primary production (Carrie et al., 2009; Outridge et al., 2007; Stern et al., 2009).

While High-Arctic peat records of Hg accumulation suggest relatively low and stable rates of Hg deposition through the mid- to late-Holocene (Givelet et al., 2004), Hg in peat is strongly influenced by diagenetic transformations of the peat matrix and related mass loss (Biester et al., 2006, 2007; Biester et al., 2003; Martínez-Cortizas et al., 2007). Moreover, applying a reliable chronological framework to peat cores is limited by problems associated with both $^{210}$Pb (Biester et al., 2007) and $^{14}$C dating (Bindler et al., 2005) of peat deposits. Lake records on the other hand appear to provide a reliable record of past Hg deposition (Lockhart et al., 2000; Rydberg et al., 2008) and can be reliably dated using both $^{210}$Pb and $^{14}$C radioisotopes (Wolfe et al., 2004). When combined with multi-proxy studies from the same lake, past Hg-climate-ecosystem relationships can be investigated. Here we present multi-proxy sediment records from Lakes CF8 and CF3 from the east coast of Baffin Island, Canada to investigate natural Hg variability and Hg-climate couplings over millennial timescales, and place the 20$^{th}$ century in a unique, long-term perspective spanning multiple interglaciations.

## Materials and Methods

### *Study Sites*

Full descriptions of both the study lakes and the recovered sediment cores have been published previously (Axford et al., 2009a, 2009b; Briner et al., 2006, 2007; Michelutti et al., 2007, 2009; Thomas et al., 2008) and so are only summarized

here (Table 6.1). Both lakes are located near the hamlet of Clyde River on east-central Baffin Island, Nunavut Territory, Arctic Canada (Fig. 6.1). Lake CF8 is small (0.3 km$^2$) and shallow ($Z_{max}$=10 m), and is situated at 195 m asl. The lake rests within a steeply sloping catchment of 0.6 km$^2$, and there is a stream that flows through the lake during the ice-free season. Lake CF3 (70° 31'N, 68° 22'W; 27 m asl) is also a small (0.2 km$^2$) and shallow ($Z_{max}$=7 m) tundra lake within a 0.6 km$^2$ catchment containing little vertical relief. Prolonged ice cover characterizes both lakes with the ice-free season currently lasting only 2 or 3 months each year. Both lakes are similar to other lakes on the east coast of Baffin Island that are characterized by oligotrophic, highly dilute, slightly acidic water.

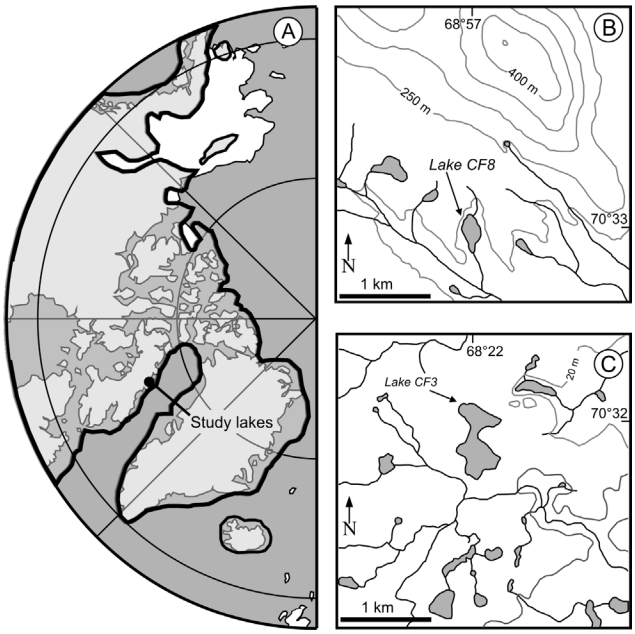


**Fig. 6.1.** (A) Map of the Canadian Arctic and the location of the two study lakes on the east coast of Baffin Island. Bold line indicates approximate extent of ice sheets during the Last Glacial Maximum. Also shown are detailed topographic maps of Lakes (B) CF8 and (C) CF3 and their catchments; contour lines are in 50 m and 20 m intervals, respectively.

**Table 6.1.** Physical characteristics of the study lakes.

| Lake | Latitude | Longitude | Elevation (m asl) | Zmax | Catchment area (km2) | Lake area (km2) | C:L area ratio | Surface inflow (Y/N) |
|---|---|---|---|---|---|---|---|---|
| CF8 | 70° 33' N | 68° 57' W | 195 | 10 | 1.5 | 0.30 | 5 | Y |
| CF3 | 70° 32' N | 68° 22' W | 27 | 7 | 0.6 | 0.20 | 3 | N |

*Core chronologies*

Our sedimentary analyses were preformed on the same cores first described by Briner et al., (2006) for Lake CF3, and by Thomas et al. (2008) and Briner et al., (2007) for Lake CF8. For Lake CF3, the sediment stratigraphy is a composite of two cores: a 21 cm surface core (Glew et al., 2001) and a 180 cm percussion core (Nesje, 1992). The Lake CF8 stratigraphy is a composite of a single surface core and multiple percussion cores which together preserve four organic-rich lake sediment units, each of which is separated by inorganic sands. Age-depth chronologies for the surface cores from both lakes were constructed using excess $^{210}$Pb activities coupled to accelerator mass spectrometry (AMS) $^{14}$C ages on aquatic bryophytes, which are demonstrably equilibrated with atmospheric $^{14}CO_2$ in arctic lakes within granitic basins (Wolfe et al., 2004). Age-depth models for both CF3 (Briner et al., 2006; Michelutti et al., 2007) and CF8 (Axford et al., 2009a; Briner et al., 2007; Michelutti et al., 2009; Thomas et al., 2008) have been discussed in detail in previous publications. The sedimentary sequence from Lake CF8 spans portions of the past three interglacial periods (Marine Isotope Stages (MIS) 1, 5e, and 7) and one interstadial (MIS 5a or 5c), and is described in detail in Briner et al. (2007).

*Sediment processing and data analyses*

New measurements of total [Hg] were determined using a DMA80 direct mercury analyzer at the University of Connecticut, Department of Marine Sciences (EPA, 1998). Average blank values, recoveries of standard reference material (mess-3 and tort-2), and the relative percent difference (RPD) between duplicate measurements are presented in Table D.1. A suite of additional proxies (loss on ignition (% LOI 550 °C), spectrally inferred Chlorophyll a (Chl *a*), and C:N), which have all been published previously (Axford et al., 2009a; Briner et al.,

2006), are also presented.

## Results

*Sediment Hg geochemistry*

At Lake CF3, [Hg] is lowest (~5 ng $g^{-1}$) immediately following deglaciation, increases gradually to ~40 ng $g^{-1}$ between 8.5 and 9.5 ka BP, and subsequently declines to ~25 ng $g^{-1}$ by ~1 ka BP (Fig. 6.2). A rapid increase in [Hg] is noted beginning ~100 years ago, and Hg concentrations reach 75 ng $g^{-1}$ during the mid-1970's (the uppermost interval measured). At Lake CF8, [Hg] displays considerable variability within all of the interglacials units (Fig. 6.3). During the early Holocene, [Hg] increases rapidly from 11 to 10.5 ka BP, rising from ~5 ng $g^{-1}$ to ~230 ng $g^{-1}$. Sediment [Hg] subsequently declines to ~45 ng $g^{-1}$ by 1 ka BP, before steadily increasing to a surface value of 70 ng $g^{-1}$ (Fig. 6.3). A similar,

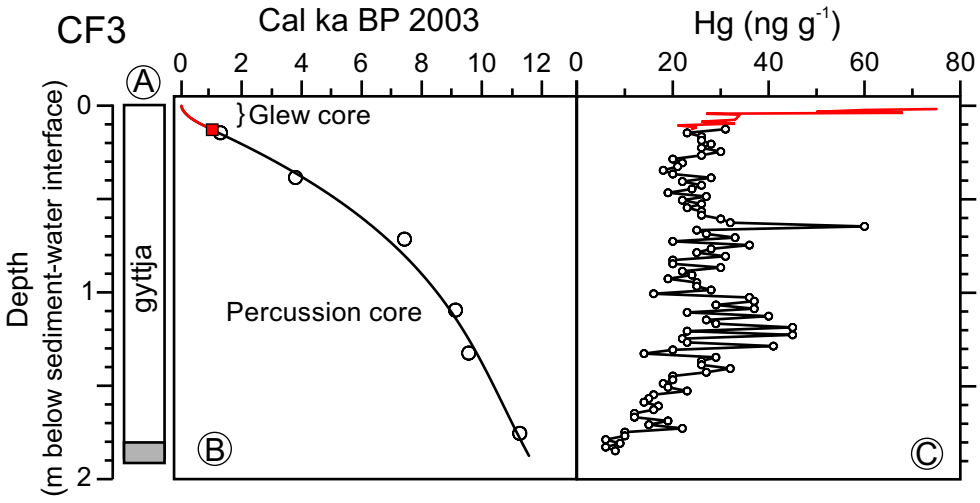


**Fig. 6.2.** (A) Sediment lithostratigraphy which is composed of gyttja overlying inorganic sediment of glacial age (grey). (B) Age-depth model for the Lake CF3 surface (red line) and percussion cores (black line) incorporating CRS $^{210}Pb$ dates (not shown), AMS $^{14}C$ dates on the Glew core (red squares), and $^{14}C$ dates on the percussion core (white circles). (C) Down-core [Hg] determined on the surface (red line) and percussion cores (black line).

though less variable, decrease in [Hg] (from 100 ng $g^{-1}$ to 30 ng $g^{-1}$) is apparent through the last interglacial *sensu stricto* (Fig. 6.3). There is therefore a consistent picture of declining [Hg] through two complete interglacials (MIS 1 and 5e). The Holocene and MIS 5e sediments are separated by ~10 cm of moss-rich gyttja, which were deposited during MIS 5a or 5c. These moss-rich sediments contain [Hg] between 20 and 120 ng $g^{-1}$. Only the latter portion of MIS 7 is captured by the CF8 sediment record, and [Hg] decreases from 30 to 2 ng $g^{-1}$ during this period. The sand layers that separate each interglacial unit contain very little Hg

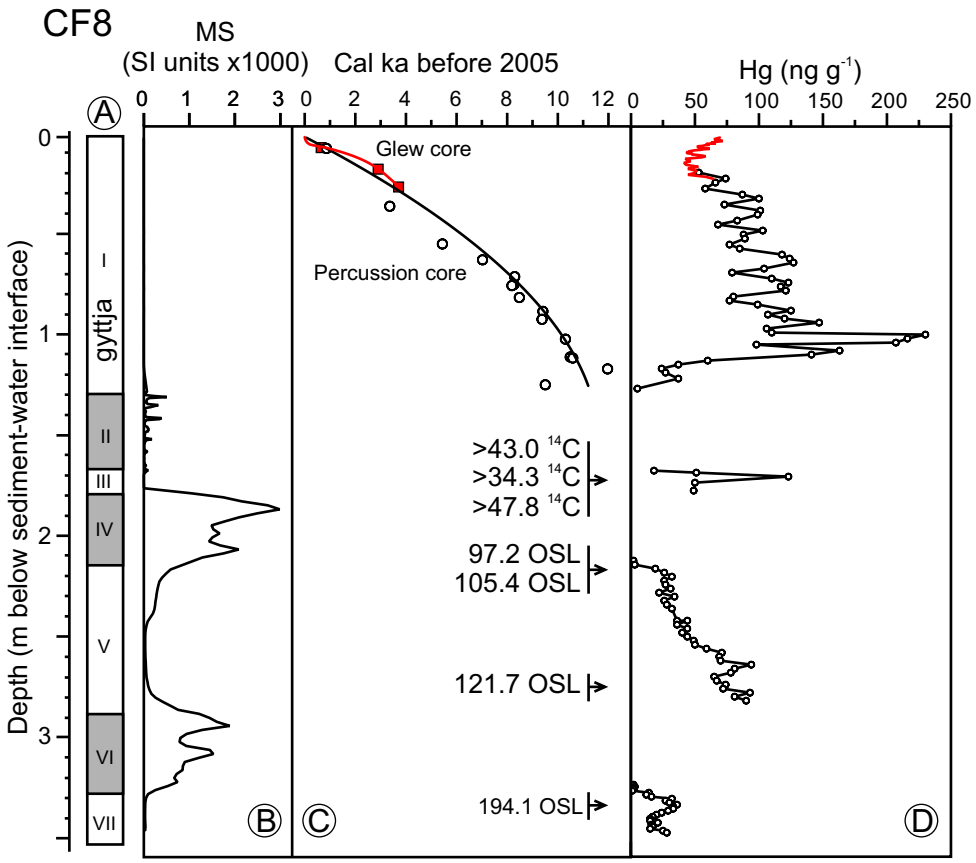


**Fig. 6.3.** (A) Sediment lithostratigraphy; organic interglacial gyttja sediments are separated by highly inorganic sediment (grey) presumably deposited during glacial retreat.(B) Down-core profile of magnetic susceptibility. (C) Age-depth model for the CF8 surface (red line) and percussion cores (black line) incorporating $^{210}$Pb dates (not shown), AMS $^{14}$C dates on the surface core (red squares), $^{14}$C dates on the percussion core (white circles), and OSL dates. (D) Down-core [Hg] determined on the surface (red line) and percussion cores (black line).

(average [Hg]=1.8±0.8 ng $g^{-1}$; n=4).

## Discussion

*Late-Holocene Hg enrichment: the last 500 years in detail*

At CF3 and CF8, sediment [Hg] is stable from 500 to 150 years before 2005 (BP) averaging ~30 ng $g^{-1}$ and ~60 ng $g^{-1}$, respectively (Fig. 6.4a, b). The Hg flux rate from 500-150 years BP is <0.5 μg $m^{-2}$ $yr^{-1}$ at both lakes. These estimates of pre-industrial flux are much lower than previous studies of Arctic mercury accumulation using lake sediments. In a survey of 18 Canadian arctic lakes, Muir et al. (2009) reported an average pre-industrial Hg flux of ~6 μg $m^{-2}$ $yr^{-1}$, while Fitzgerald et al. (2005) reported pre-industrial Hg fluxes ~1 μg $m^{-2}$ $yr^{-1}$ for five lakes from northern Alaska. Similar pre-industrial flux rates were reported by Outridge et al. (2005) for Lake DV-09 on Devon Island and Amituk Lake on Cornwallis Island. However, previous studies investigating Arctic Hg flux using lake sediment cores have relied solely on $^{210}$Pb dating and have not incorporated $^{14}$C dates into their core chronologies. However, the exhaustion of unsupported $^{210}$Pb and the onset of anthropogenic global Hg emissions converge temporally in the late 19$^{th}$ century, raising the possibility that pre-industrial Hg fluxes are poorly constrained (Cooke et al., 2010). At CF3, one AMS $^{14}$C date between 100 and 150 years ago constrains pre-industrial sedimentation rates (Fig. 6.2), while three dates are used at CF8 (Fig. 6.3). At CF3, sedimentation rates begin to increase ~1850, rising from ~20 g $m^{-2}$ $yr^{-1}$ to >120 g $m^{-2}$ $yr^{-1}$ (Fig. D.1a). A similar trend is noted at CF8, where sedimentation rates increase steadily through the 20$^{th}$ century from <10 g $m^{-2}$ $yr^{-1}$ to ~50 g $m^{-2}$ $yr^{-1}$ (Fig. D.1b). Lakes across the Arctic are undergoing profound hydrological and biological changes as a result of recent warming, including increased summer evaporation (Smol and Douglas, 2007), changes in

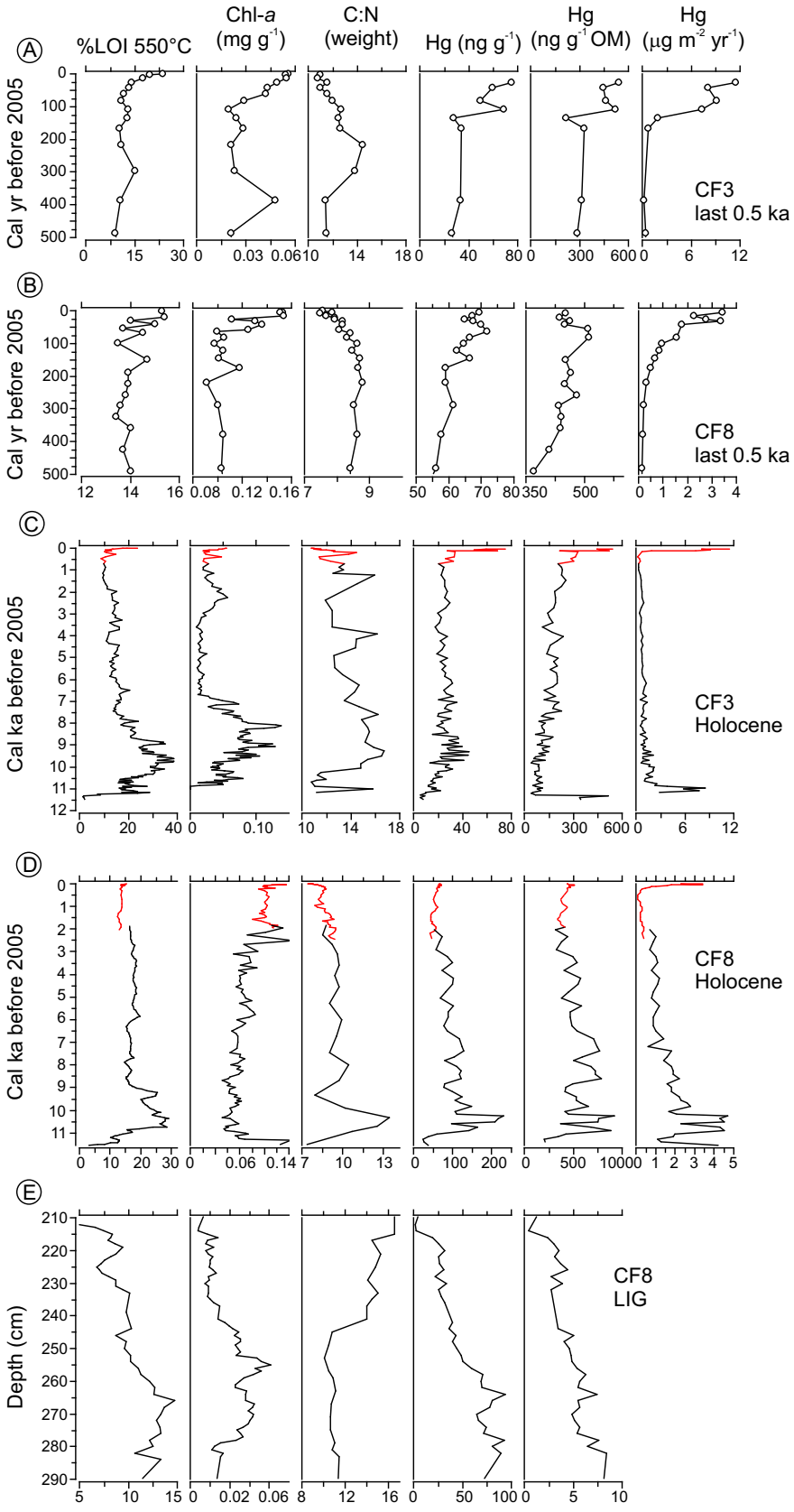
A
%LOI 550°C
Chl-a (mg g-1)
C:N (weight)
Hg (ng g-1)
Hg (ng g-1 OM)
Hg (µg m-2 yr-1)
Cal yr before 2005
CF3 last 0.5 ka
B
CF8 last 0.5 ka
C
Cal ka before 2005
CF3 Holocene
D
CF8 Holocene
E
Depth (cm)
CF8 LIG

**Fig. 6.4.** (previous page) Profiles of organic matter (%LOI 550), spectrally inferred Chl a, C:N ratio (by weight), [Hg], Hg normalized to organic matter content, and Hg flux for the past 0.5 ka for both Lakes (A) CF3 and (B) CF8. All of the data for this period (the past 0.5 ka) are from the surface cores. Also shown are the same data spanning the Holocene for both lakes (C) CF3 and (D) CF8 and the last interglacial (LIG) (E) for Lake CF8. Note that the LIG is plotted against depth not age.

---

algal community assemblages (Smol et al., 2005), and increases in both primary production (Michelutti et al., 2005) and inorganic sedimentation (Hughen et al., 2000; Thomas and Briner, 2009). It seems likely that these changes may be driving some of the increases in lake sedimentation observed here.

After ~150 years BP, [Hg] and Hg flux increase at both lakes; however, Hg flux increases to a much larger degree than [Hg], driven in large part by the dramatic increase in sedimentation rate at both sites (Fig. 6.4a, b). Enrichment ratios, comparing recent (CF3: 1977; CF8: 2001) to average pre-industrial (500-150 years BP) Hg concentrations, are ~2 and <2 for lakes CF3 and CF8, respectively. However, these enrichment ratios are much smaller than flux ratios calculated over the same periods, which are ~23 for CF3 and ~11 for CF8. This is a large discrepancy that requires careful consideration.

Insight into the difference between the Hg enrichment and flux ratios can be gleaned by examining the geochemical profiles of [Pb], Pb flux and Pb stable isotopes from CF8, which have been published previously (Michelutti et al., 2009). Sediment [Pb] and Pb stable isotopes were measured on the same core and at nearly the same resolution as these new Hg data, and thus are directly comparable. As with Hg, [Pb] displays little increase over the 20$^{th}$ century remaining constant ~5 $\mu g\ g^{-1}$, while Pb flux steadily increases (Fig. 6.5). However, the increase in Pb pollution indicated by the Pb flux profile (but not the [Pb] profile) is corroborated by a parallel decrease in $^{206}Pb/^{207}Pb$. Indeed, multi-isotope mixing models (e.g., $^{204}Pb/^{208}Pb$, $^{206}Pb/^{207}Pb$, etc.) indicate multiple industrial

global sources of Pb pollution at CF8 (Michelutti et al., 2009). Thus, while both the Pb flux and $^{206}Pb/^{207}Pb$ profiles clearly indicate increasing 20$^{th}$-century anthropogenic Pb pollution, the [Pb] data, considered alone, do not. Because sediment Pb stable isotopic ratios are not influenced by sedimentation rates, this indicates that metal concentrations, including both Pb and Hg, have been diluted in recent decades by increasing rates of lake sedimentation. Thus, we suggest that flux ratios, rather than enrichment ratios, more accurately reflect the relative increase in metal deposition within our lake sediment cores.

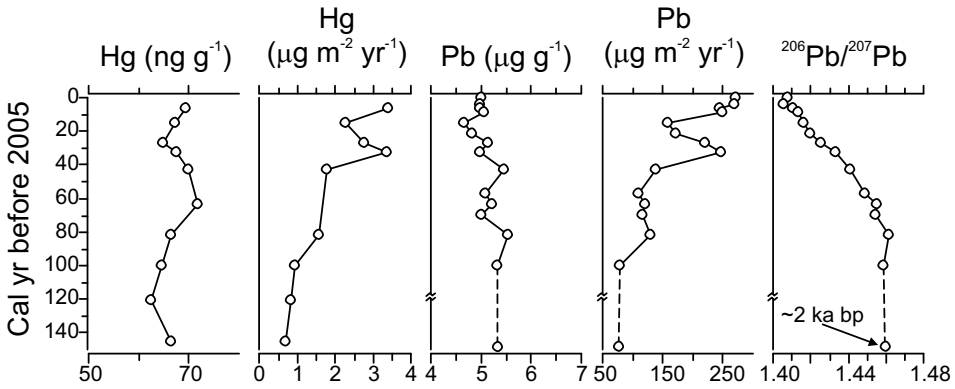


**Fig. 6.5.** Profiles of [Hg], Hg flux, [Pb], Pb flux, and $^{206}Pb/^{207}Pb$ isotopic ratios from the CF8 surface core spanning the past ~150 years. For the Pb data, note the break in the y-axis, with the lower-most datum dating to ~2 ka BP.

Recently, Outridge and colleagues (Carrie et al., 2009; Outridge et al., 2005, 2007; Stern et al., 2009) have proposed that 20$^{th}$-century warming can explain some of the recent increase in Hg recorded in lake sediments across the Arctic. The proposed mechanism is an increase in the sorptive capacity of oligotrophic arctic lakes via increases in within-lake primary production. Hg is characterized by a strong affinity for organic matter, and changes in organic matter quantity and quality can carry important implications for Hg recruitment to sediments (Kainz and Lucotte, 2006). To examine what influence organic phases might play in Hg sequestration at Lake CF3 and CF8, profiles of [Hg],

Hg normalized to organic content ($Hg_{org}$), and Hg flux are shown alongside proxies of organic matter quantity (LOI and spectrally inferred Chl *a*) and quality (sediment C:N ratios) in Figure 6.4 (panels a and b). At both lakes, LOI and Chl *a* concentrations increase over the past ~150 years, and are matched by decreasing C:N. These trends likely reflect increases in within-lake primary production over the 20$^{th}$ century, as has been observed across a suite of arctic lakes (Axford et al., 2009a; Michelutti et al., 2005). However, this increase in autochthonous organic matter supply appears unable to account for the increase in Hg noted in CF3 and CF8 sediments. The [Hg] and $Hg_{org}$ profiles are virtually identical in both lakes, suggesting organic matter supply is not driving the recent increases in Hg in these lakes. Moreover, Hg and Chl *a* are not significantly correlated over this period in CF3 ($r^2$=0.12, $p$=0.4, $n$=8) and are only weakly correlated in CF8 ($r^2$=0.28, $p$<0.001, $n$=36). This topic is explored in greater detail below, but the late-Holocene biogeochemical data presented here suggest that recent increases in Hg occur independent of, though coeval to, warming-induced increases in within-lake primary production.

*Trends in Holocene Hg accumulation*

Lakes CF3 and CF8 display very different Hg profiles over the Holocene (Fig. 6.4c, d). At Lake CF3, [Hg] rarely exceeds 40 ng $g^{-1}$ and normalizing to organic matter ($Hg_{org}$) does little to change the overall shape of the Hg profile. In contrast, both [Hg] and $Hg_{org}$ increase ~5-fold during the early Holocene at Lake CF8. While Hg flux also increases at Lake CF3 during the early Holocene, this likely represents an artifact associated with elevated dry density values at this time (Fig. D.1a), rather than a real increase in Hg delivery to the lake. In contrast, the early-Holocene increase in Hg flux observed within CF8 is driven primarily by the increase in Hg concentration (Fig. D.1b), and thus likely reflects a real increase

in the rate of Hg delivery through the early Holocene. The different Holocene Hg records from CF3 and CF8 are highlighted by the calculation of natural cumulative Holocene Hg burdens within each lake. The Holocene cumulative dry mass sediment inventory for Lakes CF3 and CF8 is ~50 g $cm^{-2}$ and ~40 g $cm^{-2}$, respectively. Yet despite the higher sediment inventory at CF3, Lake CF8 sediment contains ~3000 ng Hg $cm^{-2}$ while CF3 contains only ~1100 ng Hg $cm^{-2}$.

These differences between the CF3 and CF8 Hg records suggest different processes are driving Holocene Hg accumulation within the two lakes. Both lakes experienced similar early-Holocene climates, characterized by regional summer air temperatures 4-6 °C warmer than present (Axford et al., 2009a; Axford et al., 2009b; Briner et al., 2006). Moreover, both lakes record pronounced increases in organic matter content during the early-Holocene thermal maximum (HTM), a finding similar to other studies in high-latitude regions (e.g., Willemse and Törnqvist, 1999; Kaplan et al., 2002). However, profiles of organic matter quality suggest that the source of organic matter differs between these two lakes.

In Lake CF3, LOI and Chl *a* display similar stratigraphic profiles, suggesting autochthonous sources control organic matter supply (Fig. 6.4). Rapid declines in both proxies are noted around 8 and 7 ka BP, respectively, and this interval also marks the deceleration of sedimentation accumulation rates (Fig. 6.2), which further indicates that sedimentation in this lake is intimately related to primary production and autochthonous organic matter supply. While the C:N ratio of lake sediment is commonly interpreted as a proxy for the relative contribution of terrestrial versus aquatic organic matter (Meyers and Terranes, 2001), CF3 rests in a small and very flat catchment with no inflow stream. Therefore, this interpretation of the C:N data is not appropriate for CF3. Instead, the C:N ratio of CF3 sediment most likely reflects the relative abundance of differing aquatic plants (phytoplankton and macrophytes), an interpretation which is supported by

the observation that the CF3 sediment core contained abundant macrophytes.

The pronounced early-Holocene increase in both LOI and Chl *a*, and the subsequent decrease in both proxies at 7-8 ka BP, appears to have carried little consequence for the sequestration of Hg to CF3 sediment. Indeed, [Hg] and Hg flux remain relatively invariant over the Holocene averaging 24±8 μg $g^{-1}$ and 1.3±1.3 μg $m^{-2}$ $yr^{-1}$, respectively. Moreover, Hg displays no significant positive correlation with either LOI ($r^2$=0.14, $n$=85) or Chl *a* ($r^2$<0.07, $n$=82). Thus, despite a clear climate-driven increase in within-lake primary production during the early Holocene at CF3, there is no attendant increase in Hg recruitment to CF3 sediments. These data would therefore argue against the hypothesis that climate-driven changes in algal productivity mediate the recruitment of Hg to arctic lake sediments. Instead, we suggest atmospheric deposition controls Hg delivery to Lake CF3. If atmospheric deposition does control Hg delivery to CF3, it would suggest that little variability in the rate of atmospheric Hg deposition over the Holocene, despite dramatic changes in both Arctic climate and attendant limnological responses.

Unlike Lake CF3, Hg delivery to Lake CF8 increases dramatically during the early Holocene when the highest Hg concentrations observed within the entire ~200,000-year CF8 sediment core are recorded (Fig. 6.4d). Lake CF8 rests in a steeply sloping catchment and possesses seasonally active inflow and outflow streams. Based on these observations, we would predict that organic sediment supply at Lake CF8 would be influenced more by catchment erosion than within-lake primary production. Indeed, [Hg] is significantly correlated with LOI ($r^2$=0.49, $p$<0.001, $n$=49) and with C:N ($r^2$=0.57[1], $p$<0.001, $n$=22) but not with Chl *a* ($r^2$=0.13, $p$>0.02, $n$=38) within CF8 sediment. Unlike CF3, the CF8 sediment core did not contain abundant macrophytes, and its steeply sloping

[1] Calculated using 500-year means because C:N and [Hg] were measured on different core intervals.

catchment and seasonally-permanent inflow and outflow streams would suggest the sediment C:N does reflect the relative contribution of terrestrial versus aquatic organic matter. Thus, it appears that the export of organic-bound Hg from the catchment to the lake exerts a first-order control over Hg burdens at Lake CF8.

The affinity of Hg for terrestrial organic matter is well documented (e.g., Kainz and Lucotte, 2006). In a study of 12 subarctic lakes from northern Quebec (Canada), Lucotte et al. (1995) found lake-sediment Hg-burdens varied in direct proportion to the amount of terrestrial organic carbon supplied, while Fitzgerald et al. (2005) found that soil erosion contributes a substantial portion (15-65%) of Hg to lakes in northern Alaska. In alpine environments, springtime stream-water export of DOC is an important control on Hg delivery to lakes (e.g. Selvendiran et al., 2009). While Hg delivery mechanisms are less well studied in the Arctic, Wolfe and Härtling (1997) documented similar patterns of trace-metal (i.e., Pb, Zn, Cu, Ni, Cr) enrichment in organic-rich sediments dating to the early Holocene. More recently, Klaminder et al. (2010) noted an increase in Pb burdens in sub-Arctic lakes in Sweden, despite clear decreases in recent Pb deposition. The authors suggest that climate warming is driving an increase in the export of organic matter and organically bound Pb from the catchment to the lake. Interestingly, this Pb appears to be legacy Pb pollution, deposited over the last ~three millennia. We hypothesize that during the early Holocene, when temperatures were 4-6 °C warmer in this region (Axford et al., 2009a, 2009b; Briner et al., 2006), enhanced soil development (i.e., humus production) and invigorated spring runoff accelerated the delivery of organic-bound Hg to the lake. Unlike the recent increase in Pb delivery to Swedish lakes (Klaminder et al., 2010), this early-Holocene Hg enrichment cannot be explained via the mobilization of ancient Hg pollution. Indeed, the early-Holocene increase in Hg documented here is all the more pronounced given that both modeling and

empirical results suggest greater volatilization of Hg at higher temperatures, solar radiation, and lake-water Hg concentrations (Mackay et al., 1995; Schroeder et al., 2005), all of which would have been experienced during the early Holocene. The CF8 data therefore suggest that specific natural conditions are capable of producing a sedimentary Hg signature which is of comparable magnitude to lakes which lie proximal to industrial Hg emission sources.

*Comparing the Holocene and the last interglacial in CF8*

The sediment record from Lake CF8 offers a unique opportunity to examine Hg dynamics over multiple interglaciations. Our dataset includes Hg measurements from organic sediments dating to MIS 5a or 5c, MIS 5e, and the part of MIS 7 (Briner et al., 2007). Here, we limit our discussion to comparing the two full interglacial cycles preserved at CF8: the Holocene (MIS 1) and the last interglacial *sensu stricto* (MIS 5e). [Hg] declines as both interglacials progress. While the Holocene is characterized by a tight coupling between Hg and terrestrial organic matter supply, during the last interglacial this relationship is more complicated. Organic matter delivery and within-lake primary production both appear to have been lower than during the Holocene (Fig. 6.4e). In addition, during the first-half of the last interglacial (and unlike the early Holocene) C:N remains relatively constant ~11, suggest a steady balance between catchment erosion and within-lake primary production. The lack of an early-last-interglacial increase in [Hg] may be due to enhanced catchment stability during this time relative to the Holocene. Nonetheless, a significant positive relationship between [Hg] and LOI ($r^2$=0.75, $p$<0.01, $n$=30) is maintained during this period, suggesting that, similar to the Holocene, the export of catchment-derived organic matter mediated Hg supply to the lake.

During the last-half of the last interglacial, when Hg and organic matter

values continue to decline, C:N ratios increase to ~15 (Fig. 6.4e). The increase in C:N at this time is paralleled by an increase in MS and a decrease in Chl *a* (Fig. 6.3). This shift likely indicates an increase in the flux of catchment-derived clastic material to the lake as climatic conditions deteriorated. Relative to organic matter, sorption to mineral matter therefore only appears to play a minor role in the delivery and sequestration of trace-metals in oligotrophic arctic lakes. The differences observed between the Holocene, the early-half and late-half of the last interglacial underscore the important role catchment-derived organic phases can play in mediating Hg delivery to arctic lakes which are intimately tied to their catchments.

**Conclusion**

The records presented here place 20$^{th}$-century Arctic Hg enrichment in a well-dated multi-proxy perspective spanning multiple interglaciations. In both study lakes, 20$^{th}$-century Hg flux exceeds pre-industrial (i.e., Little Ice Age) Hg flux rates by 10-fold or greater. While, many previous studies have suggested a much smaller increase in the magnitude of anthropogenic Hg enrichment in the Arctic, these studies have failed to incorporate $^{14}$C into their chronological models. Our results suggest the incorporation of multiple dating techniques is vital if accurate reconstructions of past Hg flux are sought from arctic lake sediment cores.
Over the Holocene, lake and catchment characteristics influence Hg supply and recruitment to sediments, and edaphic processes are capable of producing [Hg] higher than present under warmer than present conditions. Given the profound climatological and biogeochemical changes currently underway in the Arctic the observation that climatically-mediated edaphic process direct Hg supply and recruitment carries profound implications. Processes that enhance the export of

labile catchment organic matter will undoubtedly result in increased Hg burdens in arctic lakes, and these increases in lake-water Hg can be rapidly communicated up food chains. Additional multi-proxy studies of climate-Hg-ecosystem linkages will only help to further our understanding of Hg in the Arctic and its future trajectory in a rapidly changing arctic environment. In addition, we suggest that further testing of the primary production hypothesis should look to well-dated core material spanning the early-Holocene climatic optima, rather than attempting to disentangle possible 20$^{th}$-century warming-driven Hg enrichment from anthropogenic pollution.

**References**

AMAP (2002) Assessment Report: Arctic Pollution 2002. Oslo, Norway, Arctic Monitoring Assessment Programme.

Axford, Y., Briner, J. P., Cooke, C. A., Francis, D. R., Michelutti, N., et al. (2009a) Recent changes in a remote Arctic lake are unique within the past 200,000 years. *Proceedings of the National Academy of Sciences,* 106, 18443-18446.

Axford, Y., Briner, J. P., Miller, G. H. & Francis, D. R. (2009b) Paleoecological evidence for abrupt cold reversals during peak Holocene warmth on Baffin Island, Arctic Canada. *Quaternary Research,* 71, 142-149.

Biester, H., Bindler, R. & Martínez-Cortizas, A. (2006) Mercury in mires. IN Martini, I. P., Martinez-Cortizas, A. & Chesworth, W. (Eds.) *Peatlands: Evolution and Records of Environmental and Climate Changes.* Elsevier.

Biester, H., Bindler, R., Martínez-Cortizas, A. & Engstrom, D. R. (2007) Modeling the past atmospheric deposition of mercury using natural archives. *Environmental Science & Technology,* 41, 4851-4860.

Biester, H., Martínez-Cortizas, A., Birkenstock, S. & Kilian, R. (2003) Effect of peat decomposition and mass loss on historic mercury records in peat bogs from Patagonia. *Environmental Science & Technology,* 37, 32-39.

Bindler, R., Martinez-Cortizas, A. & Blaauw, M. (2005) Comment on "Atmospheric Mercury Accumulation Rates between 5900 and 800 Calibrated Years BP in the High Arctic of Canada Recorded by Peat Hummocks". *Environmental Science & Technology,* 39, 908-909.

Briner, J. P., Axford, Y., Forman, S. L., Miller, G. H. & Wolfe, A. P. (2007) Multiple generations of interglacial lake sediment preserved beneath the Laurentide Ice Sheet. *Geology,* 35, 887-890.

Briner, J. P., Michelutti, N., Francis, D. R., Miller, G. H., Axford, Y., et al.

(2006) A multi-proxy lacustrine record of Holocene climate change on northeastern Baffin Island, Arctic Canada. *Quaternary Research,* 65, 431-442.

Cannon, W. F., Dean, W. E. & Bullock, J. H. (2003) Effects of Holocene climate change on mercury deposition in Elk Lake, Minnesota: The importance of eolian transport in the mercury cycle. *Geology,* 31, 187-190.

Carrie, J., Wang, F., Sanei, H., Macdonald, R. W., Outridge, P. M., et al. (2009) Increasing contaminant burdens in an arctic fish, burbot (Lota lota), in a warming climate. *Environmental Science & Technology,* 44, 316-322.

Cooke, C., Hobbs, W. O., Michelutti, N. & Wolfe, A. P. (2010) Reliance on $^{210}$Pb chronology can compromise the inference of preindustrial Hg flux to lake sediments. *Environmental Science & Technology,* 44, 1998-2003.

EPA (1998) Mercury in solids and solutions by thermal decomposition, amalgamation, and atomic absorption spectrophotometry. *EPA Method 7473 Report.* Washington, DC, Environmental Protection Agency.

Fitzgerald, W. F., Engstrom, D. R., Lamborg, C. H., Tseng, C. M., Balcom, P. H., et al. (2005) Modern and historic atmospheric mercury fluxes in northern Alaska: global sources and Arctic depletion. *Environmental Science & Technology,* 39, 557-568.

Givelet, N., Roos-Barraclough, F., Goodsite, M. E., Cheburkin, A. K. & Shotyk, W. (2004) Atmospheric mercury accumulation rates between 5900 and 800 calibrated years BP in the High Arctic of Canada recorded by peat hummocks. *Environmental Science & Technology,* 38, 4964-4972.

Glew, J. R., Smol, J. P. & Last, W. M. (2001) Sediment core collection and extrusion. IN Last, W. & Smol, J. P. (Eds.) *Tracking Environmental Change Using Lake Sediments: Basin Analysis, Coring, and Chronological Techniques.* New York, Springer.

Hughen, K. A., Overpeck, J. T. & Anderson, R. F. (2000) Recent warming in a 500-year palaeotemperature record from varved sediments, Upper Soper Lake, Baffin Island, Canada. *The Holocene,* 10, 9-19.

Intergovenmental Panel on Climate Change (2007) *Climate change 2007: Impacts, adaptation, and vulnerability*. Contribution of Working Group II to the Fourth Assessment Report of the Intergovernmental Panel on Climate Change. Cambridge University Press, Cambridge.

Jitaru, P., Gabrielli, P., Marteel, A., Plane, J. M. C., Planchon, F. A. M., et al. (2009) Atmospheric depletion of mercury over Antarctica during glacial periods. *Nature Geoscience,* 2, 505-508.

Kainz, M. & Lucotte, M. (2006) Mercury concentrations in lake sediments– revisiting the predictive power of catchment morphometry and organic matter composition. *Water, Air, & Soil Pollution,* 170, 173-189.

Kaplan, M. R., Wolfe, A. P. & Miller, G. H. (2002) Holocene environmental variability in southern Greenland inferred from lake sediments. *Quaternary Research*, 58, 149-159.

Klaminder, J., Hammarlund, D., Kokfelt, U., Vonk, J. E., Bigler, C. (2010) Lead contamination of subarctic lakes and its response to reduced atmospheric fallout: can the recovery process be counteracted by the ongoing climate change? *Environmental Science & Technology*, Arcticle ASAP.

Landers, D. H., Gubala, C., Verta, M., Lucotte, M., Johansson, K., et al. (1998) Using lake sediment mercury flux ratios to evaluate the regional and continental dimensions of mercury deposition in arctic and boreal ecosystems. *Atmospheric Environment,* 32, 919-928.

Lockhart, W. L., Macdonald, R. W., Outridge, P. M., Wilkinson, P., DeLaronde, J. B., et al. (2000) Tests of the fidelity of lake sediment core records of mercury deposition to known histories of mercury contamination. *The*

*Science of the Total Environment,* 260, 171-180.

Lucotte, M., Mucci, A., Hillaire-Marcel, C., Pichet, P. & Grondin, A. (1995) Anthropogenic mercury enrichment in remote lakes of northern Quebec (Canada). *Water, Air, & Soil Pollution,* 80, 467-476.

Mackay, D., Wania, F. & Schroeder, W. H. (1995) Prospects for modeling the behavior and fate of mercury, globally and in aquatic systems. *Water, Air, and Soil Pollution,* 80, 941-950.

Martínez-Cortizas, A., Biester, H., Mighall, T. & Bindler, R. (2007) Climate-driven enrichment of pollutants in peatlands. *Biogeosciences,* 4, 905-911.

Martínez-Cortizas, A., Pontevedra-Pombal, X., García-Rodeja, E., Nóvoa-Muñoz, J. C. & Shotyk, W. (1999) Mercury in a Spanish peat bog: Archive of climate change and atmospheric metal deposition. *Science,* 284, 939-942.

Meyers, P. A. & Terranes, J. L. (2001) Sediment orgranic matter. IN Last, W. M. & Smol, J. P. (Eds.) *Tracking Environmental Change Using Lake Sediment, 2. Physical and Geochemical Methods.* Kluwer Academic Publishers.

Michelutti, N., Simonetti, A., Briner, J. P., Funder, S., Creaser, R. A., et al. (2009) Temporal trends of pollution Pb and other metals in east-central Baffin Island inferred from lake sediment geochemistry. *Science of the Total Environment,* 407, 5653-5662.

Michelutti, N., Wolfe, A. P., Briner, J. P. & Miller, G. H. (2007) Climatically controlled chemical and biological development in Arctic lakes. *Journal of Geophysical Research,* L19715.

Michelutti, N., Wolfe, A. P., Vinebrooke, R. D., Rivard, B. & Briner, J. P. (2005) Recent primary production increases in Arctic lakes. *Geophysical Research Letters,* 32.

Muir, D. C. G., Wang, X., Yang, F., Nguyen, N., Jackson, T. A., et al. (2009)

Spatial trends and historical deposition of mercury in eastern and northern Canada inferred from lake sediment cores. *Environmental Science & Technology,* 43, 4802-4809.

Nesje, A. (1992) A Piston Corer for Lacustrine and Marine Sediments. *Arctic and Alpine Research,* 24, 257-259.

Outridge, P. M., Sanei, H., Stern, G. A., Hamilton, P. B. & Goodarzi, F. (2007) Evidence for control of mercury accumulation rates in Canadian High Arctic lake sediments by variations of aquatic primary productivity. *Environmental Science & Technology,* 41, 5259-5265.

Outridge, P. M., Stern, G. A., Hamilton, P. B., Percival, J. B., McNeely, R., et al. (2005) Trace metal profiles in the varved sediment of an Arctic lake. *Geochimica et Cosmochimica Acta,* 69, 4881-4894.

Rydberg, J., Gälman, V., Renberg, I., Bindler, R., Lambertsson, L., et al. (2008) Assessing the stability of mercury and methylmercury in a varved lake sediment deposit. *Environmental Science & Technology,* 42, 4391-4396.

Schroeder, W. H., Beauchamp, S., Edwards, G., Poissant, L., Rasmussen, P., et al. (2005) Gaseous mercury emissions from natural sources in Canadian landscapes. *Journal of Geophysical Research,* 110, D18302.

Shindell, D. & Faluvegi, G. (2009) Climate response to regional radiative forcing during the twentieth century. *Nature Geoscience,* 2, 294-300.

Stern, G. A., Sanei, H., Roach, P., DeLaronde, J. & Outridge, P. M. (2009) Historical interrelated variations of mercury and aquatic organic matter in lake sediment cores from a subarctic lake in Yukon, Canada: further evidence toward the algal-mercury scavenging hypothesis. *Environmental Science & Technology,* 43, 7684-7690.

Selvendiran, P., Driscoll, C. T., Montesdeoca, M. R., Choi, H-D. & Holsen, T. M. (2009) Mercury dynamics and transport in two Adirondack lakes.

*Limnology & Oceanography*, 54, 413-427.

Smol, J., P. & Douglas, M. S. V. (2007) Crossing the final ecological threshold in high Arctic ponds. *Proceedings of the National Academy of Sciences,* 104, 12395-12397.

Smol, J., P., Wolfe, A. P., Birks, H. J. B., Douglas, M. S. V., Jones, V. J., et al. (2005) Climate-driven regime shifts in the biological communities of Arctic lakes. *Proceedings of the National Academy of Sciences,* 12, 4397-4402.

Thomas, E. K. & Briner, J. P. (2009) Climate of the past millennium inferred from varved proglacial lake sediments on northeast Baffin Island, Arctic Canada. *Journal of Paleolimnology,* 41, 209-224.

Thomas, E. K., Axford, Y. & Briner, J. P. (2008) Rapid 20th century environmental change on northeastern Baffin Island, Arctic Canada inferred from a multi-proxy lacustrine record. *Journal of Paleolimnology,* 40, 507-517.

Vandal, G. M., Fitzgerald, W. F., Boutron, C. F. & Candelone, J.-P. (1993) Variations in mercury deposition to Antarctica over the past 34,000 years. *Nature,* 362**,** 621-623.

Willemse, N. W. & Törnqvist, T. E. (1999) Holocene century-scale temperature variability from West Greenland lake records. *Geology*, 27, 580-584.

Wolfe, A. P. & Härtling, J. W. (1997) Early Holocene trace metal enrichment in organic lake sediments, Baffin Island, arctic Canada. *Arctic and Alpine Research,* 29, 24-31.

Wolfe, A. P., Miller, G. H., Olsen, C. A., Forman, S. L., Doran, P. T., et al. (2004) Geochronology of high latitude lake sediments. IN Pienitz, R., Douglas, M. S. V. & Smol, J. P. (Eds.) *Long-term Environmental Change in Arctic and Antarctic Lakes.* Dordrecht, The Netherlands, Kluwer Academic Publishers.

Wolfe, A. P. & Smith, I. R. (2004) Paleolimnology of the Canadian Arctic

Archipelago. IN Pienitz, R., Douglas, M. S. V. & Smol, J. P. (Eds.) *Long-Term Environmental Change in Arctic and Antarctic Lakes. Developments in Paleoenvironmental Research.* Dordrecht, Springer.

# CHAPTER 7: CONCLUSION

## Summary of work and future efforts

This body of work represents a concerted effort to examine natural and anthropogenic drivers of mercury (Hg) cycling during the pre-industrial era. The objectives of this work include: (1) testing the hypothesis that pre-Colonial, Colonial, and industrial mining and metallurgy left a lasting legacy of Hg pollution in the Andes, (2) suggesting how refinements to lake sediment core chronologies can improve estimates of pre-industrial Hg accumulation rates (fluxes), and (3) placing recent Hg enrichment in the Arctic in the long-term context of multiple interglaciations.

### *The case for pre-industrial Hg pollution*

Many investigations have demonstrated the presence of preindustrial metal pollution. Despite this fact, a common conception is that the industrial revolution represents the starting point of widespread environmental pollution. While most previous studies have focused on reconstructing the pollution history of lead (Pb), new research suggests other elements, including (but not limited to) copper (Cu) (Hong et al., 1996), antimony (Sb), (Krachler et al., 2005), osmium (Os) (Rauch et al., 2010) and even carbon (C) (Ruddiman, 2003), experienced pre-industrial increases as well. The results from this dissertation suggest Hg should be added to this list as well.

Jerome Nriagu was the first to suggest that pre-industrial Hg use may have resulted in large amounts of Hg being released to the global environment (Nriagu, 1993). The records presented here are the first to confirm the existence of pre-industrial Hg pollution, and suggest that early Hg emissions originated from a

multitude of activities including: cinnabar mining and processing (Chapter 2), Hg amalgamation (Chapter 3), and the smelting of argentiferous ores (Chapter 4). The efforts presented in this dissertation were limited geographically to the Andes, so how far this Hg was circulated, and its influence on the pre-industrial global cycle of Hg, remains unknown. But the finding that so many different activities resulted in Hg emissions suggests that similar records should exist for other regions of the world where mining and metallurgy have a long history. Given the long atmospheric residence time of Hg (0.5-2 years), it remains a distinct possibility that these early anthropogenic Hg emissions were circulated at the hemispheric if not global scale.

In a broad sense, these conclusions suggest that the distinction between a world dominated by humans after ~1850 (i.e. the Anthropocene) and a natural environmental state before that date may not be a useful dichotomy. This notion is supported not only by Hg, but to other metals and greenhouse gases as well. The idea of "environmental pollution" therefore should not be applied solely to post-industrial societies. The recognition of this fact carries important ecological and climatic implications. For example, for the case of Pb, Bindler et al. (2008) have demonstrated convincingly that in Europe about half of the cumulative burden of atmospherically deposited Pb was deposited before the industrial era. This Pb remains available for ecological cycling, especially in regions which are experiencing rapid climate change (e.g. the Arctic) (Klaminder et al., 2010). In terms of climate, the early Anthropocene hypothesis (Ruddiman, 2003, 2007) emphasizes the slow but cumulative impact of millennia of farming and deforestation on the global C cycle. While the early Anthropocene hypothesis has proven controversial (c.f. Broecker, 2006; Brook, 2009; Ruddiman, 2007) there is an increasing awareness that a long-term perspective is required if we are to meaningfully address environmental conservation issues relating to biological

invasions, wildfires, climate change, and the range of natural variability in biogeochemical cycles. While the traditional idea that the Anthropocene began with industrialization continues to retain scientific traction, there is an increasing awareness that early anthropogenic activities exerted a meaningful and lasting impact on the environment. Thus, the Anthropocene as a distinct geologic era in which human activities exert an overriding control of the majority of earth's ecosystems may have ultimately been preconditioned by millennia of slow but meaningful alteration of key biogeochemical cycles and indeed climate itself.

*Estimating pre-industrial Hg flux using lake sediment cores*

Reconstructing the rate of natural, pre-pollution Hg deposition can only be accomplished using the geochemical record preserved in natural archives far removed from point sources. Because of the apparent problems with Hg retention in peat (see chapter 1), lake sediments are widely considered the most reliable archives of past Hg deposition rates (Biester et al., 2007). Previous paleolimnological studies of past Hg deposition to remote regions have relied on $^{210}$Pb dating to construct their core chronologies. The 5$^{th}$ chapter of this dissertation examined the assumptions and limitations of relying solely on $^{210}$Pb dating to calculate pre-industrial Hg fluxes from lake sediment cores. It was found that incorporating $^{14}$C dates into core chronologies significantly lowered estimates of pre-industrial flux because of apparent changes in lake sedimentation since the pre-industrial era. In the Arctic, incorporating $^{14}$C dates suggests that Hg deposition may have increased >10-fold since the Industrial Revolution, rather than the commonly quoted three-fold increase. Accurate core chronologies are thus of the utmost importance.

*Long-term variability in Arctic Hg accumulation*

There are very few records of Arctic Hg accumulation that span beyond the past few hundred years. Those that do exist are peat bog cores, and the reliability of peat geochemical records casts these reconstructions in doubt (Biester et al., 2007). The Arctic is experiencing dramatic environmental change, with important ecological consequences. These ecological and climatic changes may influence how Hg is cycled in the Arctic. For example, it has been hypothesized that climate-driven increases in within-lake primary production may accelerate Hg delivery to Arctic lake sediments (Outridge et al., 2007). Because sediments are the primary source of mercury methylation, increasing sediment Hg burdens has the potential to be passed up food chains.

Investigating natural variability in Arctic Hg deposition, and revealing possible climate-Hg couplings, requires natural archives that extend beyond human interferences in the biogeochemical Hg cycle. The multi-proxy lake records summarized in chapter 6 span the Holocene and include sediment from the last and penultimate interglaciations. It was found that natural conditions are capable of producing Hg concentrations and fluxes higher than those associated with 20$^{th}$-century anthropogenic enrichment. Careful consideration of individual lake and basin characteristics and histories are necessary if records of natural Hg variability are to be interpreted.

**Future efforts**

The research described above focuses on understanding both anthropogenic and natural drivers of pre-industrial Hg cycling. I suggest future efforts in this regard should focus on four primary areas of research:

First, new well-dated lake and ice core records are needed from remote

regions within the Southern Hemisphere. The Andean study sites presented as part of this thesis all occur within a few-hundred kilometers of major ancient and modern metallurgy centers. Lake records collected from more remote regions within the Southern Hemisphere will help to constrain the geographic range of early Hg emissions. If pre-industrial Hg enrichment is found in well-dated records from regions outside the Andes, our understanding of the pre-industrial global biogeochemical cycle of Hg will require revision.

Second, we need a better understanding of the natural biogeochemical cycle of Hg, including characterizing both spatial and temporal variability. Recent research utilizing the glaciochemical record preserved in the Dome C ice core from Antarctica has revealed dramatic fluctuations in the rate of Hg deposition to Antarctica over multiple glacial-interglacial transitions (Jitaru et al., 2009). The results presented in Chapter 5 of this thesis suggest there may have been spatial variability in the rate of pre-industrial Hg deposition as well, as the two arctic lakes suggest much lower pre-industrial Hg deposition rates than the two Andean lakes.

Third, we require new approaches to understand and quantify Hg sources, sinks, and transformations. In the case of Pb, the development of ultra-clean techniques and the application of Pb stable isotopes by Clair Patterson were invaluable in this regard, firmly establishing the case for early Pb pollution. Similarly, Hg stable isotopes appear to hold the most promise in this regard. Large variations in Hg isotope ratios have been observed in natural samples and, as a result, Hg isotopes are proving useful for tracking sources and understanding Hg transformations in the environment (Bergquist and Blum, 2007). As with other stable isotope systems, discriminating source signatures from processes that induce isotope fractionation during transport and transformation in the environment remains one of the greatest challenges in applying this new tool.

However, rapid progress is being made, and there is some indication that Hg stable isotopic profiles from lake sediment cores may provide a fingerprint for identifying natural and anthropogenic emissions.

Fourth, modeling studies are needed that incorporate not only pre-industrial Hg emissions but also attempt to model variability in pre-industrial Hg deposition (e.g., the glacial-interglacial variability in Hg deposition suggested by the Antarctic ice core). Some recent efforts have been made to include the former (Strode et al., 2009), but to date there have been no efforts aimed at modeling glacial-interglacial Hg variability. Developing new models and improving existing ones will help us to identify key drivers of natural Hg variability.

**References**


Bergquist, B. A. & Blum, J. D. (2007) Mass-dependent and-independent fractionation of Hg isotopes by photoreduction in aquatic systems. *Science,* 318**,** 417.

Biester, H., Bindler, R., Martínez-Cortizas, A. & Engstrom, D. R. (2007) Modeling the past atmospheric deposition of mercury using natural archives. *Environmental Science & Technology,* 41**,** 4851-4860.

Broecker, W. S. & Stocker, T. F. (2006) The Holocene $CO_2$ rise: anthropogenic or natural?, *Eos, Transactions American Geophyical Union*, 87, doi:10.1029/2006EO030002.

Brook, E. (2009) Atmospheric carbon footprints? *Nature Geoscience,* 2, 170-172.

Hong, S., Candelone, J-P., Patterson, C. C., Boutron, C. F. (1996) History of ancient copper smelting pollution during roman and medieval times recorded in Greenland ice. *Science,* 272, 246-249.

Jitaru, P., Gabrielli, P., Marteel, A., Plane, J. M. C., Planchon, F. A. M., et al. (2009) Atmospheric depletion of mercury over Antarctica during glacial periods. *Nature Geoscience,* 2, 505-508.

Klaminder, J., Hammarlund, D., Kokfelt, U., Vonk, J. E., Bigler, C. (2010) Lead contamination of subarctic lakes and its response to reduced atmospheric fallout: can the recovery process be counteracted by the ongoing climate change? *Environmental Science & Technology*, 44, 2335-2340.

Krachler, M., Zheng, J., Koerner, R., Zdanowicz, C., Fisher, D., et al. (2005) Increasing atmospheric antimony contamination in the northern hemisphere: snow and ice evidence from Devon Island, Arctic Canada. *Journal of Environmental Monitoring,* 7, 1169-1176.

Nriagu, J. O. (1993) Legacy of mercury pollution. *Nature,* 363**,** 589.

Outridge, P. M., Sanei, H., Stern, G. A., Hamilton, P. B. & Goodarzi, F. (2007) Evidence for control of mercury accumulation rates in Canadian High Arctic lake sediments by variations of aquatic primary productivity. *Environmental Science & Technology,* 41**,** 5259-5265.

Rauch, S., Peucker-Ehrenbrink, B., Kylander, M., Weiss, D., Martinez-Cortizas, A., et al. (2010) Anthropogenic Forcings on the Surficial Osmium Cycle. *Environmental Science & Technology,* 44**,** 881-887.

Ruddiman, W. (2003) The anthropogenic greenhouse era began thousands of years ago. *Climatic Change*, 61, 261-293.

Ruddiman, W. (2007) The early anthropogenic hypothesis: challenges and responses. *Reviews of Geophysics*, 45, RG4001.

Strode, S., Jaeglé, L. & Selin, N. E. (2009) Impact of mercury emissions from historic gold and silver mining: Global modeling. *Atmospheric Environment,* 43**,** 2012-2017.

Willis, K. J. & Birks, H. J. B. (2006) What is natural? The need for a long-term perspective in biodiversity conservation. *Science,* 314, 1261-1265.

**Table A.1.** Down-core $^{210}$Pb activities, calculated CRS sediment ages, and CRS sedimentation rates for the three study cores.

| Laguna Yanacocha 1 (LY1) Depth Interval (cm) | $^{210}$Pb activity (Bq g$^{-1}$) | Error $^{210}$Pb activity (1 σ) | CRS age | Error age (1 σ) | CRS sed. rate (g m$^{-2}$ yr$^{-1}$) | Error sed. rate (1 σ) |
|---|---|---|---|---|---|---|
| 0-0.5 | 0.673 | 0.021 | 2007 | 0 | 367 | 19 |
| 1-1.5 | 0.529 | 0.016 | 2005 | 0 | 442 | 22 |
| 2-2.5 | 0.301 | 0.017 | 2002 | 1 | 737 | 70 |
| 3-3.5 | 0.258 | 0.013 | 1998 | 1 | 783 | 69 |
| 4-4.5 | 0.273 | 0.014 | 1994 | 1 | 653 | 59 |
| 5-5.5 | 0.255 | 0.010 | 1990 | 1 | 613 | 44 |
| 6-6.5 | 0.255 | 0.010 | 1985 | 2 | 529 | 37 |
| 7-7.5 | 0.193 | 0.008 | 1980 | 2 | 638 | 53 |
| 8-8.5 | 0.181 | 0.004 | 1976 | 2 | 599 | 32 |
| 9-9.5 | 0.143 | 0.007 | 1971 | 4 | 703 | 75 |
| 10-10.5 | 0.137 | 0.007 | 1966 | 5 | 642 | 71 |
| 11-11.5 | 0.125 | 0.007 | 1959 | 6 | 579 | 71 |
| 12-12.5 | 0.141 | 0.007 | 1951 | 6 | 378 | 40 |
| 13-13.5 | 0.086 | 0.006 | 1941 | 12 | 585 | 108 |
| 14-14.5 | 0.076 | 0.005 | 1933 | 15 | 573 | 116 |
| 16-16.5 | 0.072 | 0.004 | 1910 | 22 | 312 | 69 |
| 18-18.5 | 0.052 | 0.003 | | | | |
| 20-20.5 | 0.038 | 0.003 | | | | |
| 30-30.5 | 0.032 | 0.003 | | | | |
| 40-40.5 | 0.037 | 0.003 | | | | |

* Previously published as supporting online material for: Cooke C. A., Balcom, P. H., Biester, H., & Wolfe, A. P. (2009) Over three millennia of mercury pollution in the Peruvian Andes. *Proceedings of the National Academy of Sciences*, **106**, 8830-8834.

**Table A.1 (continued).** Down-core $^{210}$Pb activities, calculated CRS sediment ages, and CRS sedimentation rates for the three study cores.

| Laguna Yanacocha 2 (LY2) Depth Interval (cm) | $^{210}$Pb activity (Bq g$^{-1}$) | Error $^{210}$Pb activity (1 σ) | CRS age | Error age (1 σ) | CRS sed. rate (g m$^{-2}$ yr$^{-1}$) | Error sed. rate (1 σ) |
|---|---|---|---|---|---|---|
| 0.5-1 | 1.060 | 0.032 | 2004 | 0 | 91 | 4 |
| 1.5-2 | 0.754 | 0.030 | 1998 | 1 | 107 | 6 |
| 2.5-3 | 0.628 | 0.016 | 1990 | 1 | 102 | 4 |
| 3.5-4 | 0.562 | 0.015 | 1983 | 1 | 91 | 4 |
| 4.5-5 | 0.434 | 0.012 | 1974 | 2 | 89 | 4 |
| 5.5-6 | 0.315 | 0.006 | 1964 | 2 | 93 | 3 |
| 6.5-7 | 0.191 | 0.004 | 1954 | 2 | 120 | 5 |
| 7.5-8 | 0.128 | 0.003 | 1946 | 4 | 149 | 9 |
| 8.5-9 | 0.096 | 0.005 | 1939 | 8 | 174 | 19 |
| 9.5-10 | 0.099 | 0.005 | 1932 | 8 | 133 | 14 |
| 10.5-11 | 0.070 | 0.004 | 1923 | 12 | 165 | 24 |
| 11.5-12 | 0.055 | 0.003 | 1916 | 18 | 193 | 39 |
| 12.5-13 | 0.049 | 0.003 | 1909 | 25 | 190 | 48 |
| 13.5-14 | 0.052 | 0.004 | 1901 | 24 | 134 | 30 |
| 14.5-15 | 0.047 | 0.003 | 1890 | 29 | 115 | 28 |
| 16.5-17 | 0.034 | 0.003 | | | | |
| 18.5-19 | 0.031 | 0.002 | | | | |
| 20.5-21 | 0.027 | 0.002 | | | | |
| 30-30.5 | 0.024 | 0.002 | | | | |
| 40-40.5 | 0.021 | 0.002 | | | | |

**Table A.1 (continued).** Down-core $^{210}Pb$ activities, calculated CRS sediment ages, and CRS sedimentation rates for the three study cores.

| Laguna Negrilla Depth Interval (cm) | $^{210}Pb$ activity (Bq $g^{-1}$) | Error $^{210}Pb$ activity (1 σ) | CRS age | Error age (1 σ) | CRS sed. rate (g $m^{-2}$ $yr^{-1}$) | Error sed. rate (1 σ) |
|---|---|---|---|---|---|---|
| 0-0.5 | 1.361 | 0.099 | 2008 | 0 | 145 | 16 |
| 1-1.5 | 0.793 | 0.060 | 2006 | 0 | 239 | 29 |
| 2-2.5 | 0.800 | 0.032 | 2004 | 0 | 223 | 16 |
| 3-3.5 | 0.711 | 0.032 | 2002 | 1 | 234 | 18 |
| 4-4.5 | 0.881 | 0.034 | 1999 | 1 | 171 | 11 |
| 5-5.5 | 0.851 | 0.036 | 1995 | 1 | 158 | 12 |
| 6-6.5 | 0.840 | 0.035 | 1992 | 1 | 143 | 10 |
| 7-7.5 | 0.877 | 0.037 | 1988 | 1 | 120 | 9 |
| 8-8.5 | 0.678 | 0.021 | 1983 | 2 | 137 | 9 |
| 9-9.5 | 0.400 | 0.015 | 1979 | 3 | 218 | 20 |
| 10-10.5 | 0.468 | 0.017 | 1976 | 3 | 168 | 14 |
| 12-12.5 | 0.403 | 0.017 | 1969 | 4 | 157 | 15 |
| 14-14.5 | 0.400 | 0.018 | 1959 | 5 | 118 | 12 |
| 16-16.5 | 0.335 | 0.019 | 1948 | 8 | 102 | 13 |
| 18-18.5 | 0.251 | 0.011 | 1935 | 10 | 94 | 13 |
| 20-20.5 | 0.189 | 0.012 | 1913 | 19 | 69 | 14 |
| 22-22.5 | 0.073 | 0.006 | 1886 | 114 | 162 | 151 |
| 25-25.5 | 0.075 | 0.004 | 1879 | 107 | 120 | 100 |
| 30-30.5 | 0.058 | 0.004 | | | | |
| 45-45.5 | 0.035 | 0.003 | | | | |

**Table A.2.** Table of radiocarbon determinations for the three study cores.

| UCI ID # | Lake | Depth (cm) | Sample size (mg C) | $^{14}$C age (BP) | 2 σ calib. range BC/AD | Median date BC/AD |
|---|---|---|---|---|---|---|
| 51338 | LY1 | 45.5-46.5 | 0.10 | 520 ± 15 | 1420-1450 AD | 1435 AD |
| 49762 | LY1 | 60-60.5 | 0.21 | 1020 ± 20 | 1020-1150 AD | 1090 AD |
| 44752 | LY1 | 80-82 | 0.11 | 2175 ± 25 | 345-50 BC | 145 BC |
| 49764 | LY1 | 90.5-91 | 0.18 | 2460 ± 20 | 730-400 BC | 475 BC |
| 49763 | LY1 | 95.5-96 | 0.11 | 2675 ± 25 | 835-675 BC | 800 BC |
| 51339 | LY2 | 36-37.5 | 0.04 | 1285 ± 30 | 690-885 AD | 790 AD |
| 49759 | LY2 | 56-57.5 | 0.18 | 2225 ± 20 | 360-115 BC | 260 BC |
| 49760 | LY2 | 87.5-89.5 | 0.14 | 3390 ± 20 | 1690-1525 BC | 1620 BC |
| 51337 | Negrilla | 49.5-50 | 0.16 | 3170 ± 15 | 1450-1610 AD | 1465 AD |
| 56388 | Negrilla | 87.5-88 | 0.04 | 2060 ± 45 | 165 BC-115 AD | 10 BC |
| 49765 | Negrilla | 112.5-114 | 0.05 | 440 ± 45 | 1495-1260 BC | 1390 BC |

**Table A.3.** Table of blank values, average relative standard deviations, and recoveries of standard reference materials associated with DMA80 measurements of Hg.

| | LY1 | LY2 | Negrilla |
|---|---|---|---|
| Blanks (ng/g) | 1.4<br>n=25 | 4.0<br>n=14 | 0.5<br>n=24 |
| Duplicates (avg. % difference) | 15%<br>n=14 | 12%<br>n=10 | 4%<br>n=20 |
| MESS-3 (avg. % recovery) | 101%<br>n=11 | 100%<br>n=7 | 97%<br>n=14 |
| PACS-2 (avg. % recovery) | 97%<br>n=11 | 101%<br>n=6 | 101%<br>n=11 |

**Fig. A.1.** Solid-phase Hg thermo-desorption curves of standard materials and selected sediment samples of the LY2 core. The Chavín and Colonial/Modern samples are from 80 and 8.5 cm depth respectively. The Colonial/Modern sample-peak lies between $Hg^0$ and cinnabar, indicating the presence of matrix-bound Hg, a fraction which is largely bound to organic matter, but may also include particulate-bound Hg. Cinnabar and $Hg^0$ standard samples were obtained from the Idrija mercury mine, Slovenia.

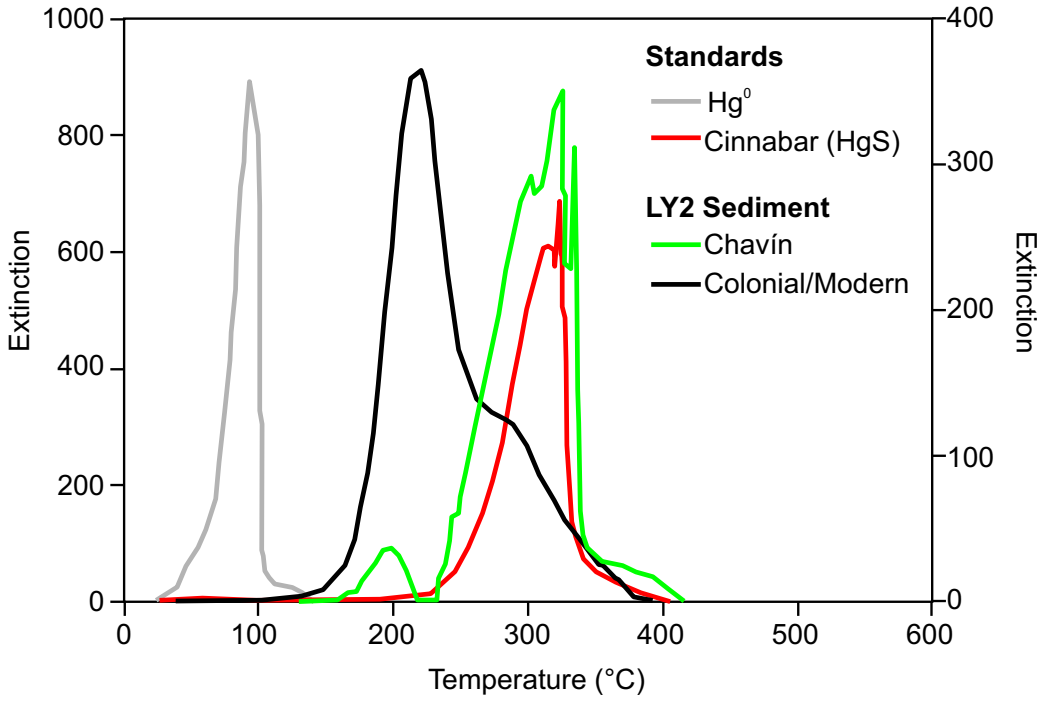

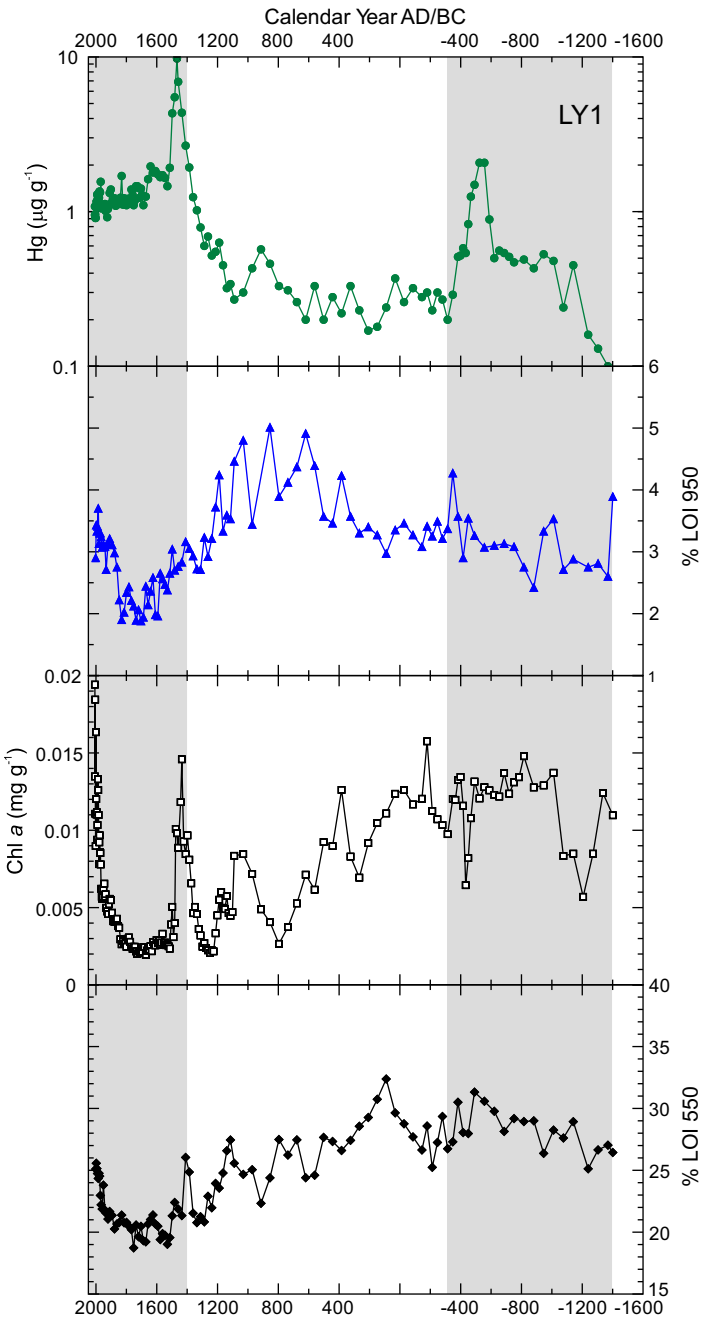


**Fig. A.2.** Geochemical and organic matter profiles from core LY1. Significant increases in Hg are shaded and cannot be attributable to rapid increases in other sediment variables. Both within-lake primary production and total organic mater burial have been shown to influence the accumulation of Hg within lake sediments. There is no correlation between Hg and Chl a ($r^2$=0.01), and Hg and % LOI 550 ($r^2$=-0.15). The exception is an obvious large peak in both Hg and Chl a centered ~1450 AD. However, similar Chl a concentrations (e.g. ca. 200 BC) yield no net increase in Hg, and no increase in Hg is noted in modern sediments when Chl a attains its highest levels (0.02 mg/g).

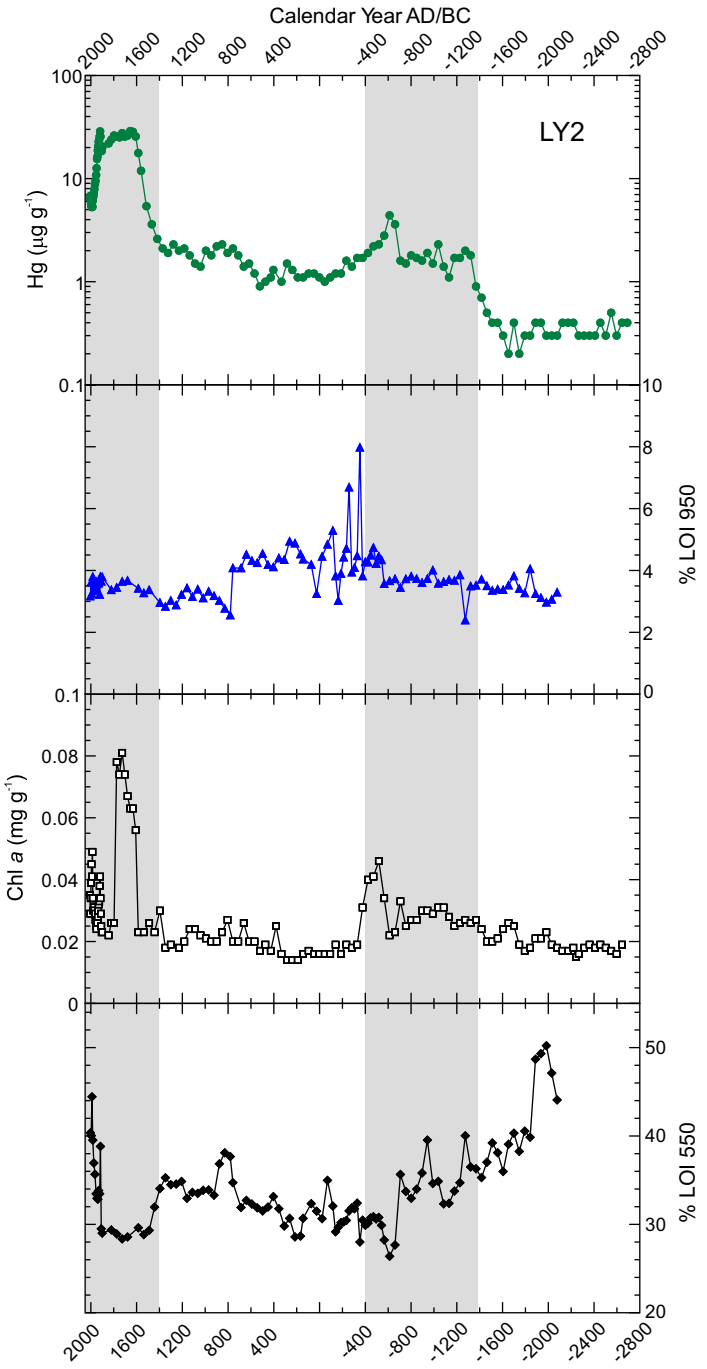


**Fig. A.3.** Geochemical and organic matter profiles from core LY2. As observed at LY1, increases in Hg are shaded and cannot be attributable to rapid increases in other sediment variables.

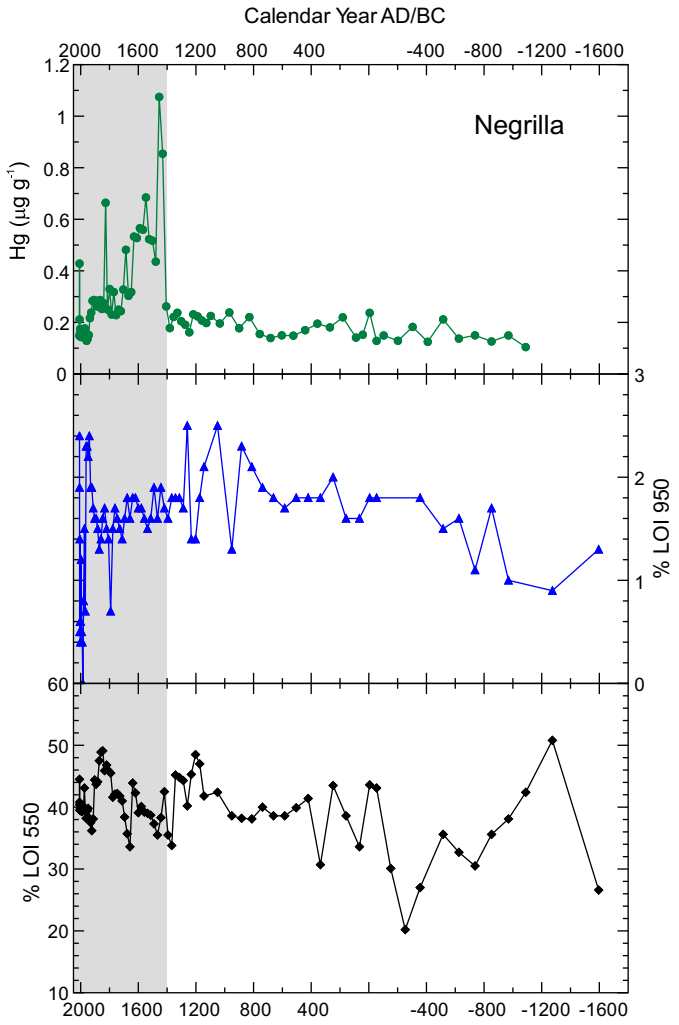


**Fig. A.4.** Geochemical and organic matter profiles from Negrilla. As with LY1 and LY2, increases in Hg are shaded and cannot be attributable to rapid increases in other sediment variables.

**Table B.1.** Measurements of total $^{210}$Pb activity, associated CRS dates, and CRS sedimentation rates for the Llamacocha core.

| Depth (cm) | $^{210}$Pb (Bq g$^{-1}$) | 1σ error | CRS date | 1σ error | CRS sed. rate (g m$^{-2}$ yr$^{-1}$) | 1σ error |
|---|---|---|---|---|---|---|
| 0-1 | 1.15 | 0.06 | 2007 | 0 | 85 | 8 |
| 2-3 | 1.20 | 0.04 | 2006 | 0 | 78 | 6 |
| 4-5 | 1.19 | 0.04 | 2004 | 0 | 73 | 5 |
| 6-7 | 1.04 | 0.03 | 2000 | 0 | 75 | 5 |
| 8-9 | 1.01 | 0.03 | 1995 | 1 | 67 | 5 |
| 10-11 | 0.93 | 0.03 | 1990 | 1 | 61 | 6 |
| 12-13 | 0.68 | 0.03 | 1981 | 2 | 66 | 6 |
| 14-15 | 0.48 | 0.02 | 1974 | 2 | 78 | 7 |
| 16-17 | 0.35 | 0.02 | 1967 | 5 | 91 | 12 |
| 18-19 | 0.38 | 0.02 | 1961 | 5 | 68 | 10 |
| 20-21 | 0.29 | 0.02 | 1950 | 7 | 66 | 12 |
| 24-25 | 0.16 | 0.01 | 1929 | 11 | 75 | 14 |
| 28-29 | 0.12 | 0.01 | 1914 | 20 | 75 | 21 |
| 32-33 | 0.11 | 0.01 | 1894 | 30 | 56 | 26 |
| 41-42 | 0.06 | 0.01 | | | | |
| 51-52 | 0.05 | 0.00 | | | | |

**Table B.2.** Table of radiocarbon dates used in the core chronology. Note that BC dates are denoted as negative.

| UCI ID | Depth (cm) | Size (mg carbon) | ± | Fraction modern | ± | $^{14}$C age (BP) | ± |
|---|---|---|---|---|---|---|---|
| 56389 | 33-36 | 0.029 | 1.5 | 0.946 | 0.004 | 445 | 40 |
| 51340 | 42-45 | 0.029 | 0.8 | 0.916 | 0.004 | 705 | 40 |
| 49761 | 56-59 | 0.065 | 4.0 | 0.865 | 0.003 | 1160 | 30 |
| 56386 | 61-64 | 0.033 | 1.2 | 0.829 | 0.004 | 1510 | 40 |
| 56387 | 85-86 | 0.033 | 1.4 | 0.768 | 0.005 | 2120 | 60 |

* Previously published as supporting online material for: Cooke C. A., Wolfe, A. P., & Hobbs, W. O. (2009) Lake-sediment geochemistry reveals 1400 years of evolving extractive metallurgy at Cerro de Pasco, Peruvian Andes. *Geology*, **37**, 1019-1022.

**Table B.3.** Table of stable Pb isotopic values for Llamacocha sediment samples.

| Depth (cm) | Calibrate year (AD/BC) | $^{206}Pb/^{204}Pb$ | 1σ | $^{207}Pb/^{204}Pb$ | 1σ | $^{208}Pb/^{204}Pb$ | 1σ |
|---|---|---|---|---|---|---|---|
| 3 | 2004 | 18.774 | 9.01E-04 | 15.647 | 1.07E-03 | 38.795 | 3.47E-03 |
| 19 | 1955 | 18.781 | 8.21E-04 | 15.648 | 9.64E-04 | 38.819 | 3.06E-03 |
| 38 | 1582 | 18.814 | 1.20E-03 | 15.651 | 1.23E-03 | 38.825 | 3.60E-03 |
| 45 | 1322 | 18.816 | 1.72E-03 | 15.640 | 1.73E-03 | 38.788 | 5.04E-03 |
| 51 | 1091 | 18.852 | 1.80E-03 | 15.649 | 1.72E-03 | 38.818 | 4.49E-03 |
| 58 | 823 | 18.936 | 1.98E-03 | 15.652 | 2.06E-03 | 38.818 | 5.24E-03 |
| 63 | 643 | 19.227 | 9.74E-04 | 15.668 | 1.09E-03 | 38.877 | 3.27E-03 |
| 69 | 453 | 19.457 | 1.52E-03 | 15.691 | 1.25E-03 | 38.943 | 3.66E-03 |
| 76 | 256 | 19.441 | 1.78E-03 | 15.688 | 1.68E-03 | 38.932 | 4.75E-03 |
| 81 | 125 | 19.454 | 1.39E-03 | 15.663 | 1.45E-03 | 38.863 | 4.26E-03 |
| 96 | -255 | 19.589 | 9.70E-04 | 15.698 | 1.16E-03 | 38.975 | 3.57E-03 |
| 101 | -350 | 19.606 | 2.01E-03 | 15.689 | 1.77E-03 | 38.937 | 4.85E-03 |
| NBS 981+ Tl | | 16.930 | 1.05E-03 | 15.485 | 1.15E-03 | 36.683 | 3.36E-03 |
| NBS 981+ Tl | | 16.931 | 1.11E-03 | 15.484 | 1.26E-03 | 36.675 | 3.09E-03 |
| NBS 981+ Tl | | 16.935 | 9.72E-04 | 15.488 | 1.08E-03 | 36.687 | 2.86E-03 |
| Certified value | | 16.941 | | 15.496 | | 36.722 | |

| Depth (cm) | Calibrate year (AD/BC) | $^{208}Pb/^{206}Pb$ | 1σ | $^{207}Pb/^{206}Pb$ | 1σ |
|---|---|---|---|---|---|
| 3 | 2004 | 2.066 | 9.11E-05 | 0.833 | 1.92E-05 |
| 19 | 1955 | 2.067 | 8.00E-05 | 0.833 | 1.56E-05 |
| 38 | 1582 | 2.064 | 7.91E-05 | 0.832 | 1.88E-05 |
| 45 | 1322 | 2.061 | 9.39E-05 | 0.831 | 2.16E-05 |
| 51 | 1091 | 2.059 | 8.04E-05 | 0.830 | 2.41E-05 |
| 58 | 823 | 2.050 | 6.88E-05 | 0.827 | 2.73E-05 |
| 63 | 643 | 2.022 | 9.57E-05 | 0.815 | 2.27E-05 |
| 69 | 453 | 2.002 | 7.02E-05 | 0.806 | 1.65E-05 |
| 76 | 256 | 2.003 | 8.82E-05 | 0.807 | 1.97E-05 |
| 81 | 125 | 1.998 | 9.30E-05 | 0.805 | 2.13E-05 |
| 96 | -255 | 1.990 | 8.13E-05 | 0.801 | 1.76E-05 |
| 101 | -350 | 1.986 | 7.25E-05 | 0.800 | 1.79E-05 |
| NBS 981+ Tl | | 2.167 | 8.17E-05 | 0.915 | 2.04E-05 |
| NBS 981+ Tl | | 2.166 | 6.33E-05 | 0.914 | 1.96E-05 |
| NBS 981+ Tl | | 2.166 | 6.34E-05 | 0.915 | 1.82E-05 |
| Certified value | | 2.168 | | 0.915 | |

**Table B.4.** Table of stable Pb isotopic values for regional ores; source references are as indicated.

| Mine | $^{206}Pb/^{204}Pb$ | $^{207}Pb/^{204}Pb$ | $^{208}Pb/^{204}Pb$ | $^{208}Pb/^{206}Pb$ | $^{207}Pb/^{206}Pb$ | Reference |
|---|---|---|---|---|---|---|
| Cerro de Pasco | 18.778 | 15.637 | 38.811 | 2.067 | 0.833 | Mukasa et al., 1990 |
| | 18.778 | 15.661 | 38.888 | 2.071 | 0.834 | |
| | 18.821 | 15.96 | 38.954 | 2.070 | 0.848 | |
| | 18.789 | 15.658 | 38.870 | 2.069 | 0.833 | |
| Cerro de Pasco | 18.776 | 15.666 | 38.902 | 2.072 | 0.834 | Sangster et al., 2000 |
| Atacocha | 18.822 | 15.681 | 38.968 | 2.070 | 0.833 | Gunnesch and Baumann |
| | 18.839 | 15.693 | 39.009 | 2.071 | 0.833 | 1984 |
| | 18.793 | 15.659 | 38.866 | 2.068 | 0.833 | |
| | 18.810 | 15.673 | 38.937 | 2.070 | 0.833 | |
| | 18.860 | 15.727 | 39.073 | 2.072 | 0.834 | |
| Atacocha | 18.823 | 15.682 | 38.969 | 2.070 | 0.833 | Gunnesch et al., 1990 |
| | 18.839 | 15.693 | 39.009 | 2.071 | 0.833 | |
| | 18.793 | 15.653 | 38.863 | 2.068 | 0.833 | |
| | 18.810 | 15.673 | 38.937 | 2.070 | 0.833 | |
| | 18.860 | 15.727 | 39.073 | 2.072 | 0.834 | |
| | 18.789 | 15.651 | 38.866 | 2.069 | 0.833 | |
| Milpo | 18.801 | 15.643 | 38.866 | 2.067 | 0.832 | Gunnesch and Baumann |
| | 18.829 | 15.673 | 38.938 | 2.068 | 0.832 | 1984 |
| | 18.851 | 15.701 | 39.047 | 2.071 | 0.833 | |
| | 18.848 | 15.685 | 38.987 | 2.068 | 0.832 | |
| | 18.819 | 15.664 | 38.91 | 2.068 | 0.832 | |
| | 18.771 | 15.667 | 38.925 | 2.074 | 0.835 | |
| | 18.835 | 15.683 | 38.967 | 2.069 | 0.833 | |
| | 18.849 | 15.697 | 39.04 | 2.071 | 0.833 | |
| | 18.832 | 15.678 | 38.958 | 2.069 | 0.833 | |
| | 18.842 | 15.673 | 38.956 | 2.068 | 0.832 | |
| | 18.826 | 15.676 | 38.959 | 2.069 | 0.833 | |
| | 18.801 | 15.649 | 38.876 | 2.068 | 0.832 | |
| | 18.819 | 15.674 | 38.932 | 2.069 | 0.833 | |
| | 18.817 | 15.665 | 38.926 | 2.069 | 0.832 | |

**Fig. B.1.** Down-core profile of (A) total $^{210}$Pb activity, (B) associated CRS dates, and (C) Sedimentation rate for the Llamacocha core.

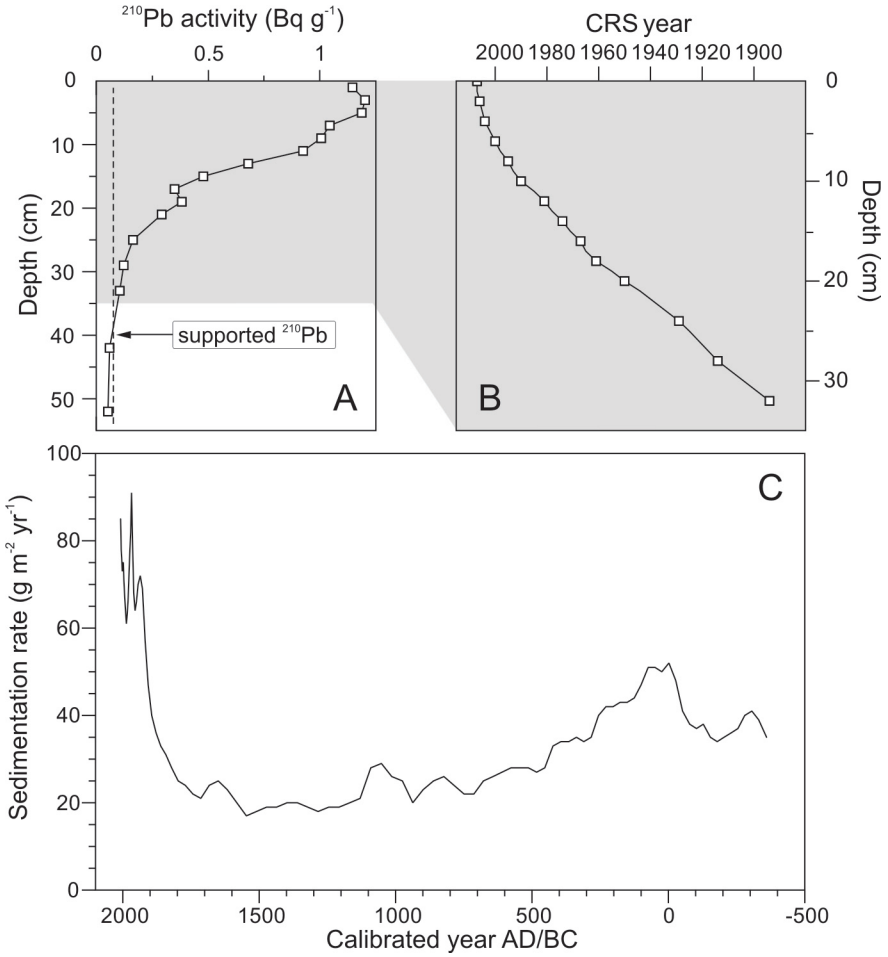

**Fig. B.2.** Elemental fluxes for each element measured. Na, Mg, Al, Ca, Ti, Mn, Fe, Zn, As, Cu, Sr, and Pb are in the units mg $m^{-2}$ $yr^{-1}$; Hg, Sb, Cr, and Sc are in the units μg $m^{-2}$ $yr^{-1}$. Note Mn, Zn, Hg, As, Pb, and Sb are plotted on a log scale.

**Fig. B.3.** Plot of $^{206}Pb/^{204}Pb$ vs. (A) $^{207}Pb/^{204}Pb$ and (B) $^{208}Pb/^{204}Pb$. Stable Pb

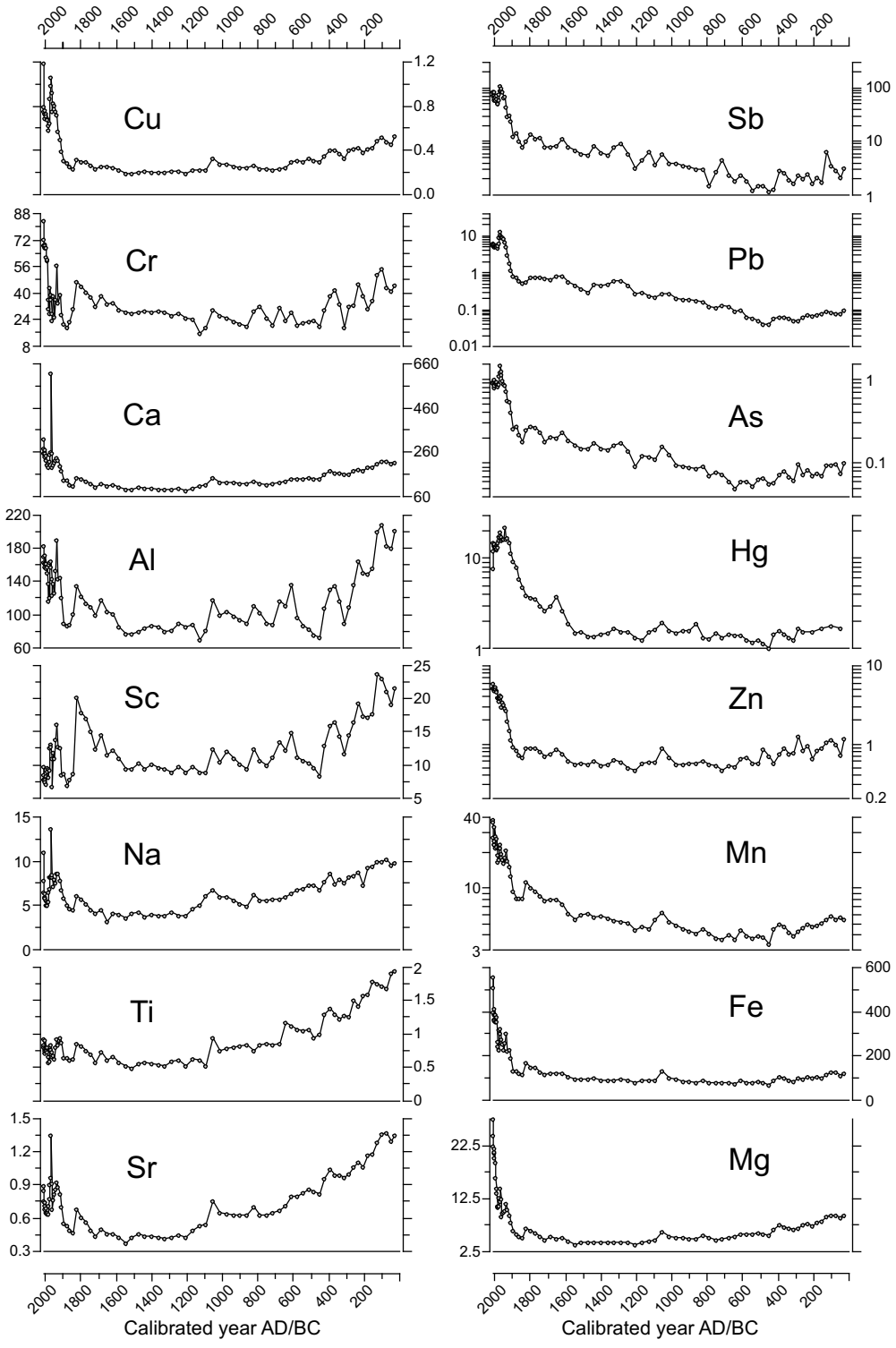

isotopic ratios for Llamacocha sediment are plotted alongside stable Pb isotopic ratios from galena (PbS) from local mines (Pb data for Llamacocha sediment are provided in Table B.3 and Pb data for ores in Table B.4). The largest and historically the most economically important of these mines is Cerro de Pasco. Milpo, Atacocha, and the St Vicenete mine are all located 10-20 km north of Cerro de Pasco. The cluster of four background samples are those intervals which pre-date ~600 AD, and thus pre-date Pb enrichment associated with the rise of regional metallurgy. Llamacocha sediment Pb ratios roughly plot along a straight line between background and 20$^{th}$ century intervals. The 20$^{th}$ century samples plot directly on top of the low-end of Cerro de Pasco ores (especially $^{208}Pb/^{204}Pb$), indicating Cerro de Pasco is the major source of anthropogenic Pb in Llamacocha sediment, though limited influence by other regional ores cannot be ruled out.

**Fig. B.4.** The down-core flux ratio profile for both Pb and Hg. Flux ratios (sample

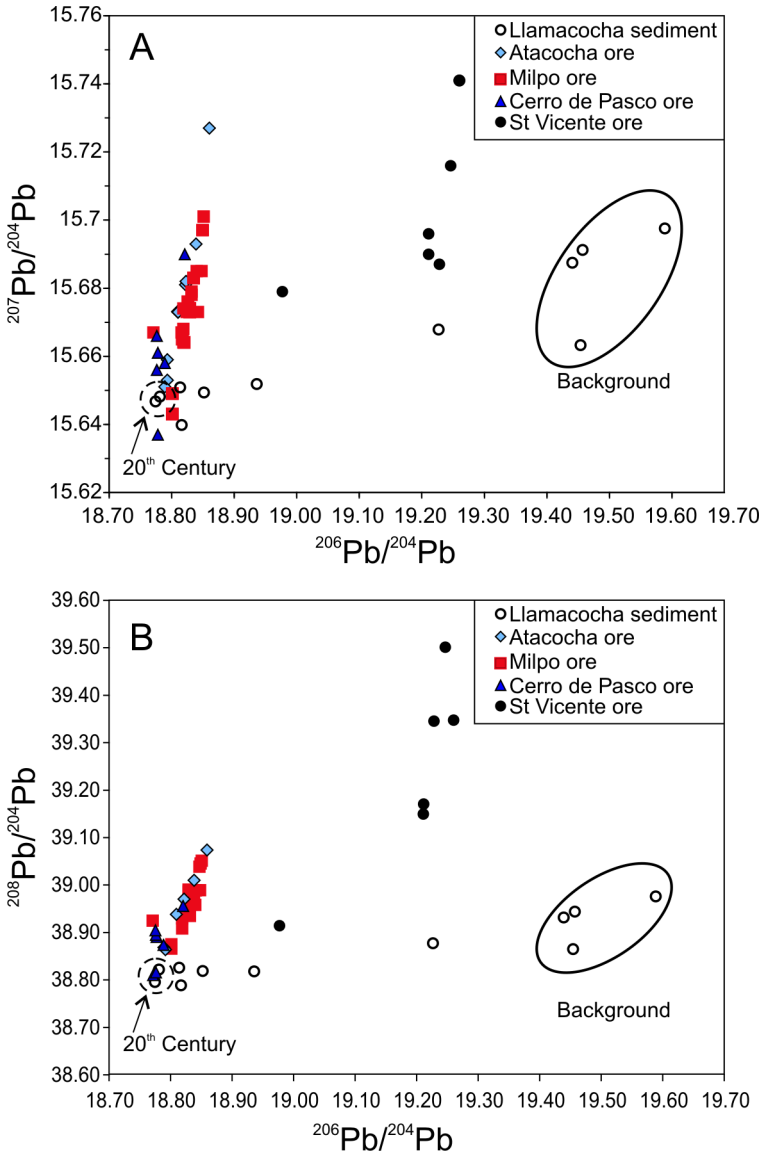

to average background fluxes) provide a unitless measure of relative increases in metal accumulation rates, and facilitate comparisons between lake records. The average background Pb flux is 0.07±0.01 mg $m^{-2}$ $yr^{-1}$ (n=35; pre-600 AD) and the average rate of background Hg flux is 1.5±0.2 μg $m^{-2}$ $yr^{-1}$ (n=49; pre-1600 AD).

**References:**

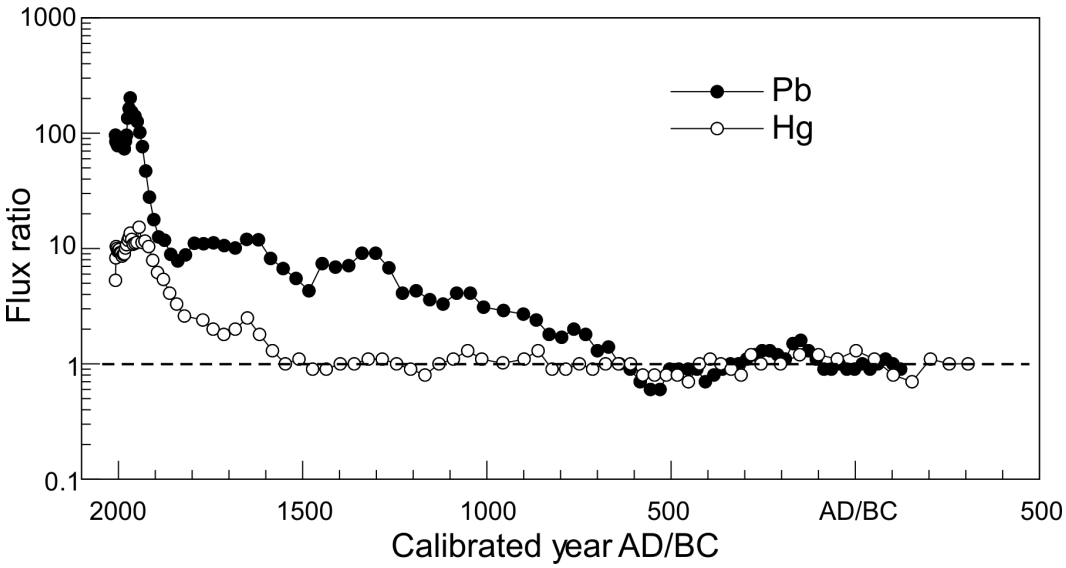


Gunnesch, K.A., & Baumann A. (1984) The Atacocha district, central Perú: Some metallogenetic aspects, IN Wauschkuhn A., Kluth, C., & Zimmermann, R.A. (Eds.) *Syngenesis and epigenesis in the formation of mineral deposits*. Berlin, Springer-Verlag, 448–456.

Gunnesch, K.A., Baumann A., & Gunnesch, M. (1990) Lead isotope variations across the central Peruvian Andes. *Economic Geology*, 85, 1384–1401.

Mukasa, S.B., Vidal, C., C.E., & Injoque-Espinoza, J. (1990) Pb Isotope Bearing on the Metallogenesis of Sulfide Ore Deposits in Central and Southern Peru. *Economic Geology*, 85, 1438–1436.

Sangster, D.F., Outridge, P.M., and Davis, W.J. (2000) Stable lead isotope characteristics of lead ore deposits of environmental significance. *Environmental Reviews*, 8, 115–147.

**Fig. C.1.** Map of North and South America indicating the location of the study sites in Canada (Lost Pack and CF8), and Peru (LY2 and Negrilla).

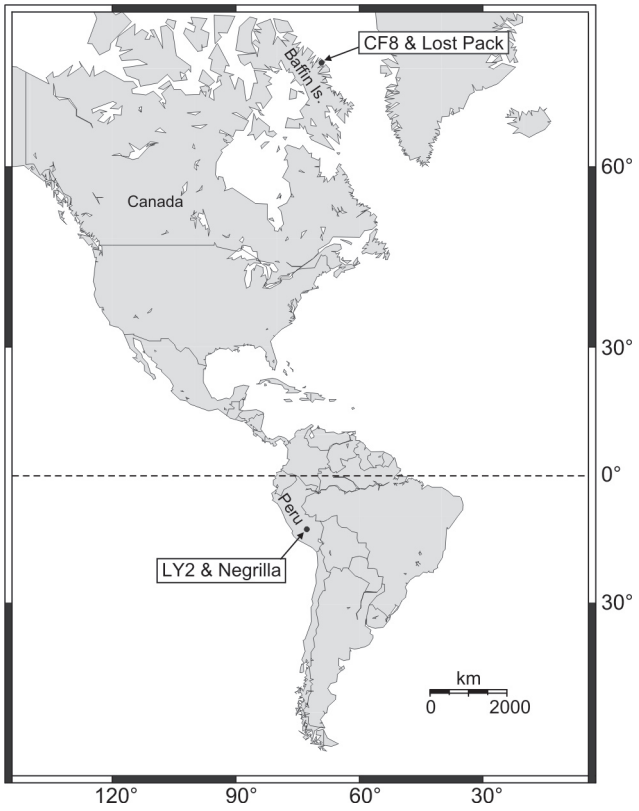


* Previously published as supporting online material for: Cooke C. A., Hobbs, W. O., Michelutti, N., & Wolfe, A. P. Reliance on $^{210}$Pb chronology can compromise the inference of pre-industrial Hg flux to lake sediments. (in press) *Environmental Science & Technology*.

**Fig. C.2.** Down-core profiles of dry density (open squares) and % LOI 550°C (red line) for (A) LY2; (B) Laguna Negrilla; (C) CF8, and; (D) Lost Pack.

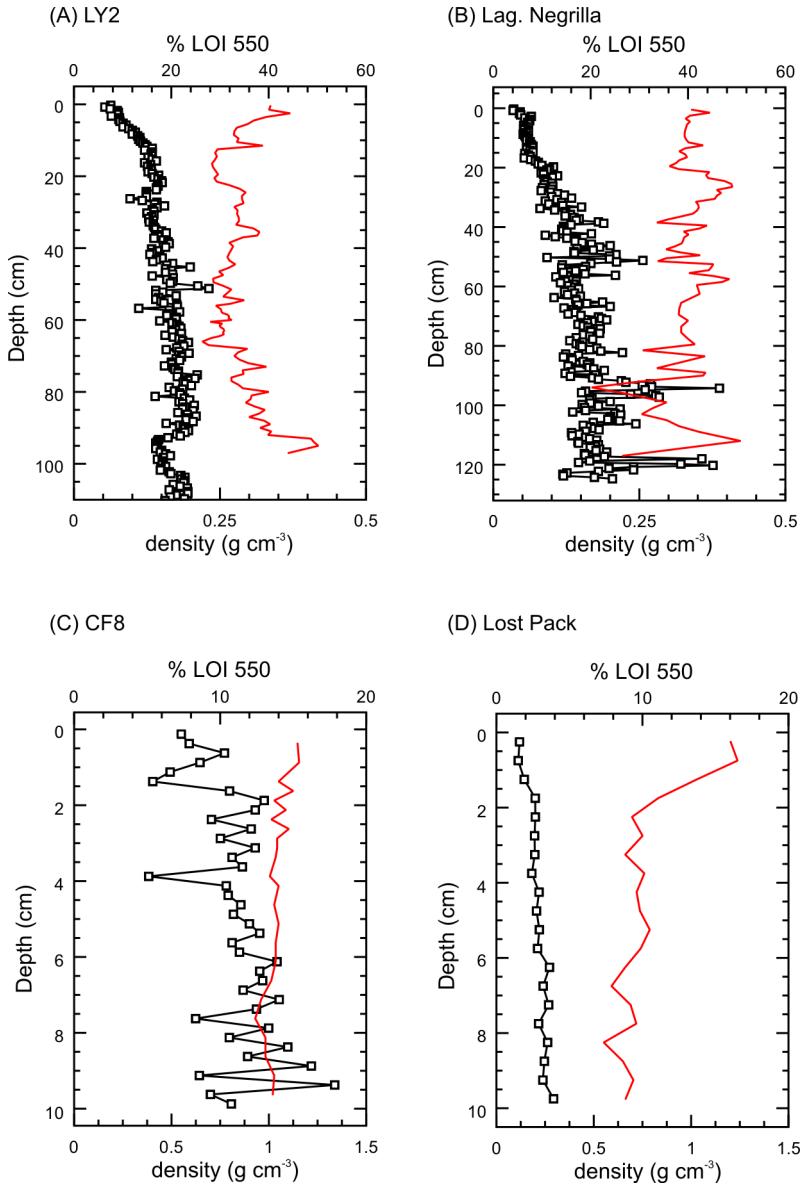

**Table C.1.** Location and physical characteristics of the study lakes.

| Lake | Latitude | Longitude | Elevation (m a.s.l.) | Lake area ($km^2$) | Catchment area ($km^2$) | Catchment: Lake area |
|---|---|---|---|---|---|---|
| LY2 | 12° 49' S | 75° 1' W | 4585 | 0.05 | 0.31 | 6.2 |
| Negrilla | 13° 9' S | 72° 58' W | 4130 | 0.06 | 0.32 | 5.3 |
| CF8 | 68° 57' N | 70° 33' W | 195 | 0.30 | 1.50 | 5.0 |
| Lost Pack | 68° 50' N | 69° 57' W | 230 | 0.15 | 0.90 | 6.0 |

**Table C.2.** Results of the different Hg flux estimates when calculated using both extrapolated $^{210}$Pb age models and the composite ($^{210}$Pb and $^{14}$C) age models. Modern accumulation rates reflect dry mass sediment flux at the sediment-water interface and are derived from the CRS model of $^{210}$Pb activities for each core.

| Lake | Background accum. rate (extrap. $^{210}$Pb) ($\mu g\ m^{-2}\ yr^{-1}\ \pm 1\sigma$) | Background accum. rate ($^{14}$C model) ($\mu g\ m^{-2}\ yr^{-1}\ \pm 1\sigma$) | Modern acccum. rate ($\mu g\ m^{-2}\ yr^{-1}$) | Modern flux ratio ($^{210}$Pb model) | Modern flux ratio ($^{14}$C model) |
|---|---|---|---|---|---|
| LY2 | 44 ±8 | 14 ±3 | 644 | 15 | 46 |
| Negrilla | 12 ±3 | 7 ±3 | 31 | 3 | 4.5 |
| CF8 | 0.70 ±0.07 | 0.25 ±0.08 | 3.23 | 5 | 13 |
| Lost Pack | 1.8 ±0.3 | 0.3 ±0.1 | 4.2 | 2 | 12 |

**Table C.3.** Table of radiocarbon dates for the four study lakes.

| | Depth (cm) | Lab no. | Material dated | Fraction modern | AMS 14C date (± 1σ) | Cal year AD/BC (2σ range) |
|---|---|---|---|---|---|---|
| LY2 | 36-37.5 | UCI-51339 | Charcoal | 0.852±0.003 | 1285±30 | 690-885 AD |
| | 56-57.5 | UCI-49759 | Charcoal | 0.759±0.002 | 2225±20 | 360-115 BC |
| | 87.5-89.5 | UCI-49760 | Charcoal | 0.656±0.002 | 3390±20 | 1690-1525 BC |
| Negrilla | 49.75 | UCI-51337 | Charcoal | 0.947±0.002 | 3170±15 | 1450-1610 AD |
| | 87.75 | UCI-56388 | Charcoal | 0.774±0.004 | 2060±45 | 165 BC-115 AD |
| | 113 | UCI-49765 | Charcoal | 0.674±0.004 | 440±45 | 1495-1260 BC |
| CF8 | 5.875 | CURL-8269 | macrofossil | 0.888±0.004 | 955±35 | 1020-1160 AD |
| | 16.875 | CURL-8138 | macrofossil | 0.705±0.002 | 2810±20 | 1010-910 BC |
| | 25.5 | CURL-8141 | macrofossil | 0.652±0.001 | 3440±20 | 1870-1690 BC |
| Lost Pack | 10.25 | CURL-7499 | Humic acid | 0.677±0.001 | 3130±15 | 1440-1330 BC |
| | 21.25 | CURL-7519 | Humic acid | 0.586±0.001 | 4295±20 | 2920-2890 BC |
| | 21.25 | CURL-7500 | macrofossil | 0.597±0.001 | 4150±20 | 2870-2630 BC |

**Fig. D.1.** Down-core profiles of dry density, sedimentation rate, and Hg flux from Lakes CF3 (A) and CF8 (B). For Lake CF8, the dry density of the entire sediment record is shown, while sedimentation rate and Hg flux are restricted to the Holocene. At CF8, dry density values for the percussion core (black line) were ~2x those from the surface core during the late Holocene. Unlike the surface core, the percussion cores collected at CF8 were not extruded in the field. Thus, the difference in dry density values between the two cores likely results from de-watering of the core during collection and transport. To correct for this artifact, dry density values were multiplied by 0.5. Corrected dry density values were then included in the calculation of sedimentation rate and Hg flux and are shown in blue.

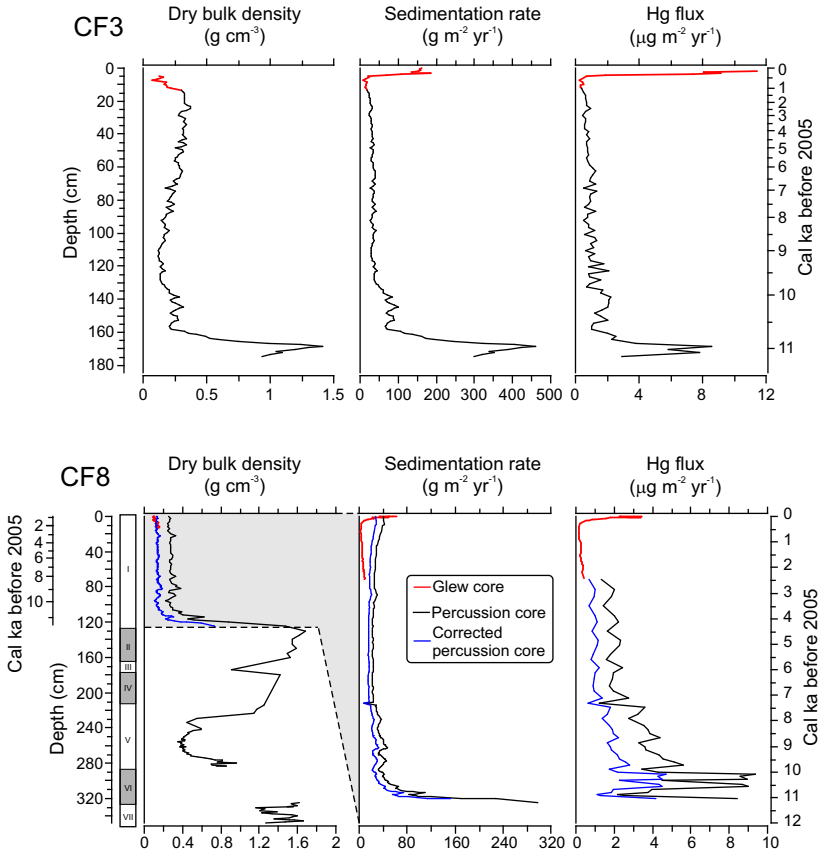

**Table D.1.** List of the sediment cores used in this study and associated QA/QC Hg values which includes average blank concentrations, average % recovery of standard reference materials, and the average % difference between duplicate measurements of the same sediment interval.

| Lake: core designation | Avg. blank (ng g-1) (*n* ) | Avg. % recovery reference materials (MESS-3, PACS-2) (*n* ) | Avg. % difference between duplicates (*n* ) |
|---|---|---|---|
| CF3: 2003 Surface core | 0.08 | 93% | 4% |
| | 4 | 2 | 2 |
| CF3: 2002 Percussion core | 0.08 | 97% | 4% |
| | 17 | 10 | 22 |
| CF8: 2005 Surface core | 0.18 | 97% | 4% |
| | 17 | 22 | 22 |
| CF8: 2002 CF8 (Unit I) | 0.53 | 98% | 6% |
| | 10 | 8 | 11 |
| CF8: 2006 CF8-P1 (UNIT III) | 0.08 | 99% | 5% |
| | 3 | 3 | 4 |
| CF8: 2004 CF8-02 (Unit V) | 0.54 | 98% | 2% |
| | 7 | 5 | 6 |
| CF8: 2005 CF8-01 (Unit VII) | 0.22 | 102% | 4% |
| | 5 | 5 | 3 |